STUDY OF FLUID FLIGHT PATH CONTROL SYSTEM

NASA CR-758

STUDY OF FLUID FLIGHT PATH CONTROL SYSTEM

Distribution of this report is provided in the interest of information exchange. Responsibility for the contents resides in the author or organization that prepared it.

Issued by Originator as Report No. 20175-FR1

Prepared under Contract No. NAS 4-763 by
HONEYWELL INC.
Minneapolis, Minn.

for Flight Research Center

NATIONAL AERONAUTICS AND SPACE ADMINISTRATION

FOREWORD

This report was prepared by the Fluid Flight Systems
Section of Honeywell Inc., Aero Engineering Depart-
ment. It fulfills Contract NAS 4-763 for the NASA
Flight Research Center and constitutes the final engineer-
ing report for that contract. Four progress reports
have been submitted at monthly intervals as required by
Article II (a) of the contract. Copies of the final report
are submitted in accordance with Article II (b).

ABSTRACT

Advanced concepts for lateral and pitch flight
path stabilization of light aircraft were studied.
A major consideration was the suitability of the
concept configuration for pure-fluid mechaniza-
tion. The concept configurations were evaluated
on an analog simulation of the Cessna 310 air-
plane. Ramp and step wind inputs were used as
disturbances in the evaluation. The results of
the study are tabulated and compared with cer-
tain pilot acceptance and ease of mechanization
criteria.

CONTENTS

ILLUSTRATIONS

SUMMARY

A total of 14 lateral axis flight path control concepts suitable for fluid
mechanization are evaluated with respect to their capability to achieve
specific predetermined primary and secondary design goals. These
design goals are discussed in detail in Appendix A.

The primary design goal is to achieve lateral flight path control which
limits the maximum flight path error to 1.3 miles + 0.04 mi/mph of
cross-course wind change in a 15-minute interval.

A secondary design goal is also specified which seeks to find a simpler
configuration at the cost of an acceptable compromise in performance.
The performance requirement for the secondary goal is to achieve a
significant improvement over the flight path performance of the conven-
tional attitude hold autopilot in the presence of a 20-mph change in cross-
wind velocity.

The lateral flight path configurations studied were classified into the
following groups:

    A.   Single-Axis Concepts

    B.   Tight Roll Concepts

    C.   Biased Heading

    D.   Dual-Mode

    E.   "Constant Heading" Flight Path

The "Single-Axis" Concepts are the simplest, employing no attitude loops. The "Tight Roll" configurations employ a roll control loop but not heading hold. The remaining three concepts employ both roll and heading attitude loops. The design and analysis approach employed was to seek a configuration which reduced the effect of lateral wind variation on flight path deviation, since, for the conventional attitude autopilot, this is the largest cause of lateral flight path error.

In all configurations studied, the effects of cross-course wind variations are reduced by considerably more than 85 percent (See Table 1, Page 93). However, such effects as system mistrims, biases, drifts and parameter variation cause considerably different amounts of lateral path error for each class of system.

To meet the primary design goal the lateral flight path deviation due to all effects except lateral wind variation must be less than 1.3 miles in 15 minutes. Only the Biased Heading Hold and Dual-Mode concepts can possibly achieve this performance in the presence of system mistrims, biases, etc., since these employ both roll and heading hold loops. The most promising of these configurations was found to be the Biased Heading Hold concept employing the integral of sideslip feedback.

To achieve the secondary design goal, the selected configuration must perform better than the conventional attitude hold autopilot in the presence of a 20-mph lateral wind change. The effect of such a wind on the flight path performance of a perfect attitude hold A/P can be to cause a lateral flight path error of:

$$0.25 \text{ hrs} \times 20 \text{ mph} = 5 \text{ miles}$$

in 15 minutes.

2

Thus, a Flight Path Control concept which drastically reduces (or completely eliminates) the flight path error due to the lateral wind variation can incur 5 miles of lateral deviation due to mistrims, biases, drifts, etc., and still equal the performance of the conventional attitude autopilot (in the presence of a 20-mph cross-wind velocity change).

To meet the secondary design goal the lateral deviation or error due to mistrims, etc., must therefore be substantially less than 5 miles in 15 minutes and the configuration must be simpler than the Biased Heading Hold configuration.

The Tight Roll configurations certainly satisfy the requirement for configuration simplicity and conceivably will also satisfy the performance requirement. The most promising configuration of this group is the "Roll Attitude Control with Sideslip Feedback". The other concepts studied do not meet either the primary or secondary design goals.

It was recommended that a fluid control system consisting of the Biased Heading Hold with the integral of sideslip feedback be designed, fabricated and flight tested to evaluate and demonstrate its performance capabilities and that the same hardware and facilities be used to evaluate the "Roll Attitude Control with Sideslip Feedback" configuration.

Four Pitch Flight Path Control concepts were considered. The major emphasis was on a descent rate mode suitable for use during landing approach. It was concluded that two concepts were equally suitable from a performance standpoint. They are:

- Altitude rate feedback command
- Lagged pitch attitude feedback command

The choice of a descent mode concept for mechanization and flight test can be made on the basis of sensor availability and quality.

3

A conventional altitude hold mode is recommended for Pitch Flight Path Control during the cruise portion of a flight.

A discussion of criteria and procedures for the evaluation of the flight test system is presented in Appendix A. Appendix A also contains a tabulation of the cost and weight breakdown of the fluid mechanization and equivalent conventional hardware mechanization of the recommended configuration. It is estimated that the fluid system can be mechanized at one-half the cost and weight of the conventional system.

SECTION I

INTRODUCTION

As a result of the experienced and predicted further increase in light aircraft traffic, attention has been directed to the need for a reliable, low-cost control system to assist the pilot in cross-country flying and landing approach. Pure-fluid mechanization appears particularly attractive for these system requirements.

With this need in mind, a research study program was undertaken to define control concepts that are amenable to present or near-future pure-fluid mechanization. The primary aim was to provide the broadest possible coverage of the theoretically feasible concepts within the time and cost constraints of the contract. The theoretical concepts were then screened to select the most attractive configurations for more detailed analysis and, ultimately, for mechanization and flight test.

Initially, studies were undertaken to define the effects of specific error sources such as control surface mistrim, multi-engine thrust differentials and system thresholds. However, it soon became apparent that other error sources were equally important and to include them all would severely curtail the number of concepts that could be studied. For this reason, the scope of the study was limited to study of the theoretical feasibility of the concepts, with lesser consideration of the effects of mechanization and operational error sources.

Concept validity was evaluated using an analog computer simulation of the Cessna 310 as a test vehicle. This aircraft was chosen as a typical light, twin-engine aircraft since it is in the current NASA inventory and also because some aerodynamic data is available.

The emphasis in the lateral axis study was on flight path control concepts which would minimize lateral displacements resulting from changes in cross-course wind velocity. Fourteen lateral control configurations were studied and are described in Section II, "Lateral Flight Path Control Concepts". The introduction to that section outlines study scope and certain detail considerations. A comparison of concepts follows the discussion of individual configurations.

Section III, "Pitch Flight Path Control", discusses control concepts for the cruise and landing approach mission phases. A comparison of pitch configurations follows the detailed discussion.

Four lateral flight path concepts and two pitch axis configurations are recommended for further study in Section IV, "Conclusions and Recommendations". The areas of study to be applied to the recommended configurations are noted. These are chosen, in particular, to select and optimize a system for mechanization and flight test.

A discussion is presented in Appendix A, "Evaluation Criteria and Procedures", of a basis for evaluating flight path control concepts and evaluation procedures are outlined. An estimated cost and weight comparison of a conventional and FFPC autopilot is given in Appendix A.

In Appendix B, "Lateral Flight Path Concept Analysis", the mathematical derivation of design and performance relationships are presented.

Additional appendixes are included to cover the definition of symbols used in this report, analog computer diagrams, and Cessna aerodynamic data. Discussions of wind profiles and engine mistrim effects are given in Appendixes G and F, respectively.

SECTION II
LATERAL FLIGHT PATH CONTROL CONCEPTS

GENERAL

The lateral control problem was investigated with the primary aim of developing concepts that showed promise of enabling a light aircraft to fly a straight-line flight path with a completely self-contained system. At the same time, the system to be developed had to show promise of being sufficiently simple and inexpensive to be practical for use in a light plane. Because of this, concepts which used minimum numbers of sensors and seemed most compatible with conventional autopilots were emphasized.

Two areas of simplification are theoretically possible:

- In the mechanization of the outer loop (i.e., replacing of the "beam-follower" type of lateral flight path error detector by a simpler outer loop) or omitting the outer loop altogether

- In simplification of the inner loops

The approach adopted is to obtain a simplification over the conventional "Omni" system by:

- Simplifying the task of the flight path control system and, therefore, requiring a simpler outer loop or none at all. Specifically in the concepts studied, the primary task of the configuration is reduced to diminish the effect of a cross-course wind on the cross-course velocity. In the conventional "Omni" system, an outer loop is required to reduce lateral flight path position errors from all sources.

7

- Simplifying the inner loop by taking advantage of the lesser dynamical requirements placed on the inner loop by a dynamically simple outer loop (or by the omission of the outer loop). That is, with a simpler outer loop (or none at all), it is possible to remove one or both attitude feedbacks of the inner loop, whereas in the "Omni" system, a full attitude control autopilot is required for stability reasons.

This approach can provide significant flight path control with a given configuration only if the cross-course wind effects remains a major contribution to lateral flight path error.

However, the relative size of cross-course wind effects and effects of other factors such as system mistrims, biases, etc., is grossly affected by the type of inner loop.

Thus, for example, for full attitude-hold inner loops, the effects on flight path error of mistrims and biases are relatively small compared to wind effects. As attitude loops are discarded, the effects of mistrims and biases become much larger and may swamp out wind effects.

In this study, effort was concentrated on discovering as many concepts with progressively more complicated inner loops - from the simplest (no attitude feedbacks) to inner loops which include both roll and heading feedbacks which would provide effective reduction in cross-wind effects. The goal set is a reduction of 85 percent, or to limit lateral deviation developed in 15 minutes by a 20-fps cross-wind to 2700 feet (see Appendix A).

The feasibility investigation of concepts was restricted to evaluation of performance for lateral wind step inputs and ramps. Effects of mistrims, thresholds, and similar non-linearities, as well as disturbances other than the lateral wind steps and ramps were not, in general, considered in this phase of the study. These limitations were imposed in the interest of touching on a larger number of possible solutions to the lateral flight path control problem in the study period.

CONCEPTS INVESTIGATED

The concepts investigated are generally described and classified in the following paragraphs:

Single-Axis Control

The inherent directional stability of the airplane is augmented by simple feedbacks to the aileron or rudder. Attitude sensors are omitted in this category. If the airplane does not accumulate any significant amount of lateral velocity with respect to the flight path during its initial response to a lateral wind change, the amount of yaw angle change will compensate for the effect of the wind change. If a roll angle is kept from developing during the initial transient, the compensating yaw angle change will be maintained.

Tight Roll Control

A roll attitude hold loop is employed to force the roll angle to zero at the end of the initial response to a lateral wind change. This assures maintenance of the yaw angle achieved at the end of the control transient. Additional feedbacks are employed to force this initial yaw angle to provide the correct amount of compensation for the wind change.

Biased Heading Control

In this group, a heading hold mode is used which is biased by a signal that is continuously computed. The bias signal is maintained equal to an amount required to offset the effect of the cross-course wind component on the desired flight path.

Dual-Mode Control

This group is similar in concept to the "Biased Heading Control". As in the "Biased Heading" approach, the airplane is normally controlled by the heading hold plus an increment required to compensate for the effect of the cross-course velocity. However, in the dual-mode approach, the bias signal is not continuously computed. Instead, the heading hold mode is switched out, and the necessary change in heading is computed by allowing the augmented directional stability of the airplane to cause the proper yaw change to take place. The heading hold loop is sychronized to the new heading before re-engagement.

"Constant Heading" Flight Path Control

In this group, roll angle is used to reduce all or part of the side force produced by a lateral wind. The result is a reduction in the net change in yaw angle necessary to maintain a straight line-flight path in the presence of a lateral wind change.

Miscellaneous

In addition to the above concepts, there are three general approaches listed in the following detailed classification which are not covered by the categories cited above.

DETAILED CONCEPT CLASSIFICATION

The concepts studied in each group are as follows:

A. <u>Single-Axis Control</u>

    A1. Free airplane - control locked

    A2. Single-axis with sideslip feedback to rudder

    A3. Single-axis with sideslip feedback to aileron

    A4. Single-axis with yaw rate feedback to aileron

B. <u>Tight Roll Control</u>

    B1. Roll attitude control

    B2. Roll attitude with sideslip feedback to rudder

    B3. Roll attitude with sideslip feedback to aileron

    B4. Roll attitude with servoed sideslip feedback to aileron

C. <u>Biased Heading Control</u>

    C1. Heading hold biased by side velocity

    C2. Heading hold biased by integral of sideslip angle

D. <u>Dual Modes</u>

    D1. Dual Mode: Roll attitude with sideslip feedback to aileron

    D2. Dual Mode: Wings leveler with sideslip feedback to aileron

    D3. Dual Mode: Wings leveler with yaw rate feedback to aileron

    D4. Dual Mode: Heading feedback to rudder

E. <u>Constant Heading Lateral Flight Path Control</u>

Heading hold through rudder with sideslip bias to roll angle.

F. Miscellaneous Control Systems

    F1. Strapped-down navigator

    F2. P-Matrix

    F3. Balanced attitude

Each concept of this list is discussed in the following subsections. Descriptions, block diagrams and representative computer performance recordings are presented for each concept. Reference should be made to appendixes for the detailed derivation of relationships (Appendix B) and for definition of symbols (Appendix E). A computer diagram is given in Appendix C, and the aerodynamic data for the Cessna 310 for cruise, approach and climb conditions are given in Appendix D.

SINGLE-AXIS CONTROL SYSTEMS (A)

In these concepts the inherent directional stability of the airplane is augmented by simple feedbacks to the aileron or rudder. The objective is to determine how flight path control can be achieved without attitude sensing.

Because of its inherent directional stability, the airplane tends to "weathercock" into the wind when a step change in the lateral wind component causes a change in orientation of the relative wind. If, during the "weathercocking" activity the airplane does not attain a cross-course component of velocity, the final value of yaw will be the proper amount to maintain the cross-flight-path velocity at zero -- that is, the final value of the yaw angle, ψ_{ss}, will equal the initial value of the sideslip angle, β_o (see Appendix B).

Two sources of error arise due to cross-course wind variation: (1) During the weathercocking activity, the airplane does attain a cross-flight path velocity so that when the sideslip goes to zero (or nearly zero, thus ending the weathercocking action) the yaw angle is less than the initial sideslip angle, β_o.

(2) A roll angle may be developed during the weathercocking activity, so that an equilibrium condition is not attained at the end when the sideslip angle reaches an essentially zero value. This roll angle will cause the airplane to continue to yaw away from or back to zero.

In these single-axis concepts, the feedbacks are used to maintain a zero roll angle during the initial transient response. It is shown in Appendix B that satisfying the conditions for a zero roll angle also results in a neutrally stable "spiral" mode. That is, the roll angle is zero, if

$$N_\beta L_r - L_\beta N_r = 0 \qquad\qquad (1)$$

where L_r, N_β, L_β and N_r are defined in Appendix E.

If Equation (1) is not satisfied, then we have a spiral divergent or convergent case. In the former case, where

$$N_\beta L_r - L_\beta N_r > 0$$

both the roll and yaw angles increase exponentially. In the latter case, where

$$N_\beta L_r - L_\beta N_r < 0,$$

the roll and yaw angles return exponentially to their initial zero value, with a time constant inversely proportional to $|N_\beta L_r - L_\beta N_r|$.

The free airplane is discussed first, for a basis of comparison. This is followed by three approaches in which the effective N_β, L_β and L_r are modified by appropriate feedbacks of sideslip (for L_β and N_β) and yaw rate (for L_r) in order to satisfy Equation (1).

In these schemes the effective N_r is adjusted by yaw rate feedback to the rudder to provide a decoupled yaw damping factor of about 0.3 to 0.5.

Free Airplane - Controls Locked (A1)

As a basis for reference, the behavior of the free airplane (controls locked) was investigated. The details of the analysis are given in Appendix B, Section A1. It is shown there that, for the cruise flight conditions, the yaw angle after the initial transient, ψ^* is quite close to β_o, and that the time constant of the convergent spiral mode, $\tau = \frac{1}{a}$, is quite long. Using the expressions developed in Appendix B [Equations (B14) and (B13)], we have evaluated ψ^* and τ for cruise, approach and climb conditions:

Flight Conditions	ψ^*	τ (sec)
Cruise	$0.97\beta_o$	135
Approach	$0.96\beta_o$	- 68
Climb	$0.98\beta_o$	- 45

It will be noted that, for the cruise condition, τ is positive (spiral mode is convergent), but, for the approach and climb conditions, τ is negative and a spirally divergent condition exists.

For a 20-fps step in lateral wind, the lateral deviation from the flight path, ε_{Y_G}, due to the error in ψ^*, after 15 minutes can be found from:

$$\varepsilon_{Y_G} = (\psi^* - \beta_o) U_1 T \qquad (2)$$

and

$$\beta_o = \frac{-\dot{Y}_{WG_o}}{U_1} = \frac{-20}{313} = -0.064 \ \text{rad.} \qquad [\text{Eq. (B6), App. B}]$$

where ψ^*, β_o, U_1 are defined in Appendix E and T = reset time = 900 secs.

For cruise conditions, $\epsilon_{Y_G} = 540$ feet. However, due to the time constant of 135 seconds there will be an error of 7000 feet at the end of 15 minutes (see Appendix B, Page B9), which exceeds the maximum allowable of 2880 feet (see Appendix A).

The free airplane (controls locked) configuration was simulated on the analog computer. Responses to a step change in lateral wind was recorded for cruise, approach and climb conditions. These recordings are reproduced in Figures 1, 2, and 3.

The values of ψ^* for a 20-fps step read from these recordings compare closely to the values computed from Equation (B14).

Single Axis with Sideslip to Rudder (A2)

In this configuration, sideslip angle is fed back to the rudder to make

$$\underline{N}_\beta L_r - L_\beta \underline{N}_r = 0 \tag{3}$$

equal to zero and thus achieve a neutrally stable spiral mode. In addition, yaw rate feedback is employed to provide the decoupled yaw response with a damping factor of 0.32 ($\delta_{rr} = 0.15$ and $\underline{N}_r = -3.2$ at cruise conditions). The block diagram for this configuration is shown in Figure 4. The bars under N_r and N_β in Equation (3) signify that these are values of the stability derivation with the effect of the yaw rate and sideslip feedbacks to the rudder accounted for. [See Equation (B23) in Page B11 in Appendix B.]

15
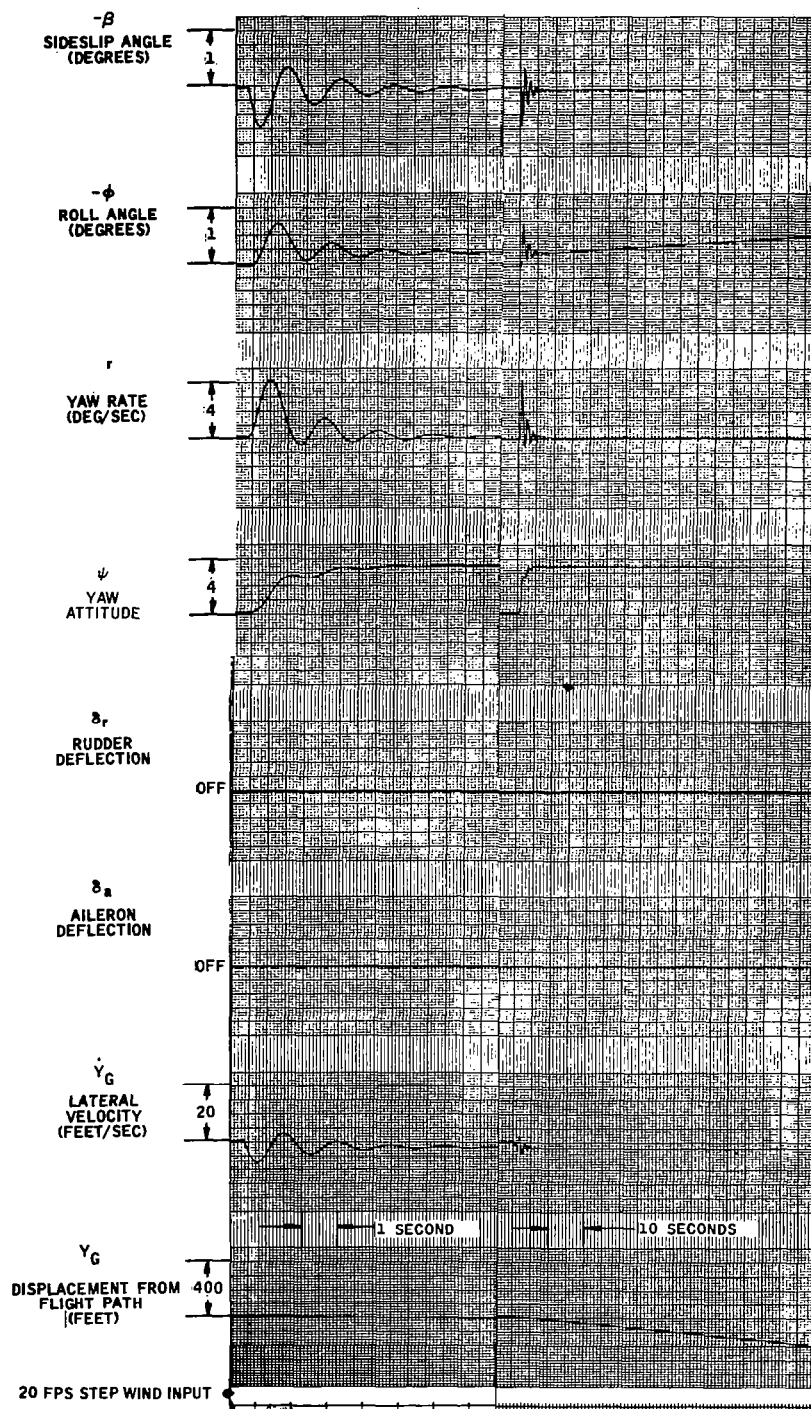
Figure 1. Free Airplane, Cruise
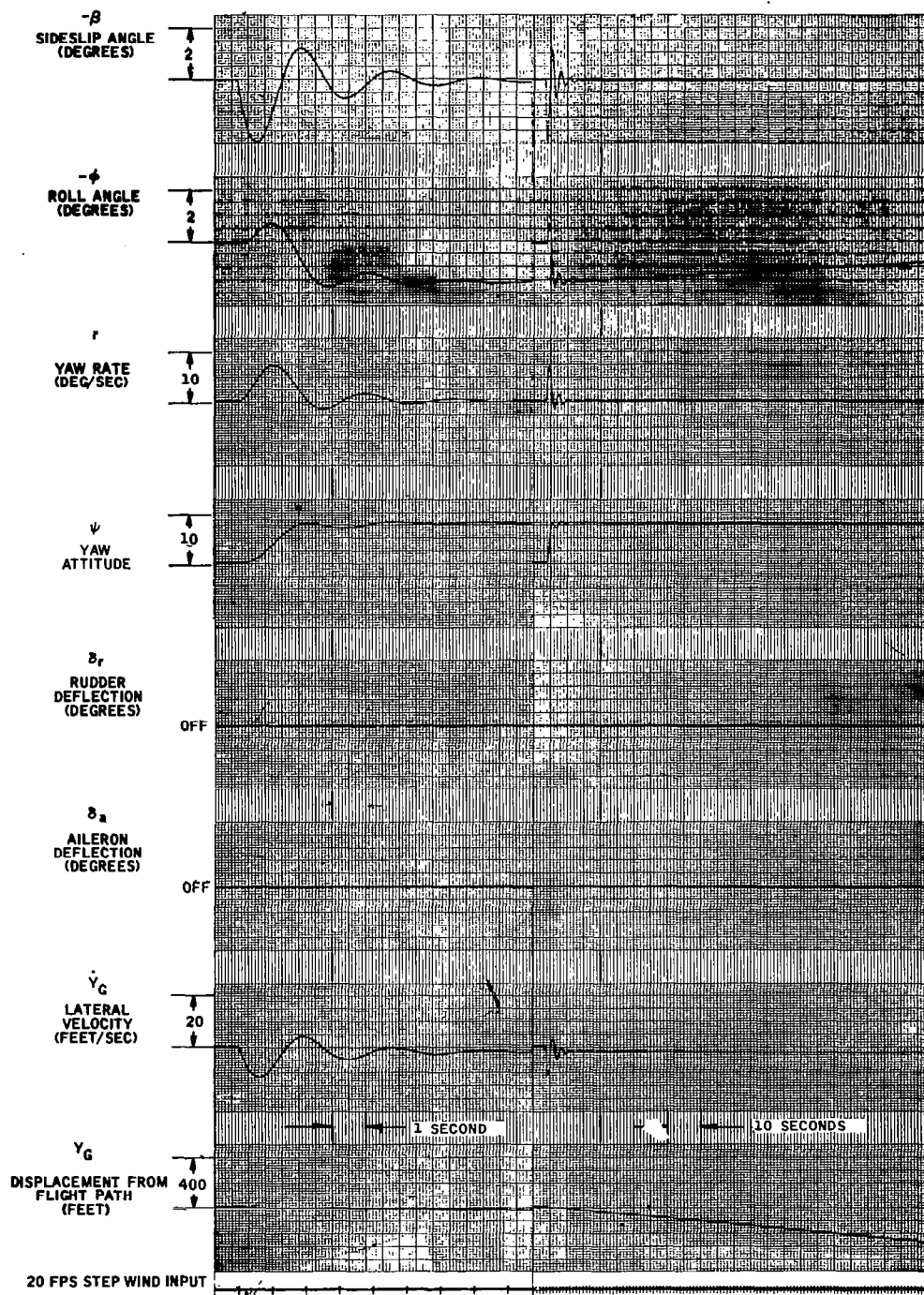
Figure 2. Free Airplane, Approach

17
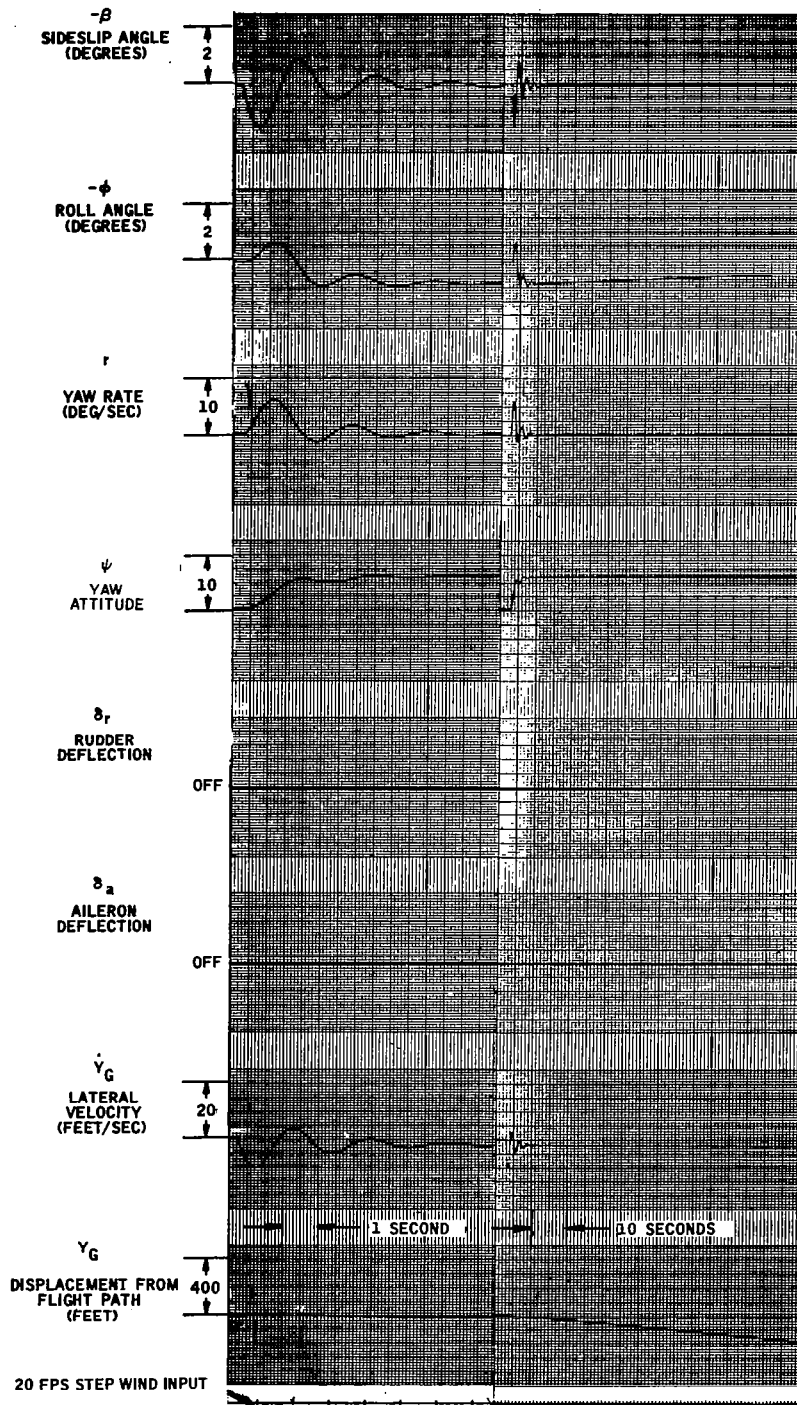
Figure 3. Free Airplane, Climb

18
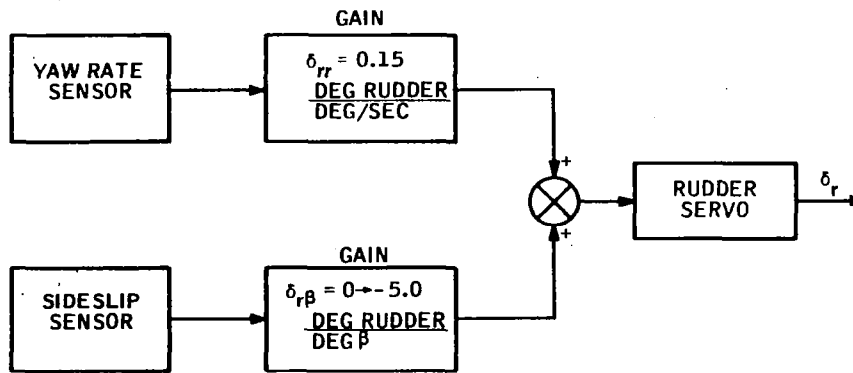
Figure 4.   Single Axis with Sideslip Feedback to Rudder (A2)

At cruise conditions Equation (3) is satisfied with

$$\underline{N}_\beta = \frac{(-23.4)(-3.2)}{0.892} = 83.8$$

or, from Equation (B23), the degrees of rudder per degree sideslip angle, $\delta_{r\beta}$,

$$\delta_{r\beta} = \frac{83.8 - 17.84}{-14.24} = -4.63$$

From Equation (B21):

$$\psi^* = 0.976 \beta_o$$

and from Equation (2), with $\dot{Y}_{WG_o} = 20$ fps ($\beta_o = -0.064$ rad.) and T= 900 sec. we have:

$$\psi^* = 0.0625 \text{ rad} = 3.58 \text{ degrees}$$

and

$$\epsilon_{Y_G} = 430 \text{ feet,}$$

which is less than the 2880-foot maximum allowable.

The analog computer was used to record the response of this configuration to a 20-fps step in lateral wind for cruise flight conditions and with autopilot gains of Figure 4 for values of

$$\delta_{r\beta} = 0, -1, -3, -5,$$

and

$$\delta_{rr} = 0.15 \text{(which corresponds to a damping ratio of 0.32)}$$

These recordings are shown in Figures 5 and 6. The recordings of Figure 6 were made with a higher paper speed-in order to show the details of the short-term response. It should also be noted that, for the traces of Figure 6, a 0.1-second low-pass filter normally used to shape the wind step was removed and a smaller step was used (10 fps). The filter is normally included so that larger step inputs could be employed without exceeding the simulator yaw rate amplifier limits. The effect of this filter is negligible after one second and therefore does not significantly effect the portion of the response we are interested in.

From the traces of Figure 5, it can be seen that for some value of $\delta_{r\beta}$ in the range

$$-5.0 < \delta_{r\beta} < -1.0$$

ψ^* is maintained constant, which agrees with the results above.

Also from the traces of Figure 5 we have confirmation that $\psi^* \cong 3.58^{\circ}$ which was computed before. Obtaining ϵ_{Y_G} by direct recording was not attempted except for the free airplane (controls locked) case for single-axis configuration. (It is extremely time-consuming to obtain ϵ_{Y_G} for 15 minutes by direct recording because of the sensitivity to mistrim experienced with configurations not provided with attitude loops. The relative sensitivity of the simulation of these configurations to mistrims reflects a similar relative sensitivity to be expected for the operation configurations.) From the traces of Figure 6, we note that increasing the magnitude of sideslip feedback to rudder tends to decrease the coupled yaw damping. Interpolating these curves we see that at $\delta_{r\beta} = -4.63$, the decrease in damping over $\delta_{r\beta} = 0$ is not significant.
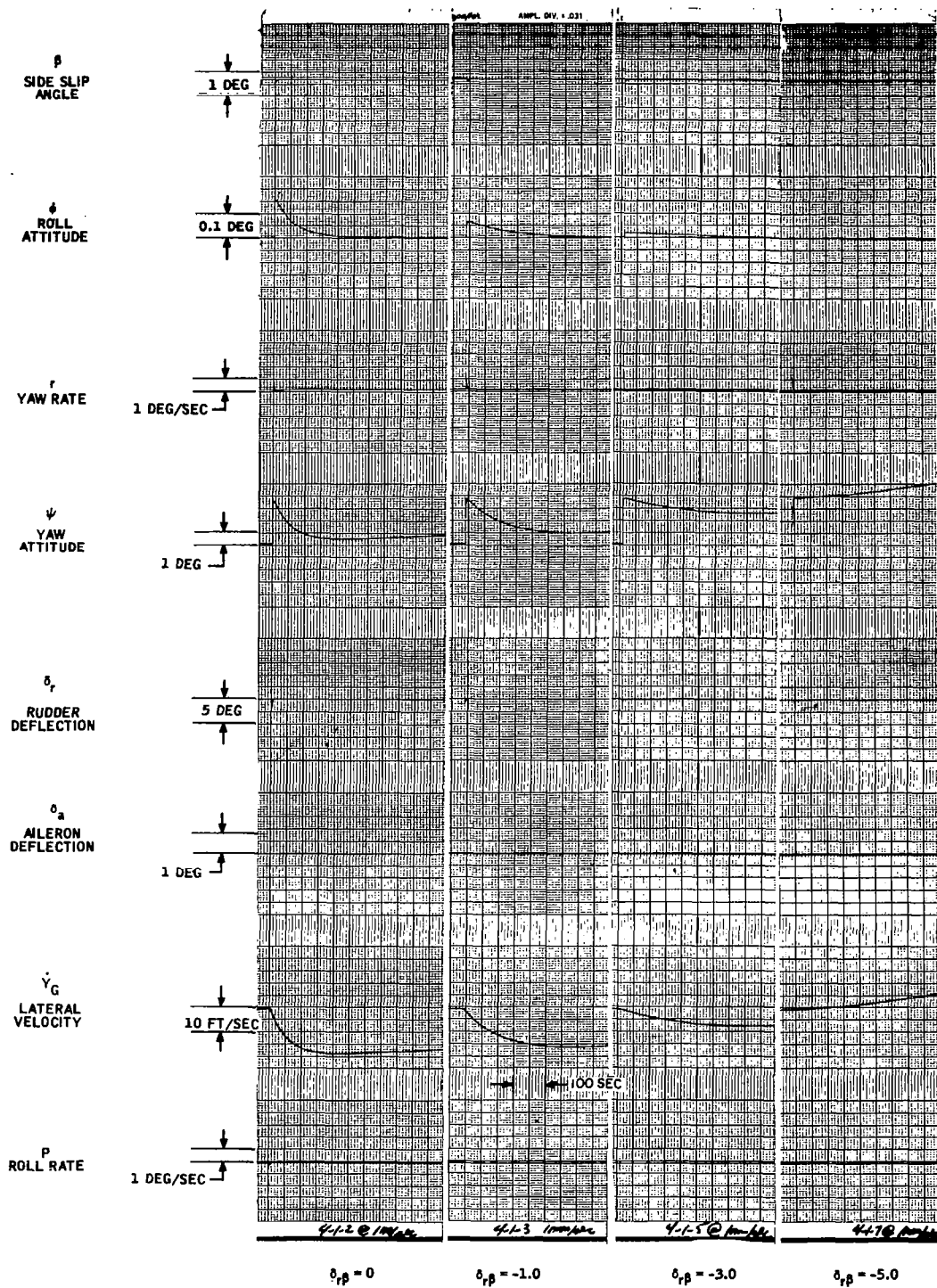
Figure 5. Single Axis with Sideslip Feedback to Rudder (A2)
- Response to 20-fps Step

21
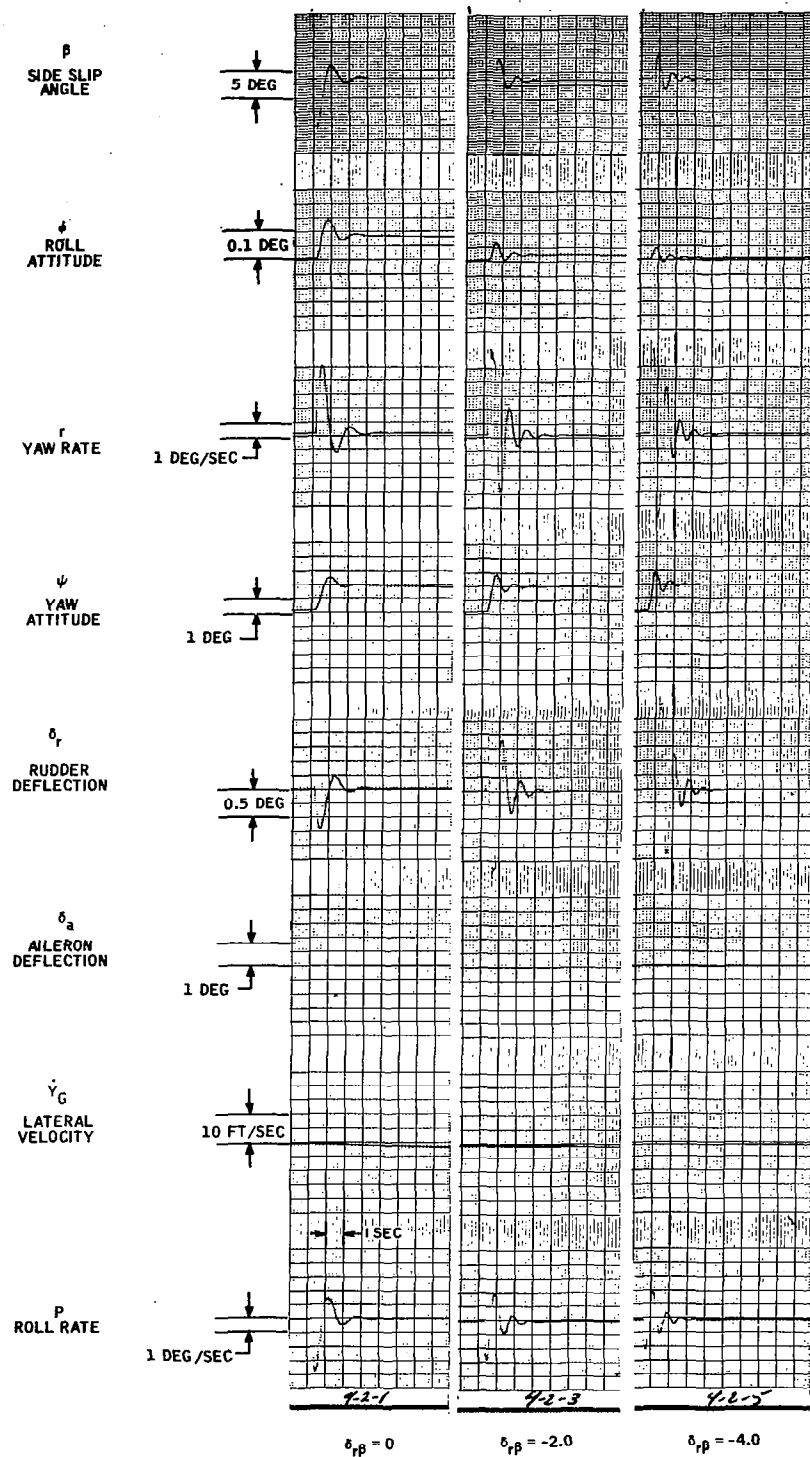
Figure 6. Single Axis with Sideslip Feedback to Rudder (A2)
- Short-Term Response

Single Axis with Sideslip Feedback to Aileron (A3)

In this configuration, the sideslip angle is fed back to the aileron to modify the effective value of L_β in order to achieve a neutrally stable spiral mode. That is, to make

$$N_\beta L_r - \underline{L}_\beta \underline{N}_r = 0$$

Again N_r is also modified by yaw rate feedback to achieve a decoupled yaw damping of 0.32. A block diagram of this configuration is shown in Figure 7. At cruise conditions, with $\underline{N}_r = -3.2$, a neutrally stable spiral condition is achieved with

$$\underline{L}_\beta \cong \frac{N_\beta L_r}{\underline{N}_r} \cong \frac{(17.84)(0.892)}{-3.2} = -4.96$$

or, from Equation (B28)

$$\delta_{a\beta} = \frac{\underline{L}_\beta - L_\beta}{L_{\delta a}} = \frac{-4.96 - (-23.4)}{-36.8} = -0.5$$

With this value of $\underline{L}_\beta$, we find from Equation (B21)

$$\psi^* = -0.955\,\beta_o$$

and from Equation (2) with $\dot{Y}_{WG_o} = 20$ fps, $(\beta_o = -0.064$ rad.$)$ and T = 900 sec, we have:

$$\psi^* = 0.061 \text{ rad.} = 3.50 \text{ degrees}$$

and

$$\epsilon_{Y_G} = 810 \text{ Feet}$$
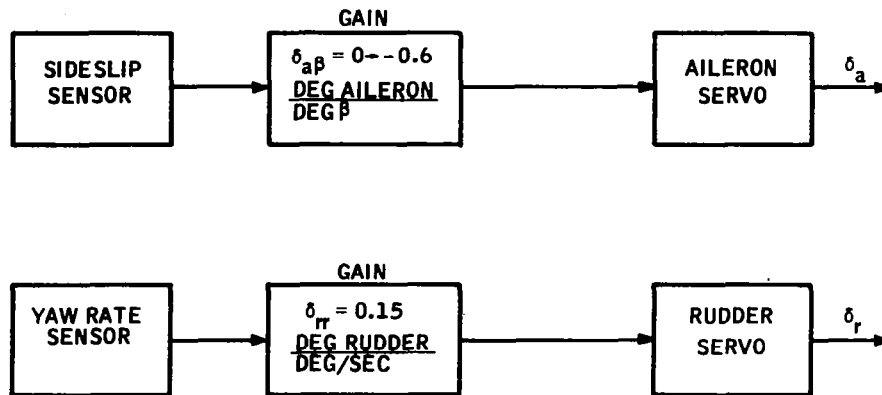
Figure 7. Single Axis with Sideslip Feedback to Aileron (A3)

Recordings were made of the response of this configuration for a lateral wind step input of 20 fps, with the autopilot gains shown in Figure 7, and $\delta_{a\beta}$ = 0, -0.4, -0.5, and -0.6. These are shown in Figures 8 and 9. The recordings of Figure 9 were made with a faster paper speed to show up the short-term response, and, as for the previous high-speed recording (Figure 6), the low-pass filter on the wind step input was removed. From the traces of Figure 8, it is seen that for a value of $\delta_{a\beta}$ in the range

$$-0.4 < \delta_{a\beta} < -0.6$$

ψ^* is maintained. That is, a neutrally stable condition is attained. This agrees with the computed result.

Also, from these traces, we confirm that

$$\psi^* \approx 3.66 \text{ degrees}$$

as computed previously.

From the traces of Figure 9 we can see that the change in yaw damping is not significant as we go from $\delta_{a\beta}$ = 0 to $\delta_{a\beta}$ = -0.5.
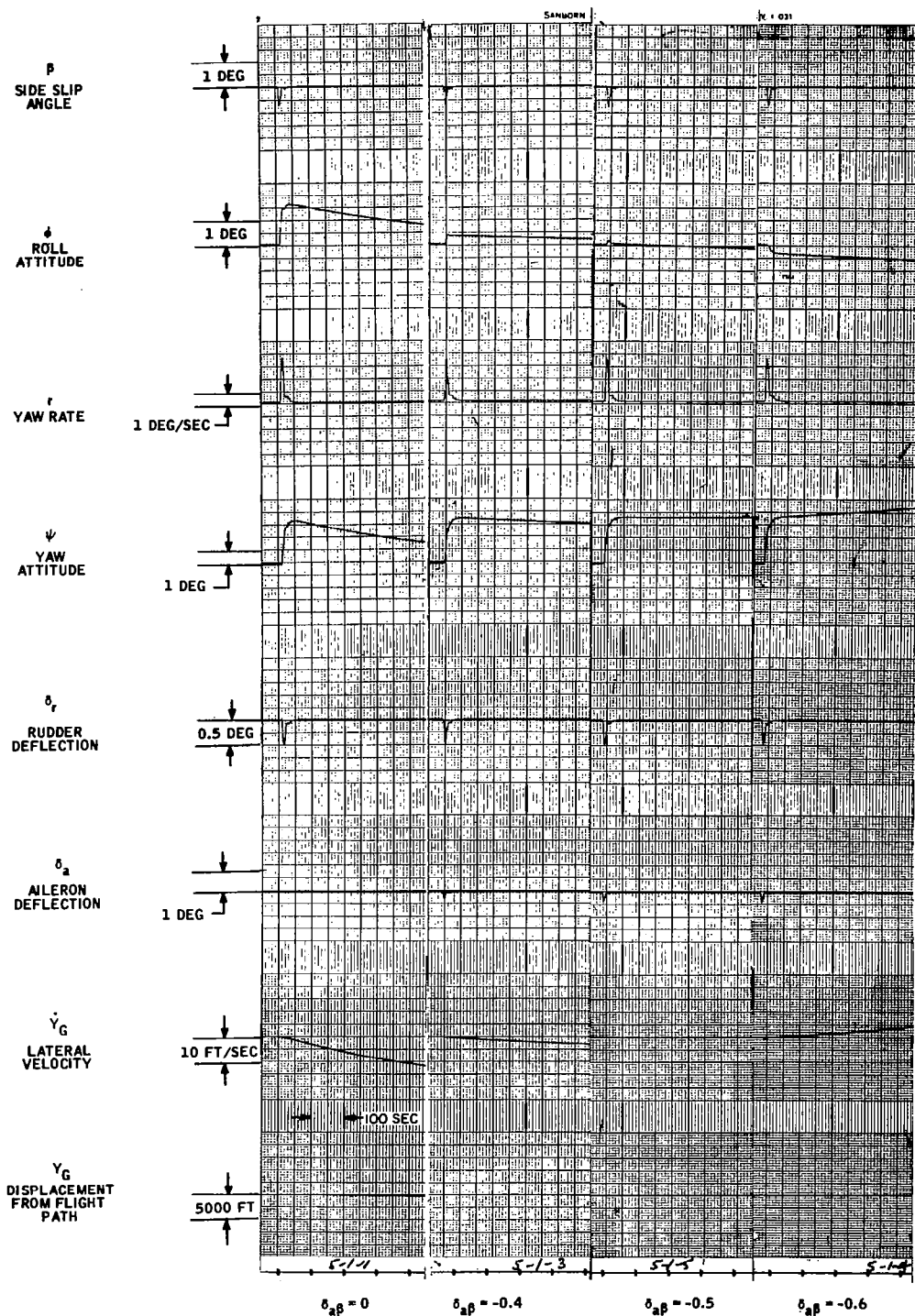
Figure 8.   Single Axis with Sideslip Feedback to Aileron (A3)
         - Response to 20-fps Step
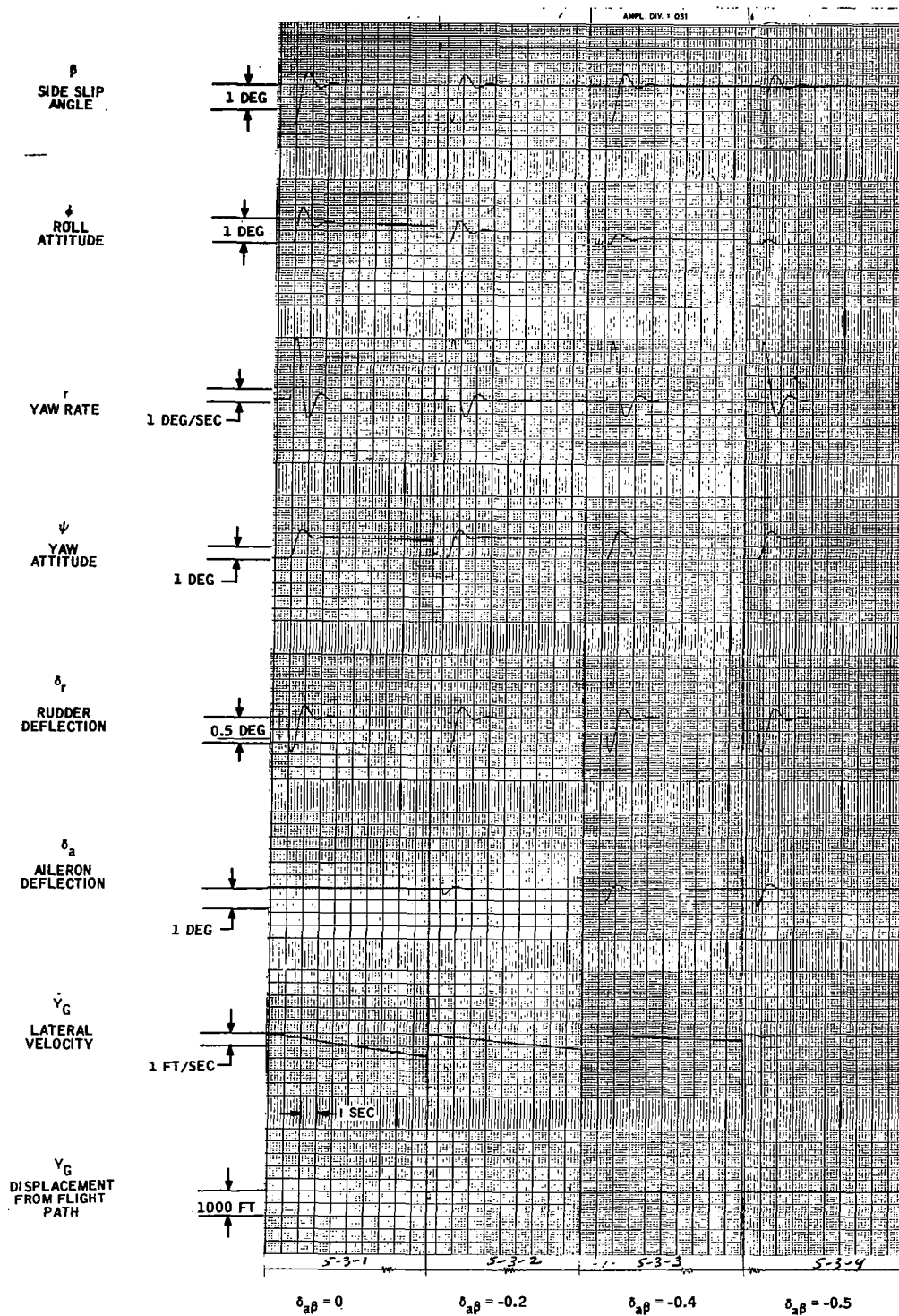
Figure 9. Single Axis with Sideslip Feedback to Aileron (A3)
- Short-Term Response

Single Axis with Yaw Rate Feedback to Aileron (A4)

Yaw rate feedback to the aileron is used in this configuration to modify the effective L_r and achieve a neutrally-stable spiral mode. The necessary value of $\underline{L}_r$ (modified L_r) is obtained by solving

$$N_\beta L_r - L_\beta \underline{N}_r = 0$$

In this configuration, $\underline{N}_r$ is made equal to -8.91 ($\delta_{rr} = 0.55$), at cruise conditions by yaw rate feedback to the rudder to give an uncoupled yaw damping factor of about 0.50. A block diagram of this configuration is shown in Figure 10.
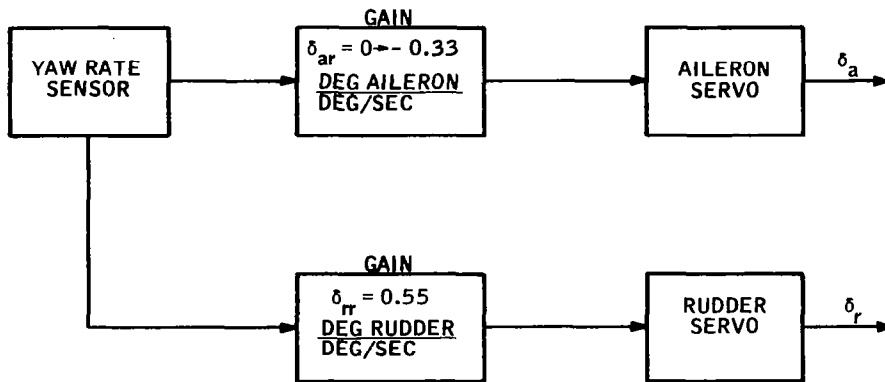
Figure 10. Single Axis with Yaw Rate Feedback to Aileron (A4)

(It is interesting to note that yaw rate feedback to the aileron is also the basis of the "Wings Leveler" technique for roll attitude control. In that instance, however, the objective is to employ enough feedback, in the proper direction, to make the spiral mode rapidly convergent, whereas in the present case a neutrally-stable spiral mode is sought.)

Solving for L_r and evaluating at cruise conditions, we have

$$\underline{L}_r = \frac{L_\beta \underline{N}_r}{N_\beta} = \frac{(-23.4)\,(-8.91)}{17.84} = 11.70$$

Using Equation (B29a), we obtain for the yaw rate to aileron autopilot gain:

$$\delta_{ar} = \frac{\underline{L}_r - L_r}{L_{\delta_a}} = \frac{11.7 - 0.892}{-36.8} = -0.295$$

With the value of $\underline{L}_r$ obtained above, we find from Equation (B21) that

$$\psi^* = 0.943\,\beta_o$$

and from Equation (2) for $\dot{Y}_{WG_o} = 20$ fps ($\beta_o = -0.064$ rad) and T = 900 seconds

$$\psi^* = -0.060 \text{ rad} = 3.46 \text{ degrees}$$

and

$$\epsilon_{Y_G} = 1020 \text{ feet.}$$

The response of this configuration to a 20-fps step in lateral wind was recorded. These traces are reproduced in Figure 11. The autopilot gains of Figure 10 were used; that is, $\delta_{rr} = 0.55$ and $\delta_{ar} = 0, -0.32, -0.32,$ and -0.33.

From these traces, it is seen that a value of δ_{ar} in the range $-0.33 < \delta_{ar} < -0.3$ achieves a neutrally-stable spiral mode. This agrees within instrumentation errors, with the computed result of $\delta_{ar} = -0.295$. From the traces we also find that the computed value of $\psi^* = 3.46$ degrees is confirmed.

TIGHT ROLL" CONTROL CONCEPTS (B)

In the "Tight Roll" concepts a roll attitude control loop is added to prevent any residual roll angle from remaining after the initial transient response to a lateral step, without interfering with the weathercocking due to inherent directional stability of the airplane.
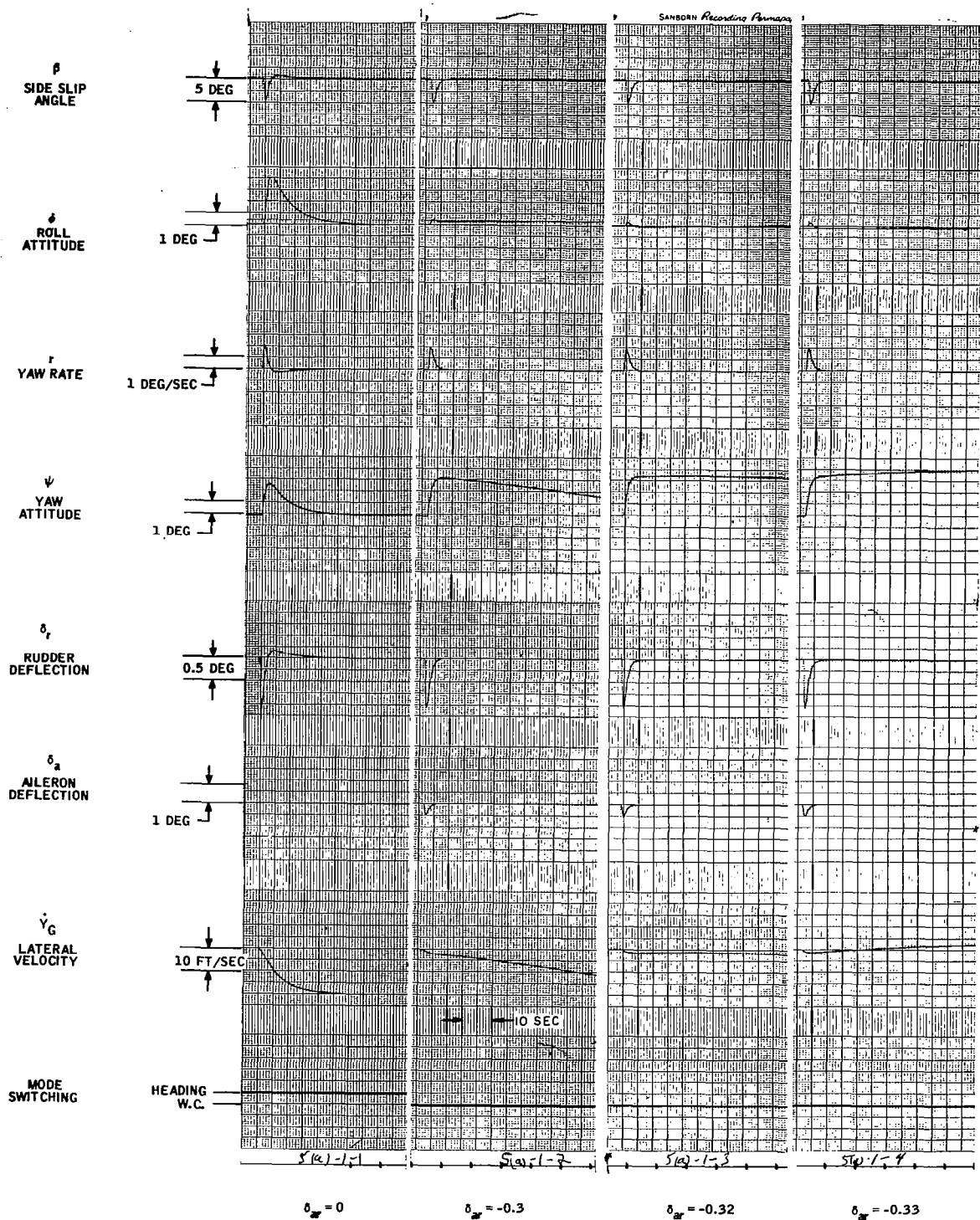
Figure 11. Single Axis with Yaw Rate Feedback to Aileron (A4)
- Response to 20-fps Step

Such a roll attitude control loop eliminates the effect of the spiral mode experienced in the single-axis concepts and the yaw achieved after the initial transient is maintained as a steady-state value. It is shown in Appendix B that roll attitude control achieved by feedback of a roll attitude sensor to the aileron eliminates the spiral mode by essentially decoupling the roll and yaw axis in the steady state, and is therefore used in the Tight Roll Control configurations. (On the other hand, the "Wings Leveler" techniques of roll control do not eliminate the spiral mode. Instead they force the yaw angle developed during the initial response to a wind step, as well as the roll angle, to zero in the steady state.)

The additional feedbacks in the Tight Roll Concepts are selected to force the steady-state yaw angle, ψ_{ss}, developed in response to a step change in cross-course wind to exactly compensate for the effect on the flight path.

In the first Tight Roll configuration discussed (B1), only yaw damping is employed, and the performance is discussed as a reference against which to compare the effect of additional feedbacks.

In the next configurations (B2 and B3), sideslip angle is fed back to the rudder and aileron respectively to reduce the difference between ψ_{ss} and β_o.

In the last concept discussed (B4), a technique for circumventing a threshold in the roll attitude sensor is explored. This is the "servoed β" concept. It was initially investigated as a means of providing biased heading operation, but proved to have the same performance as an attitude hold plus sideslip to aileron. Adding a threshold to the roll attitude sensor, in the presence of large sideslip feedback gain, causes a limit cycle that overcomes the effect of the roll attitude on flight path performance.

Roll Attitude Control (B1)

In this configuration, a roll attitude control loop is provided by roll attitude and rate feedback to the aileron. The gains were selected to give a decoupled roll response with a natural frequency of ~ 6 rad/sec and a damping factor of about 0.7. The decoupled yaw damping factor is made nominally equal to 0.5 with yaw rate feedbacks to the rudder. The amount of yaw damping was varied, however, to demonstrate the effect on flight path control. The block diagram of this configuration is shown in Figure 12.
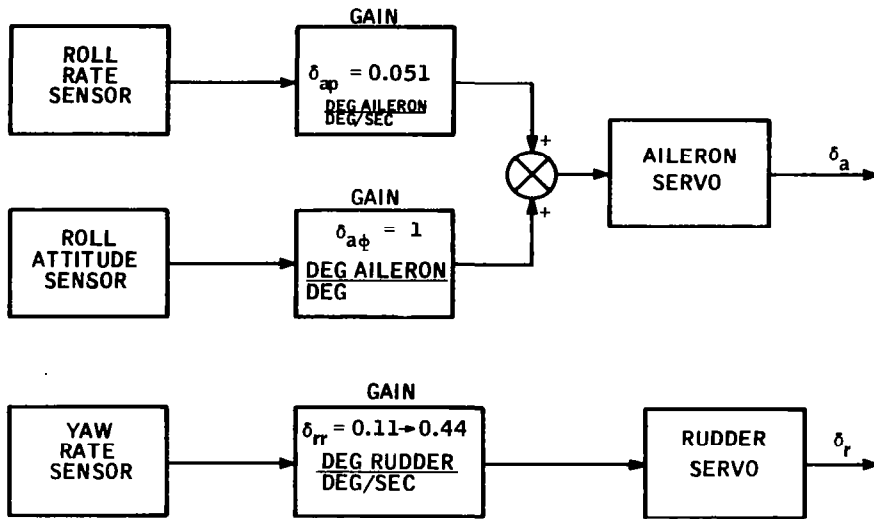
Figure 12. Roll Attitude Control (B1)

In Appendix B, an expression for ψ_{ss} is derived [Equation (B32)]. From this equation, it is seen that ψ_{ss} is nearly equal to β_o, and we can therefore expect that the flight path deviation at the end of the reset interval will be small. The expression of the deviation from the lateral flight path can be found in Equation (2), repeated here

$$\epsilon_{Y_G} = (\psi_{ss} - \beta_o) U_1 T$$

Evaluating for cruise conditions and the autopilot gains of Figure 12 (with δ_{rr} = 0.22, $\underline{N}_r$ = -4.2), we have, for a lateral wind step change of 20 fps,

$$\psi_{ss} = 0.982 \beta_0 = 0.062 \text{ rad} = 13.66 \text{ degrees} \quad \left[\text{From Equation (B32)}\right]$$

and

$$\varepsilon_{Y_G} = 324 \text{ feet in 15 minutes} \quad \left[\text{From Equation (2)}\right]$$

The response of this configuration to a 20-fps step was also recorded. The traces are reproduced in Figure 13. The responses for three different values of yaw damping are shown, corresponding to δ_{rr} = 0.11, 0.22, and 0.44. It is to be noted that the error in cross-course velocity increased with damping. From the traces for δ_{rr} = 0.32, we find ψ_{ss} compares closely with the value obtained from Equation (B32).

Roll Attitude with Sideslip to Rudder (B2)

In this configuration, sideslip feedback to rudder is added to the preceding configuration. The resulting configuration is shown in block diagram form in Figure 14.

The purpose of sideslip feedback to rudder is to modify the effect of N_β in order to reduce the error in ψ_{ss}. Equation (B32) can be used to evaluate ψ_{ss} for this configuration if N_β is replaced by $\underline{N}_\beta$, determined by the amount of sideslip to rudder feedback, $\delta_{r\beta}$:

$$\underline{N}_\beta = N_{\delta r} \delta_{r\beta} + N_\beta \qquad \text{(Page B20)}$$

Evaluating for cruise conditions and for the gains shown in Figure 14 ($\delta_{r\beta}$ = -4.0), we have for a 20-fps step (β_0 = -0.064 rad) and T = 15 minutes:

β
SIDE SLIP
ANGLE

1 DEG

φ
ROLL
ATTITUDE

1 DEG

r
YAW RATE

1 DEG/SEC

ψ
YAW
ATTITUDE

1 DEG

δ_r
RUDDER
DEFLECTION

0.5 DEG

δ_a
AILERON
DEFLECTION

1 DEG

$\dot{Y}_G$
LATERAL
VELOCITY

1 FT/SEC

100 SEC

Y_G
DISPLACEMENT
FROM FLIGHT
PATH

1000 FT

$\delta_{rr} = 0.11$ $\delta_{rr} = 0.22$ $\delta_{rr} = 0.44$
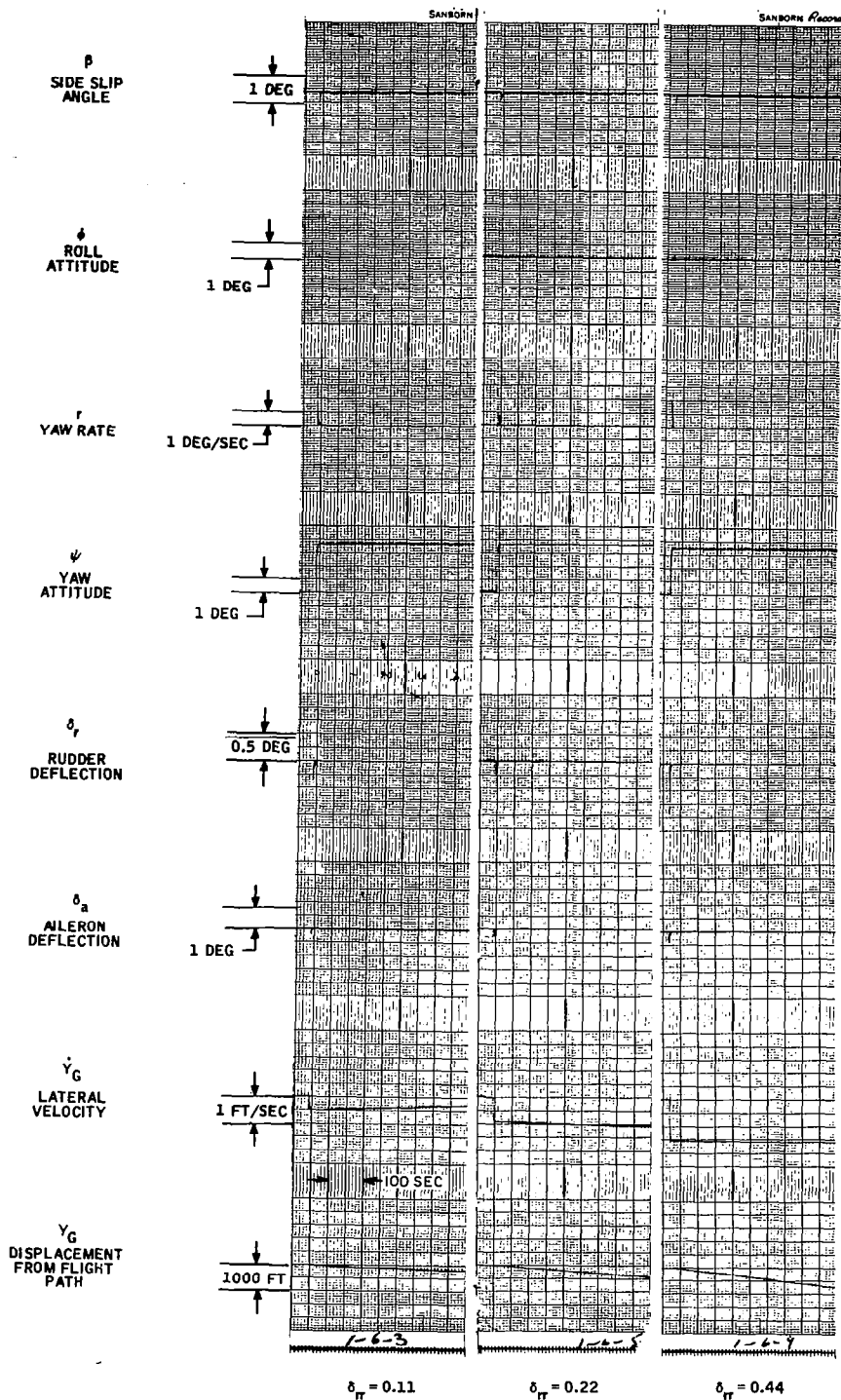
Figure 13.   Roll Attitude Control (B1)   - Response to
             20-fps Step

33
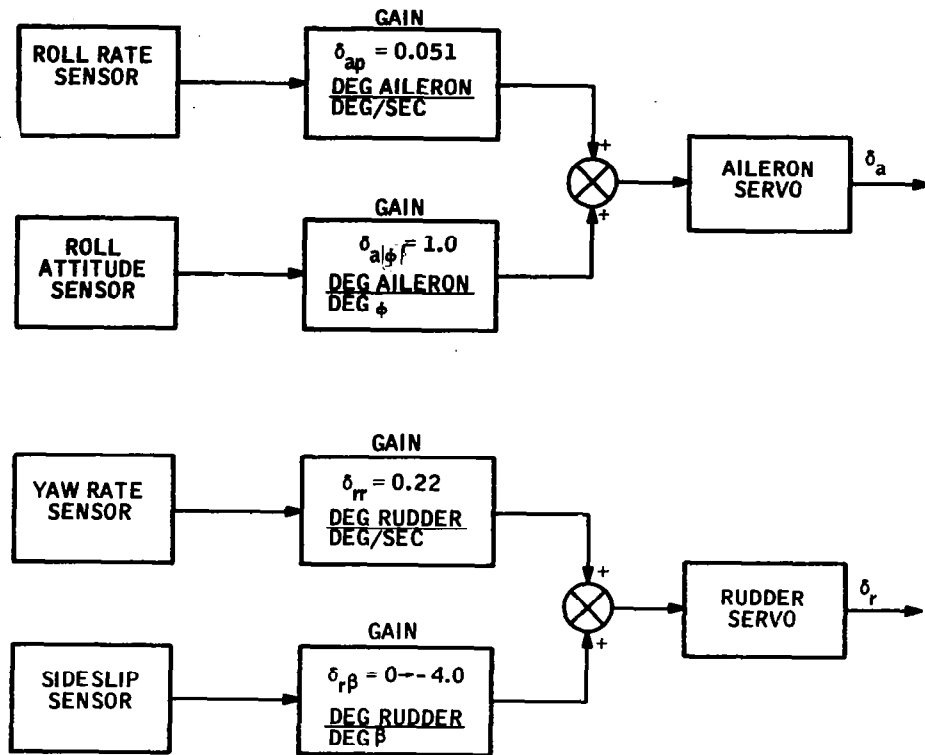
Figure 14. Roll Attitude Control with Sideslip
Feedback to Rudder (B2)

$$\underline{N}_\beta \;=\; (-14.\ddot{2}4)\,(-4.0) + 17.84 \;=\; 74.84$$

$$\psi_{ss} \;=\; 0.996\,\beta_o \;=\; 0.0639 \text{ rad} \qquad \left[\text{From Equation (B32)}\right]$$

$$\epsilon_{Y_G} \;=\; 77.9 \text{ feet in 15 minutes} \qquad \left[\text{From Equation (2)}\right]$$

Note, that for this configuration, ϵ_{Y_G} is 23.8 per cent of the preceding
case by this inclusion of sideslip feedback to rudder. The response of
this configuration a 20-fps step and a 20-fps/15-min ramp in lateral
wind are shown in Figures 15 and 16. The short-term input response
to a 10-fps step is shown, with an expanded scale, in Figure 17 (for
Figure 17 the 0.1-sec low-pass filter on $\dot{Y}_{W_G}$ was removed).
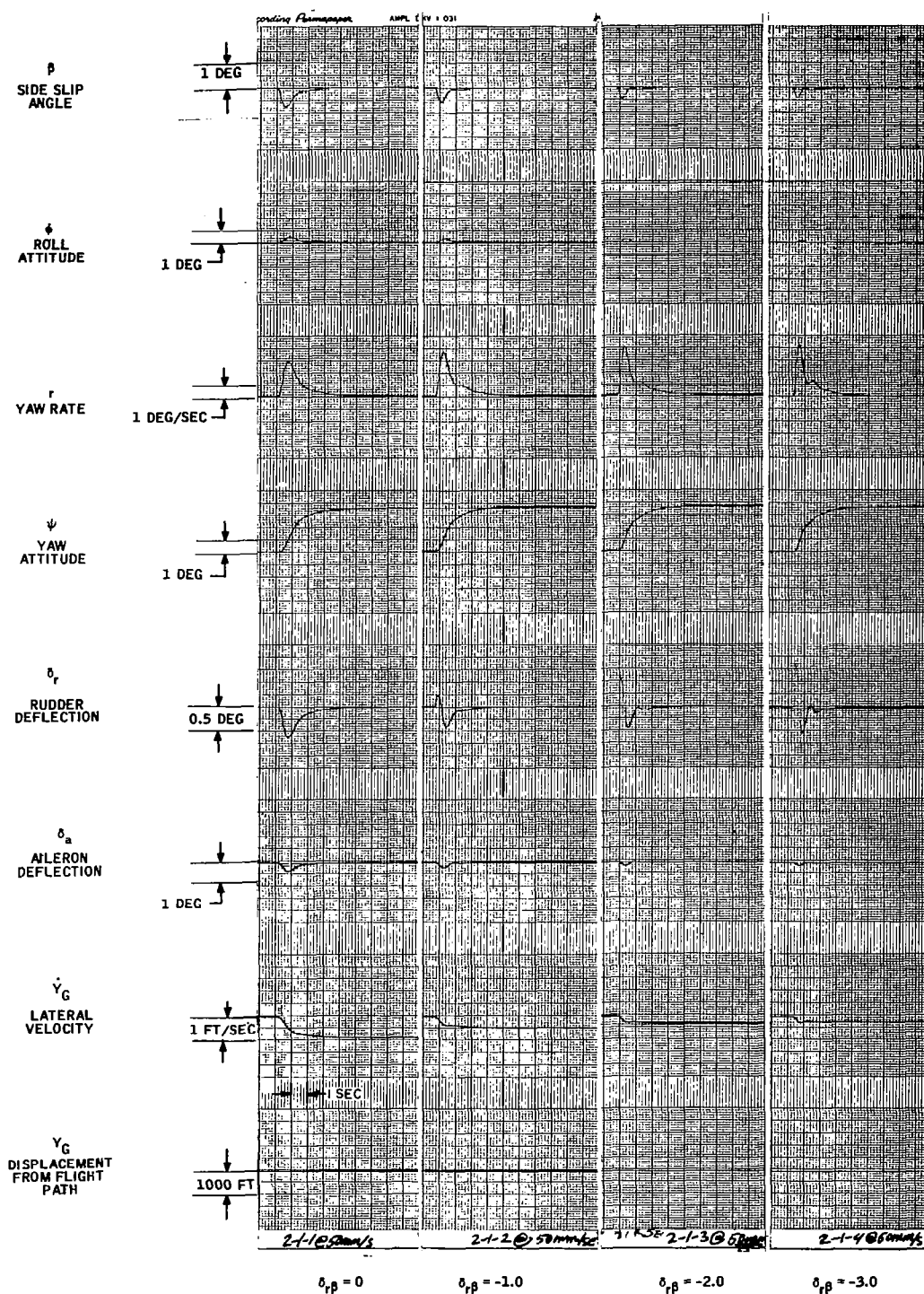
Figure 15. Roll Attitude Control with Sideslip Feedback to Rudder (B2) - Response to 20-fps Step
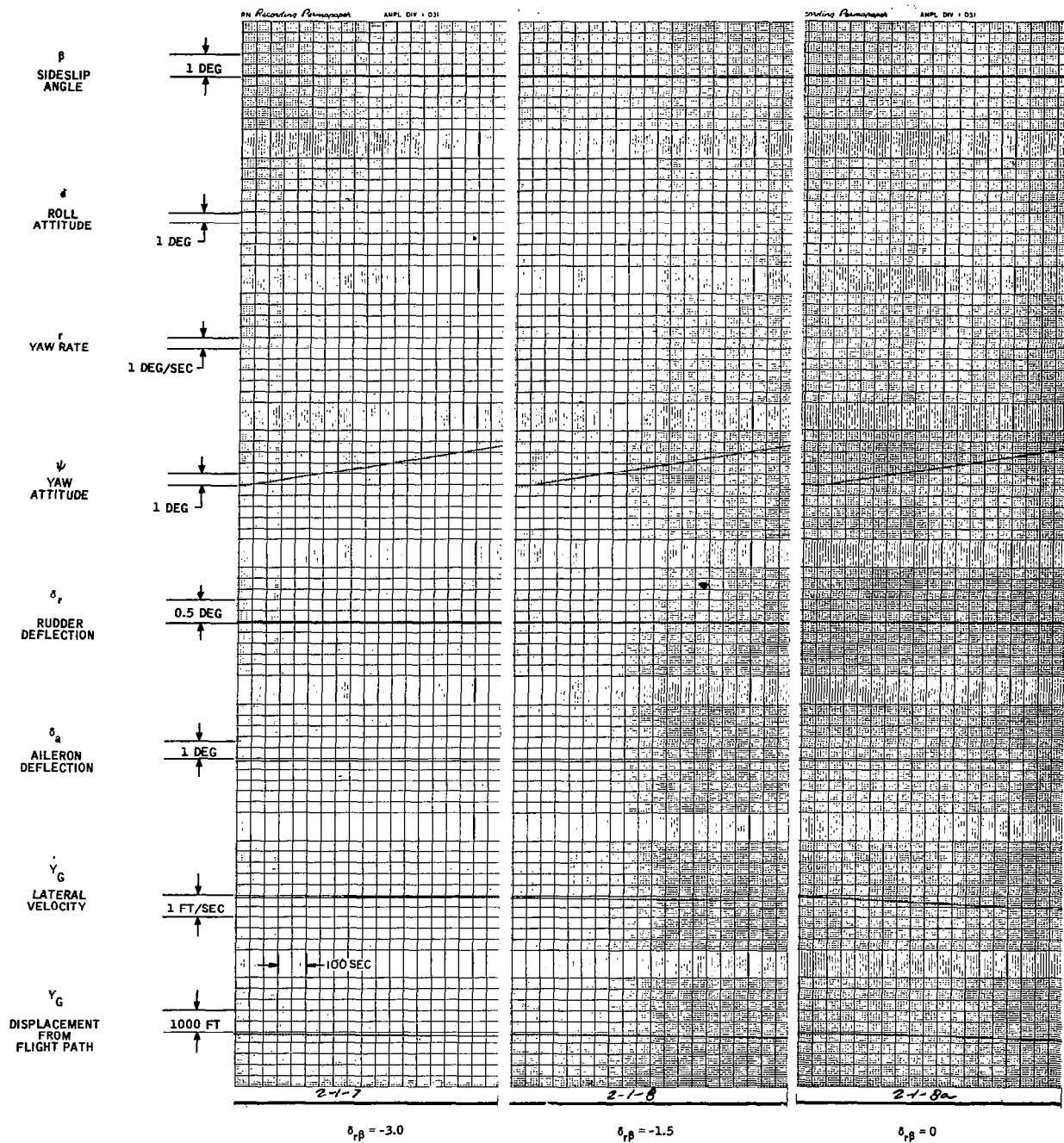
Figure 16. Roll Attitude Control with Sideslip Feedback to
Rudder (B2) - Response to 20 fps/15 min Ramp

36
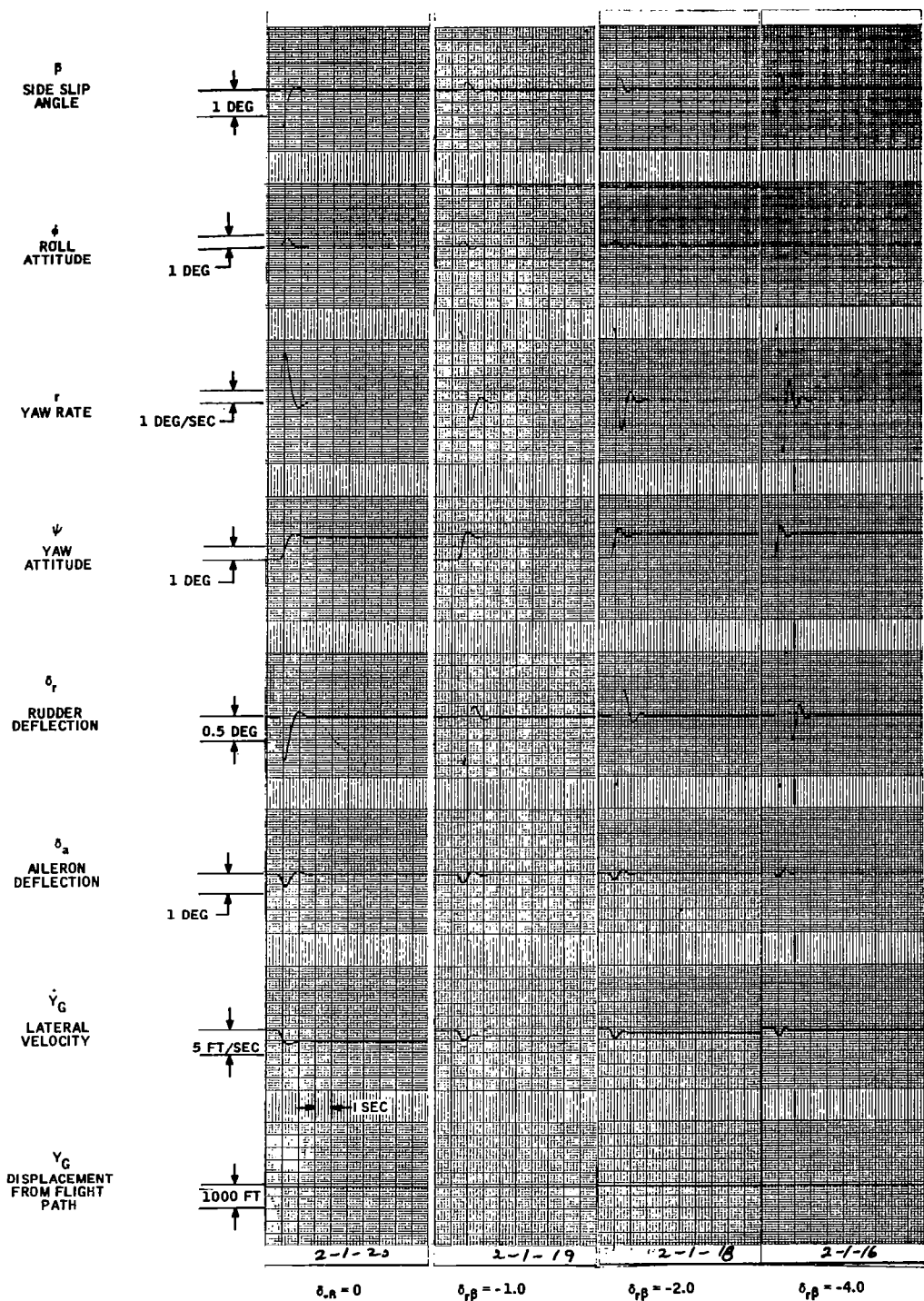
Figure 17. Roll Attitude Control with Sideslip Feedback to
Rudder (B2) - Short-Term Response

In this response, $\delta_{r\beta}$ was varied from 0 to -0.4. It can be seen from Figure 15 that the error in ψ_{ss} is reduced as $|\delta_{r\beta}|$ is increased. The value of ψ_{ss} read from the traces for $\delta_{r\beta}$ = -0.4 compares closely to the computed value given above.

From Figure 17, it is seen that increasing sideslip feedback decreases yaw damping. This is a disadvantage, since attempting to restore the value of yaw damping by increasing $\underline{N}_r$ increases the error in ψ_{ss} (as seen in Concept B1).

There is a net gain in damping in the process, however, since the damping factor is inversely proportioned to the square root of $\underline{N}_\beta$ but directly proportioned to $\underline{N}_r$.

Roll Attitude with Sideslip to Aileron (B3)

This configuration is produced by adding a sideslip to aileron feedback path to the Roll Attitude Control configuration (B1). This configuration is shown in Figure 18.
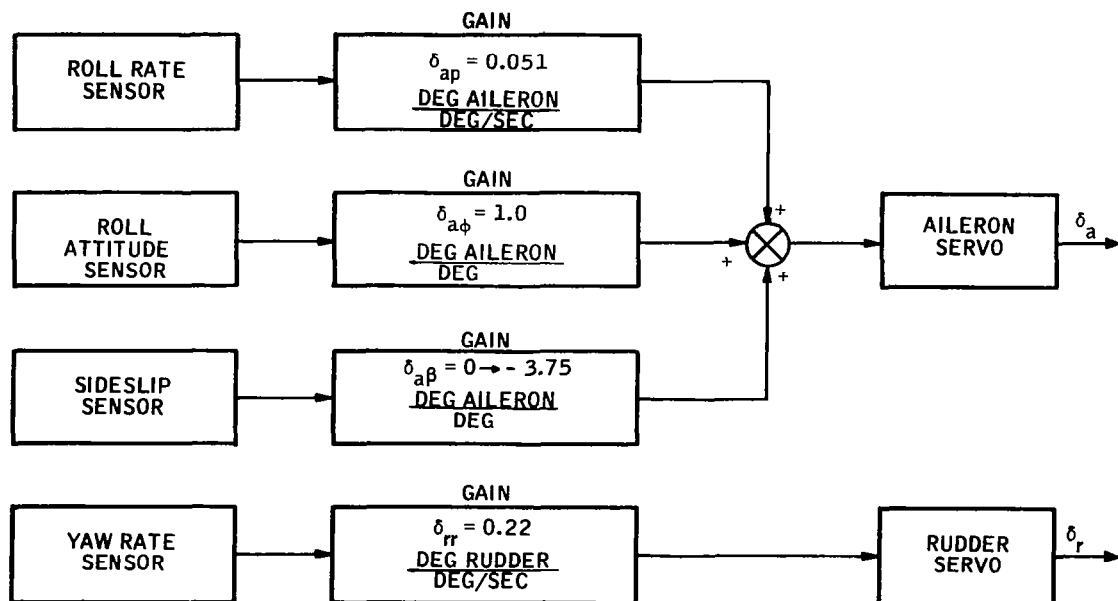
Figure 18. Roll Attitude Control with Sideslip
Feedback to Aileron (B3)

38

Feedbacks of sideslip to aileron modifies L_β (see Appendix B) and can be used to eliminate the error in ψ_{ss} completely for a given flight condition and set of autopilot gains.

For this configuration, the error in ψ_{ss} can be expressed as

$$\epsilon_{\psi_{ss}} = \frac{\beta_o \left[\underline{N}_r K_\phi Y_v + \frac{g}{U_1} (\underline{N}_\beta L_r - L_\beta N_r) \right]}{N_\beta K_\phi} \qquad \text{[From Equation (B33)]}$$

The bar under L_β indicates that effective $\underline{L}_\beta$ replaces the unmodified L_β, which exist when sideslip to aileron feedback is not used.

$\underline{L}_\beta$ is related to the sideslip to aileron feedback gain $\delta_{a\beta}$, as follows:

$$\underline{L}_\beta = L_{\delta a} \delta_{a\beta} + L_\beta$$

It can also be seen from Equation (B33) that by satisfying the relationship

$$\underline{N}_r K_\phi Y_v + \frac{g}{U_1} (N_\beta L_r - L_\beta \underline{N}_r) = 0 \qquad (4)$$

$\epsilon_{\psi_{ss}}$ can be made equal to zero.

For cruise conditions and the autopilot gains of Figure 18, Equation (4) is satisfied by making:

$$\underline{L}_\beta = 85.6$$

or

$$\delta_{a\beta} = 2.96$$

39

The response of this configuration to a 20-fps step and a 20-fps/15-min ramp in lateral wind are shown in Figures 19 and 20. The short-term step input response to an expanded time scale, is shown in Figure 21. The value of $\delta_{a\beta}$ was varied from 0 to -3.75.

It can be seen from Figure 19 that the value $\delta_{a\beta}$ necessary to cancel all errors in ψ_{ss} is near -3.0, which is in agreement with the computation performed above.

From Figure 21 it can be seen that with $\delta_{a\beta}$ at -3.0, the yaw damping has not been materially decreased.

Roll Attitude with "Servoed Sideslip" to Aileron (B4)

This configuration was originally conceived as a means of providing a biased heading hold. It was visualized as containing a sideslip sensor mounted on a platform that was servoed to heading and provided a feedback signal to the aileron. In addition, a heading sensor signal was sent directly to the aileron.

In addition to these feedbacks, the roll attitude hold and yaw damping loops of the preceding "Tight Roll" configuration were employed. A block diagram of this configuration is shown in Figure 22.

After some analysis and anlog computer experience, it became clear that the signal generated by the platform-mounted sideslip sensor (servoed sideslip signal) under ideal conditions, is equal to

$$\beta \cdot \delta_{a\beta_s} + \psi\delta_{a\psi_s}$$

Therefore, the sum of the servoed sideslip sensor and the heading sensor signal could be expressed as

$$\beta \cdot \delta_{a\beta_s} + \psi(\delta_{a\psi_s} + \delta_{a\psi})$$
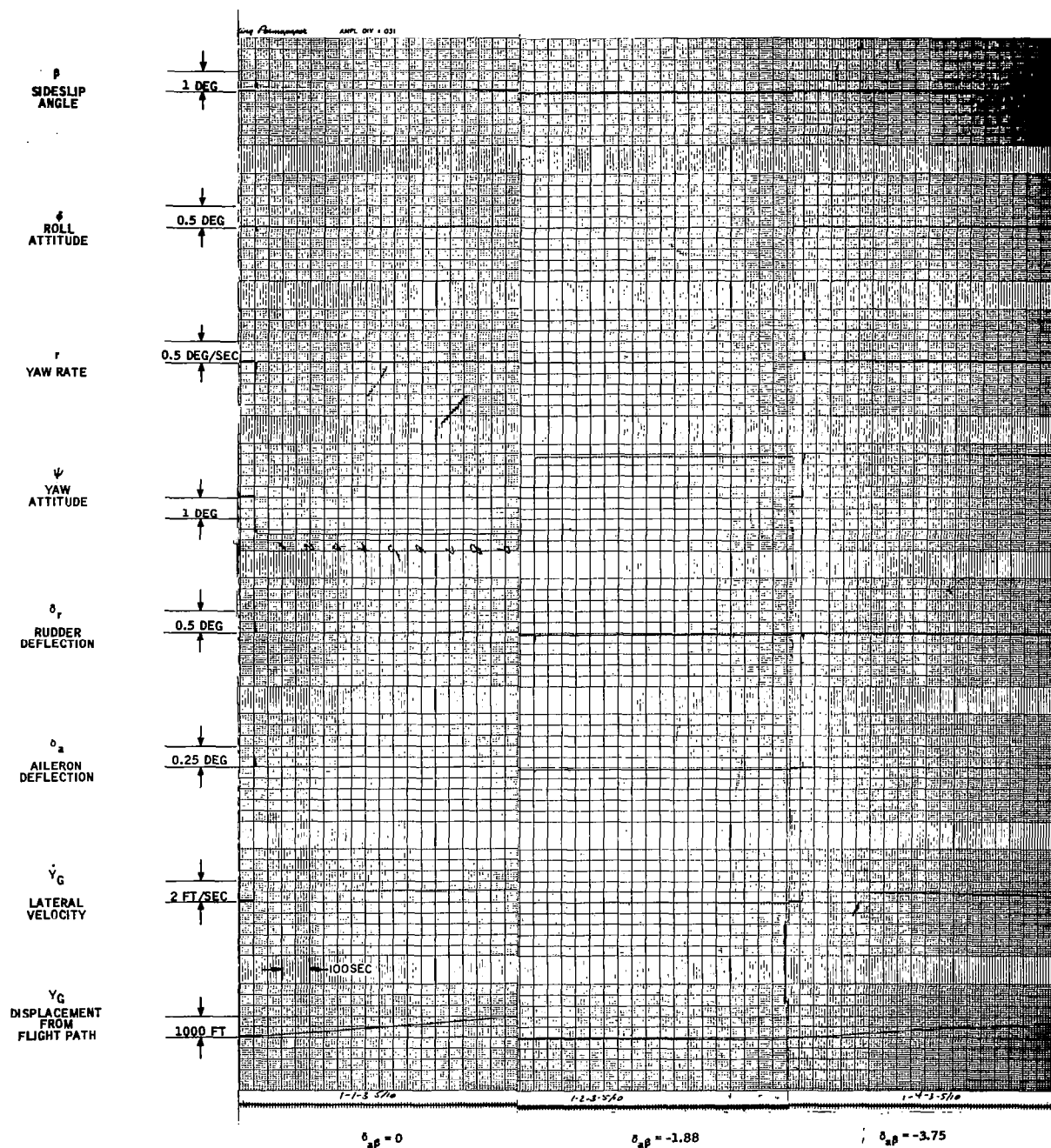
Figure 19. Roll Attitude Control with Sideslip Feedback to
Aileron (B3) - Response to 20-fps Step

41
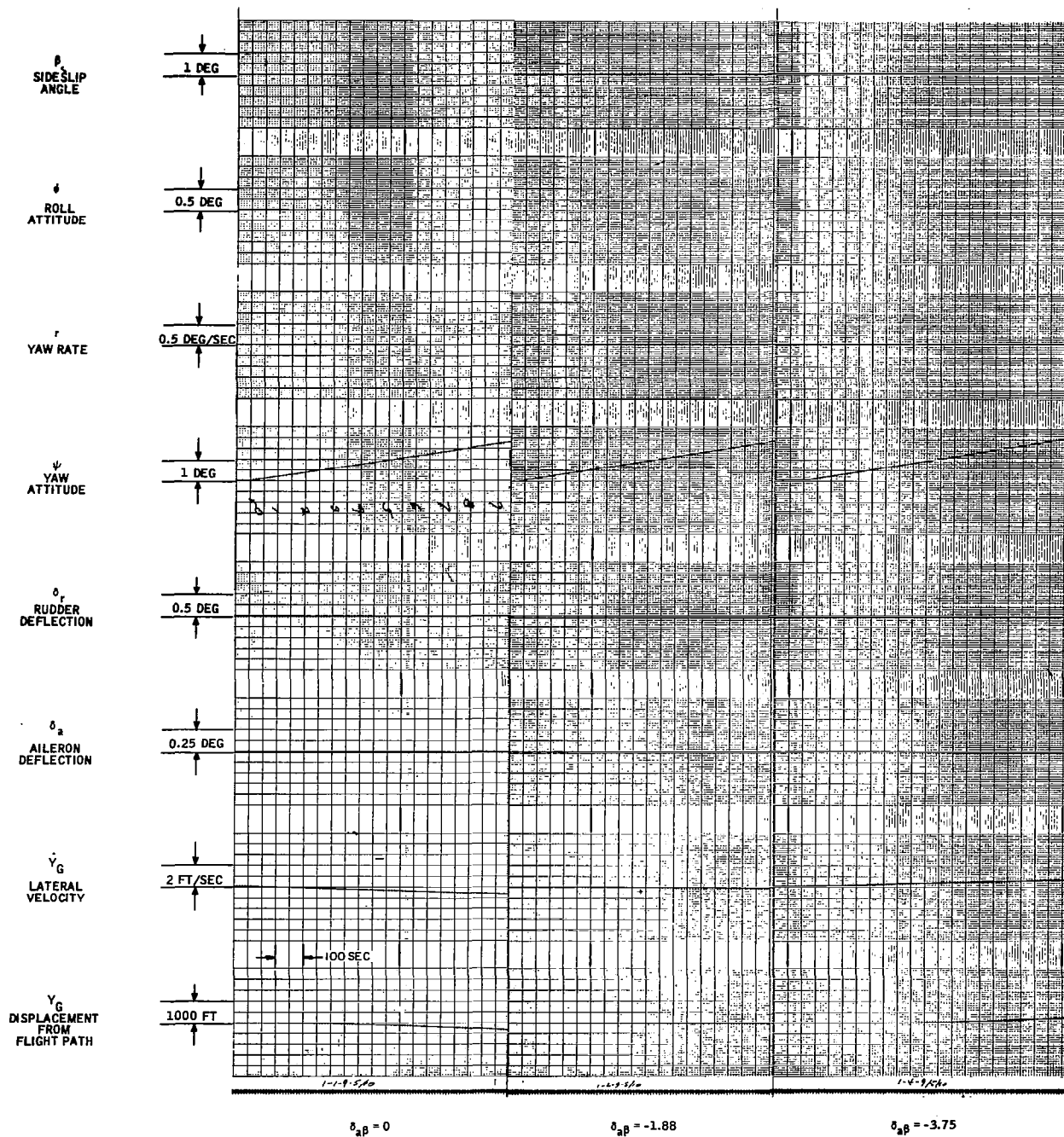
Figure 20. Roll Attitude Control with Sideslip Feedback to
Aileron (B3) - Response to 20 fps/15 min Ramp

42
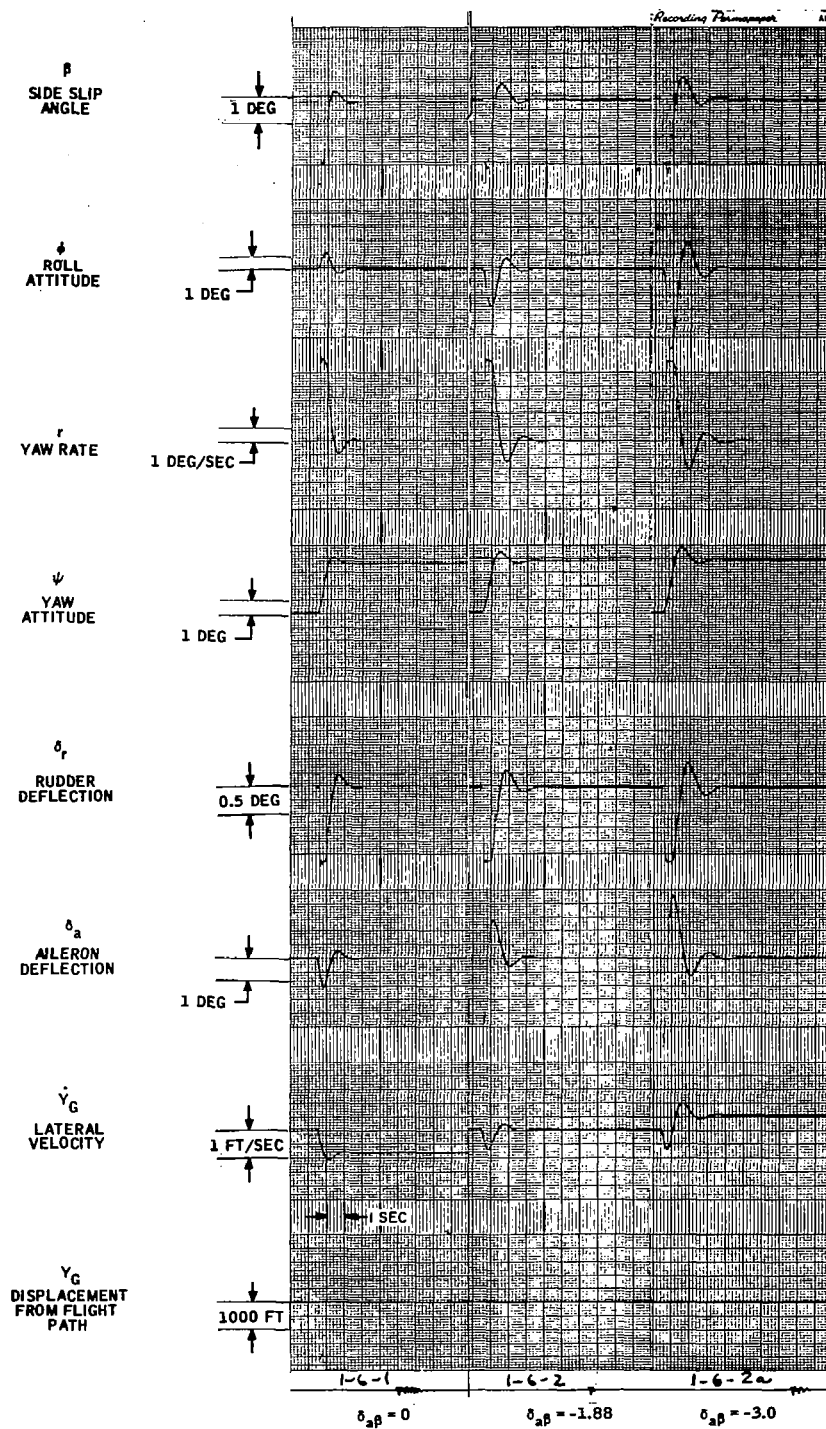
Figure 21. Roll Attitude Control with Sideslip Feedback to
Aileron (B3) - Short-Term Response

Figure 22. Roll Attitude Control with "Servoed Sideslip" Feedback to Aileron (B4)

$*_\epsilon = 0 > 0.2$

44

This relation suggests that the configuration is equivalent to one which contains a conventionally-mounted sideslip sensor (i.e., fixed to the aircraft) and that the heading gain be adjusted to equal $(\delta_{a\psi_s} + \delta_{a\psi})$ instead of the servoed sideslip sensor of Figure 22. This configuration with the conventionally-mounted sensor is shown in Figure 23.

From Figure 22, it is clear that if $\delta_{a\psi} > 0$, the configuration is similar to a conventional heading loop (except that L_β would be modified by the sideslip to aileron feedback). Therefore, after a lateral wind step, the steady-state heading change would be zero for this configuration.

If $\delta_{a\psi} = 0$, then the configuration reduces to "Roll Attitude Plus Sideslip Feedback to Aileron" (see Figure 18). This is borne out by the response traces reproduced in Figure 24. The traces are the response to a 20-fps step in lateral wind for the configuration of Figure 23 with:

$$\delta_{a\beta_s} = -1.0$$

$$\delta_{a\psi_s} = \delta_{a\psi}$$

Compare these to the traces of Figure 19 taken for "Roll Attitude Plus Sideslip to Aileron".

A unique response occurs for the "servoed sideslip" configuration if a threshold of 0.1 degree is added to the roll sensor. In this case, the response to a step in lateral wind does produce a ψ_{ss} that is fairly close to β_o. However, there is an oscillation in roll and yaw that is objectionable . An intuitive explanation for this oscillation is given in Appendix B, Section B4. The frequency and amplitude depend on the amount of sideslip feedback. Response traces for $\delta_{a\psi_s} + \delta_{a\psi} = \epsilon = 0$ and a roll threshold of 0.1 degree is given in Figure 25 for a 20-fps step input and for a 20-fps/15-min ramp.
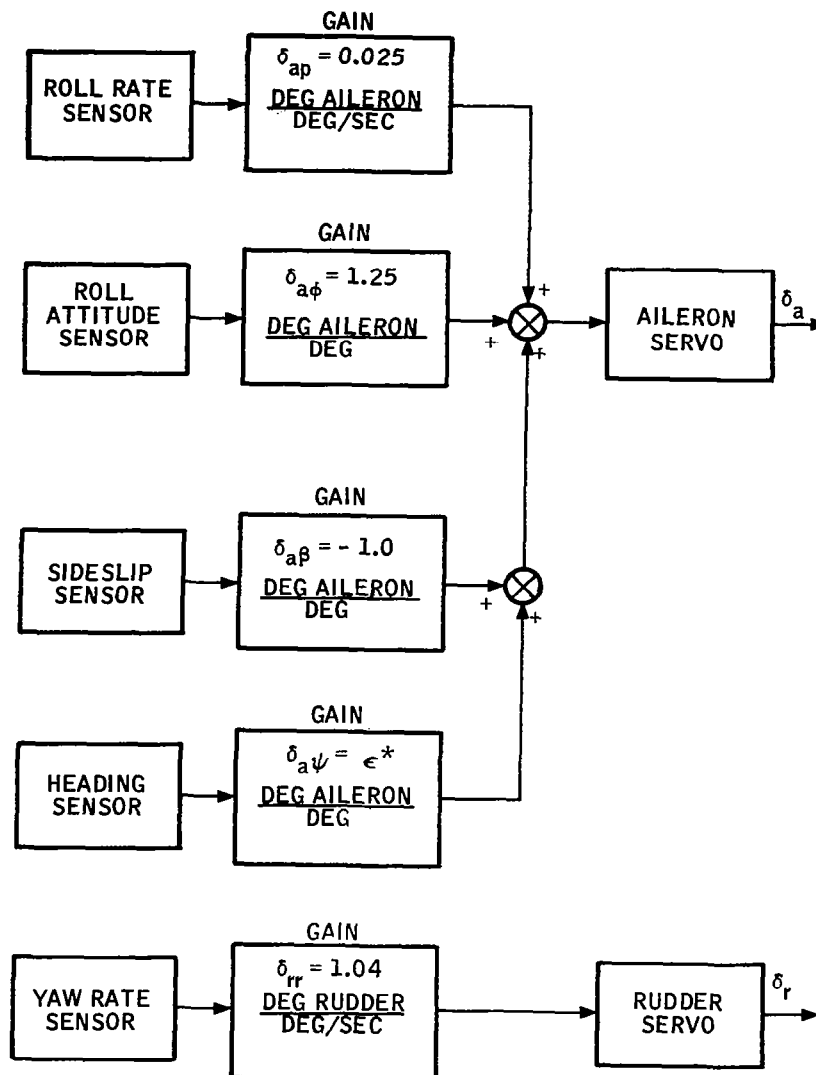
Figure 23.   Tight Roll Control with "Servoed Sideslip"
             Feedback by Conventional Means (B4 alt.)

$*_\epsilon = 0 \rightarrow 0.2$

46
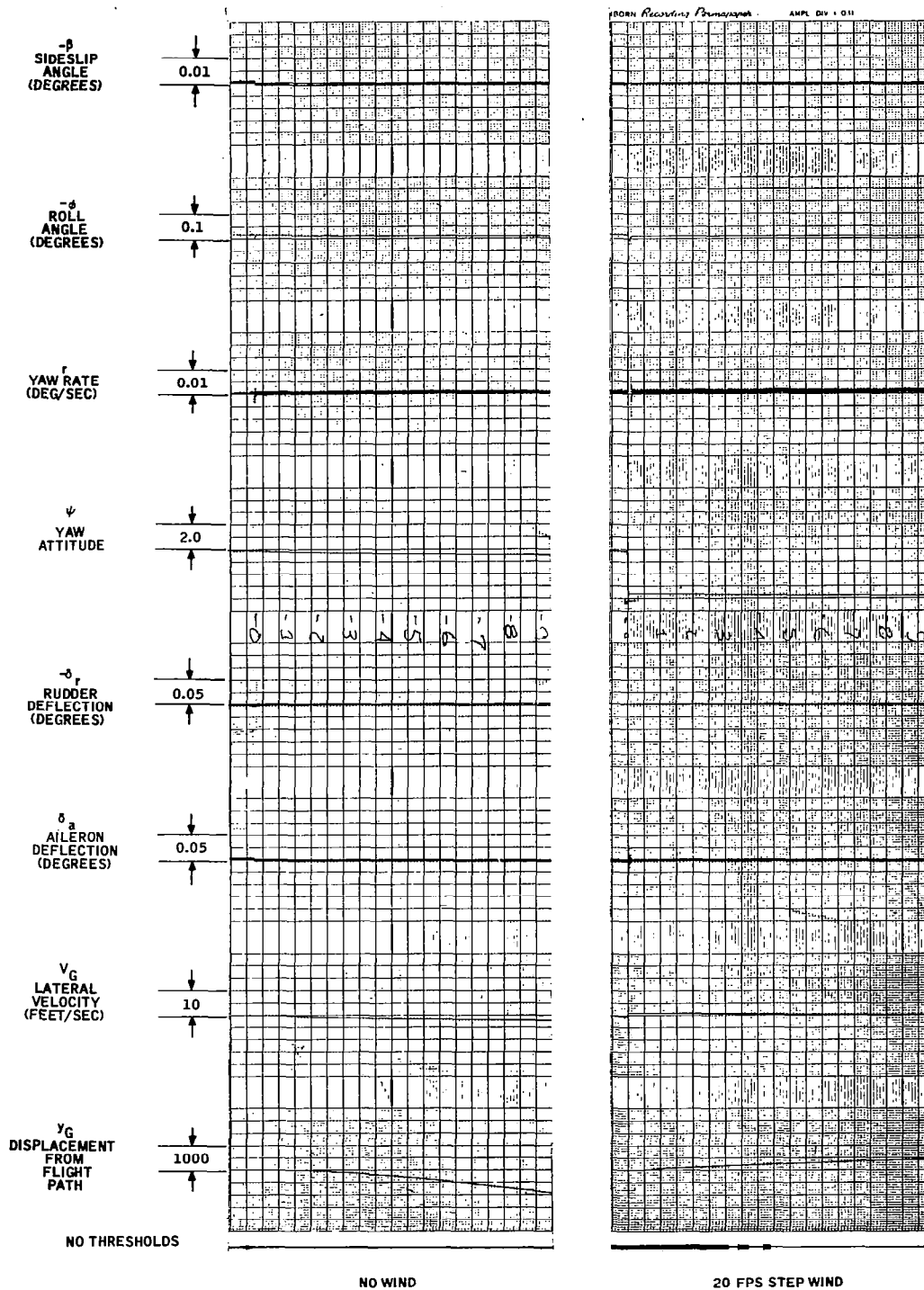
Figure 24. Roll Attitude Control with "Servoed Sideslip"
Feedback to Aileron (B4) - Response to 20-fps Step

47
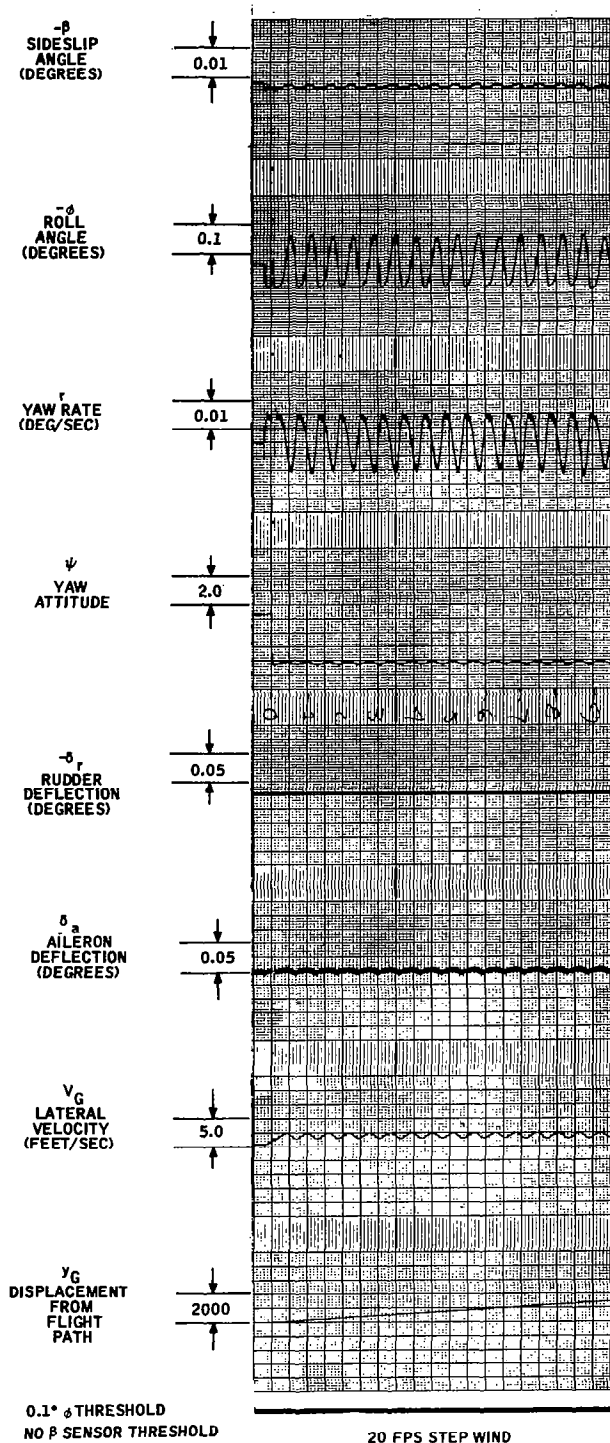
Figure 25. Roll Attitude Control with "Servoed Sideslip" Feedback to Aileron (B4) - 0.1-degree Roll Attitude Sensor Threshold - Response to 20-fps Step

From Figure 25, the error in 15 minutes appears to be about 1000 feet for the 20-fps step. The limit cycle is seen to consist of a roll amplitude of 0.1 degree and a yaw amplitude of 0.2 degree with a period of 50 seconds.

(It is important to note that the limit cycle also is attainable with the preceding configuration, "Roll Attitude Plus Sideslip to Aileron", if a roll attitude sensor threshold is introduced and the sideslip feedback gain increased beyond the point where spiral divergence occurs when the roll angle is less than the threshold.)

This seems to offer a means of tolerating small roll sensor thresholds provided parameters can be chosen to limit roll and yaw oscillation amplitude and frequency to an acceptable range.

BIASED HEADING HOLD (C)

Unless the airplane lateral axis trim is particularly good, an autopilot will require a heading hold loop for long periods of flight under autopilot control. In these concepts, lateral flight path control is added to an autopilot configuration containing such a heading hold loop.

In each of these concepts, a signal is computed and added to the heading command to cause a change in the yaw angle proportional to the change in the cross-course component of wind. The resulting change in the yaw angle is of an amount necessary to maintain the aircraft on its original straight-line flight path.

In the first concept discussed, "Heading Hold Biased by Side Velocity" (C1), side velocity is computed by summing all the components of sideforce as computed from sensor outputs and then integrated to obtain side velocity.

In the second concept (C2), sideslip angle alone is integrated and used as a heading bias. The original motiviation was to obtain in this way an approximation of side velocity, since the sideslip angle under some conditions is the major contributor to side force. However, as shown in Appendix B, Section C2, autopilot gains can be chosen so that when the integral of sideslip angle is forced to zero following a step change in cross-course wind, the airplane will have yawed sufficiently to compensate for the wind change.

Heading Hold Biased by Side Velocity (C1)

Side velocity is computed by integrating the sum of sideslip, roll rate, roll attitude, yaw rate and rudder deflection. This side velocity is summed with heading error and provides the feedback to the rudder servo. A yaw rate damper is also provided. The roll axis feedbacks consist of roll attitude and roll rate. Autopilot gains are selected to provide reasonable heading response and roll and yaw damping. A block diagram of the system is shown in Figure 26.

The principle of operation of this concept is to compute the yaw angle change necessary to maintain a straight-line path when there is a step change in the cross-course wind velocity. This quantity is then used to "bias" the heading command.

This amount of yaw angle change is the aircraft's side velocity divided by the longitudinal velocity. Since the longitudinal velocity can be assumed to be constant (for a given flight condition) the heading "bias" is proportional to the side velocity.

Appendix B, Section C1, develops the relationships between the side velocity gain to rudder, δ_{rv}, and the yaw gain to rudder, $\delta_{r\psi}$, for theoretically perfect flight path control. This relationship is

$$\delta_{rv} = - \frac{\delta_{r\psi}}{U_1}$$

where U_1 is the aircraft longitudinal velocity.
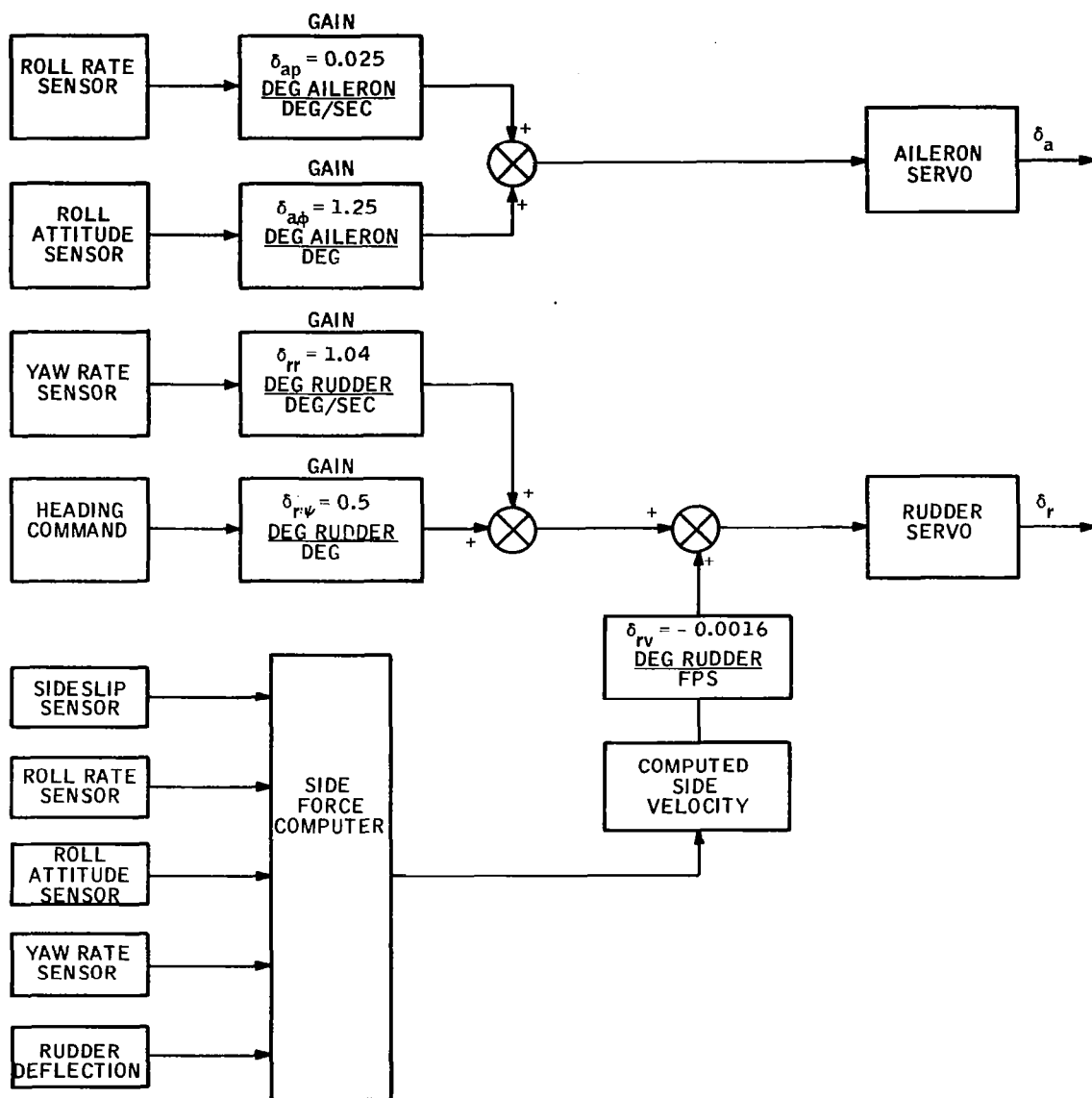
Figure 26. Heading Hold Biased by Side Velocity (C1)

The same flight performance can be expected if the heading error and side velocity are introduced in the aileron channel (rather than the rudder).

The analog recordings of the response of this configuration to a 20-fps step in lateral wind are shown in Figure 27. The lateral deviation from the flight path is seen to be less than 200 feet in 15 minutes of flight time.

Theoretically the error should be zero (see Appendix B). The discrepancy between theoretical and simulation results are well within instrumentation and setup errors.

Heading Hold Biased by Integral of Sideslip (C2)

In this configuration, the integral of sideslip replaces the side velocity feedback used in the preceding concept. The block diagram is shown in Figure 28.

In Appendix B, Section C2, it is shown that forcing the integral of sideslip developed during the response to a step change in lateral wind to zero will cause the aircraft to yaw almost the correct amount to compensate for the wind change. Forcing the integral of sideslip to zero in this configuration requires opening the heading loop.

For theoretically perfect compensation, some heading feedback is required. The ratio of heading gain, $\delta_{r\psi}$, to the "integral of sideslip" gain, $\delta_{r\beta}$, however, is about 1 to 100 for perfect compensation (see Appendix B, Page B31).

However, ratios of $\delta_{r\psi}$ to $\delta_{r\beta}$ = 0.1 also give acceptable performance as shown by the following computation. The value of ψ_{ss} is computed for cruise condition from Equation (B40). The following gains are employed:
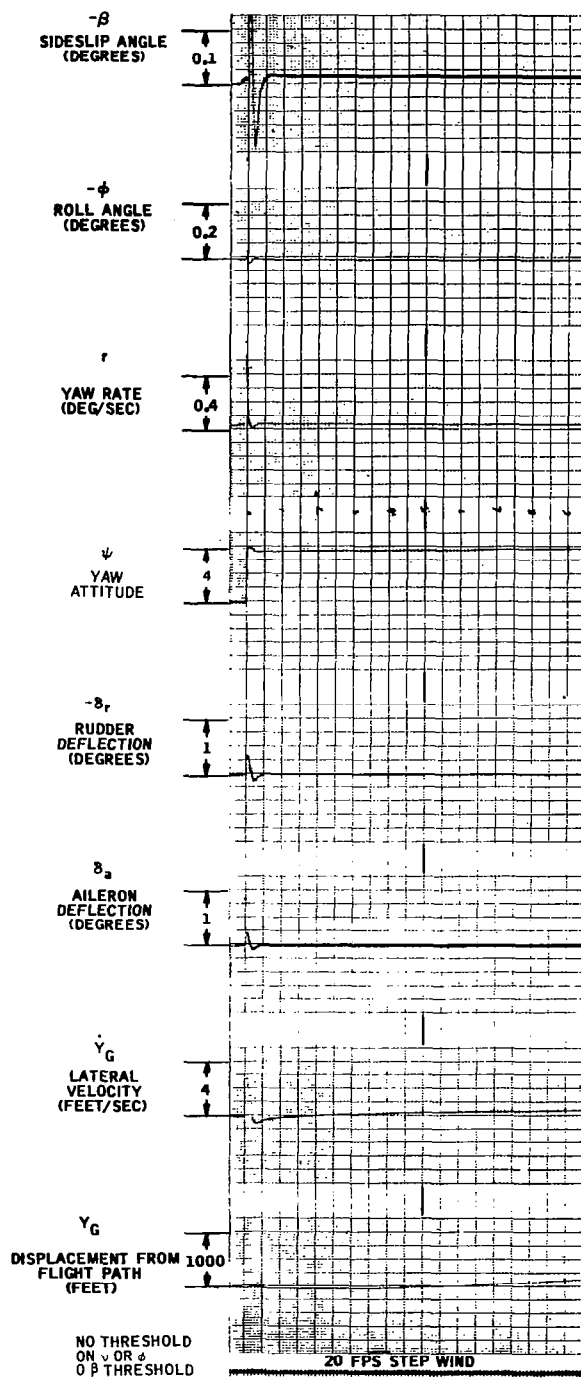
Figure 27. Heading Hold Biased by Side Velocity (C1)
- Response to 20-fps Lateral Wind Step

53

GAIN
ROLL RATE SENSOR
$\delta_{ap} = 0.25$
$\dfrac{\text{DEG AILERON}}{\text{DEG/SEC}}$

GAIN
ROLL ATTITUDE SENSOR
$\delta_{a\phi} = 1.25$
$\dfrac{\text{DEG AILERON}}{\text{DEG}}$

AILERON SERVO δ_a

GAIN
YAW RATE SENSOR
$\delta_{rr} = 1.04$
$\dfrac{\text{DEG RUDDER}}{\text{DEG/SEC}}$

GAIN
HEADING COMMAND
$\delta_{r\psi} = 0.5*$
$\dfrac{\text{DEG RUDDER}}{\text{DEG}}$

RUDDER SERVO δ_r

SIDESLIP SENSOR

SIDESLIP INTEGRATOR

GAIN
$\delta_{r\beta\,INT} = -0.5$
$\dfrac{\text{DEG RUDDER}}{\text{DEG}}$
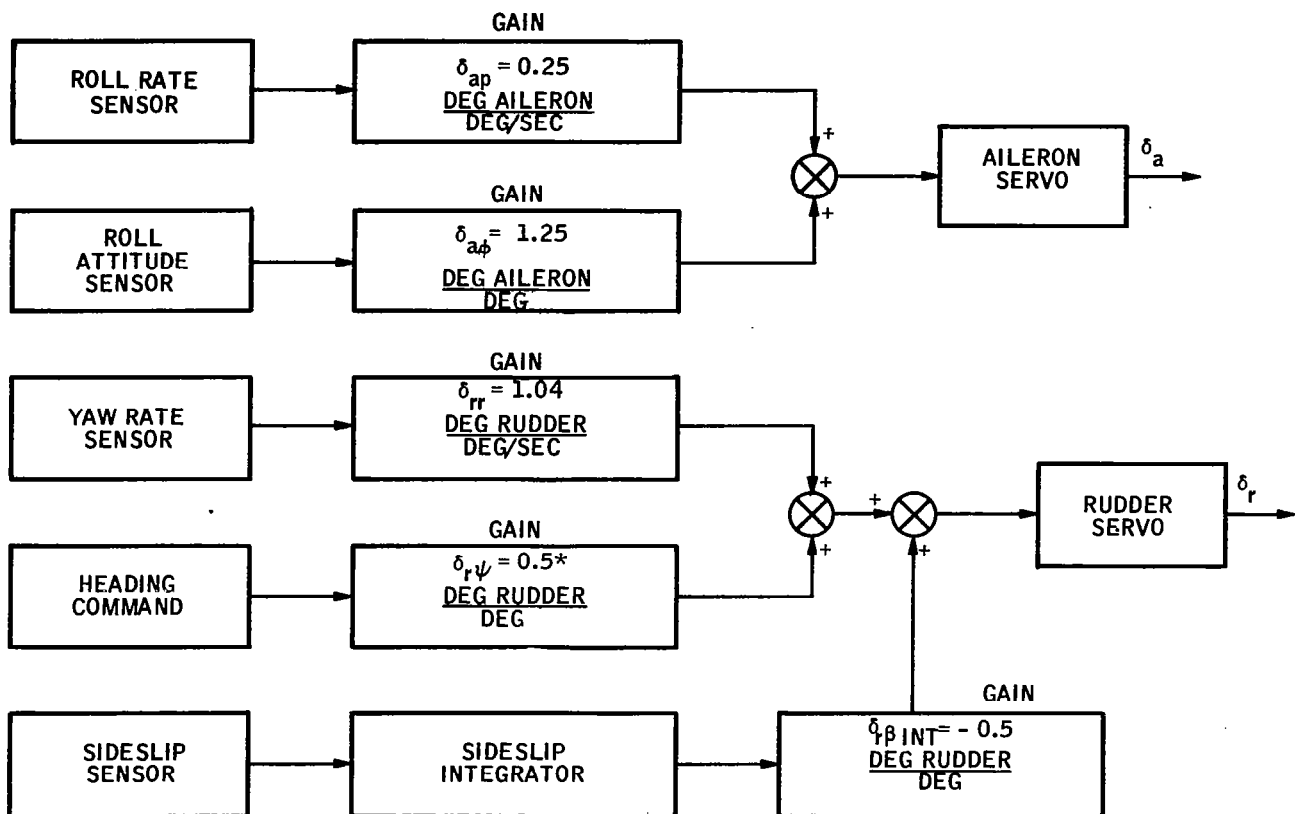
* $\dfrac{\delta_{r\psi}}{\delta_{r\beta}}$ IS - 1; AS USED FOR RESPONSES OF FIG. 29
SHOULD BE -0.1 FOR ACCEPTABLE PERFORMANCE
(i.e. $\delta_{r\psi}$ SHOULD BE 0.05)

Figure 28. Heading Hold Biased by Integral of Sideslip (C2)

$$\delta_{a\phi} = 1.25 \text{ or } K_\phi = L_{\delta a} \delta_{a\phi} = -46.0$$

$$\delta_{r\beta} = -0.5 \text{ or } K_\beta = N_{\delta r} \delta_{r\beta} = 7.12$$

$$\delta_{r\psi} = 0.05 \text{ or } K_\psi = N_{\delta r} \delta_{r\psi} = -0.712$$

From which we obtain

$$\psi_{ss} = 0.93 \beta_o$$

For a 20-fps step ($\beta_o = -0.064$ rad), we have

$$\psi_{ss} = -0.0595 \text{ rad} = -3.40 \text{ degrees.}$$

The lateral deviation in 15 minutes from Equation (2) is

$$\varepsilon_{Y_G} = (\psi_{ss} - \beta_o) U_1 T = 485 \text{ feet.}$$

The responses of Figure 29 were taken with the gains of Figure 28. It will be noted that

$$\frac{\delta_{r\psi}}{\delta_{r\beta}} = -1.0$$

in this configuration. The computed value for ψ_{ss} with these gains is

$$\psi_{ss} = 0.71 \beta_o$$

or, for a 20-fps step

$$\psi_{ss} = -0.0456 \text{ rad} = -2.62 \text{ degrees.}$$
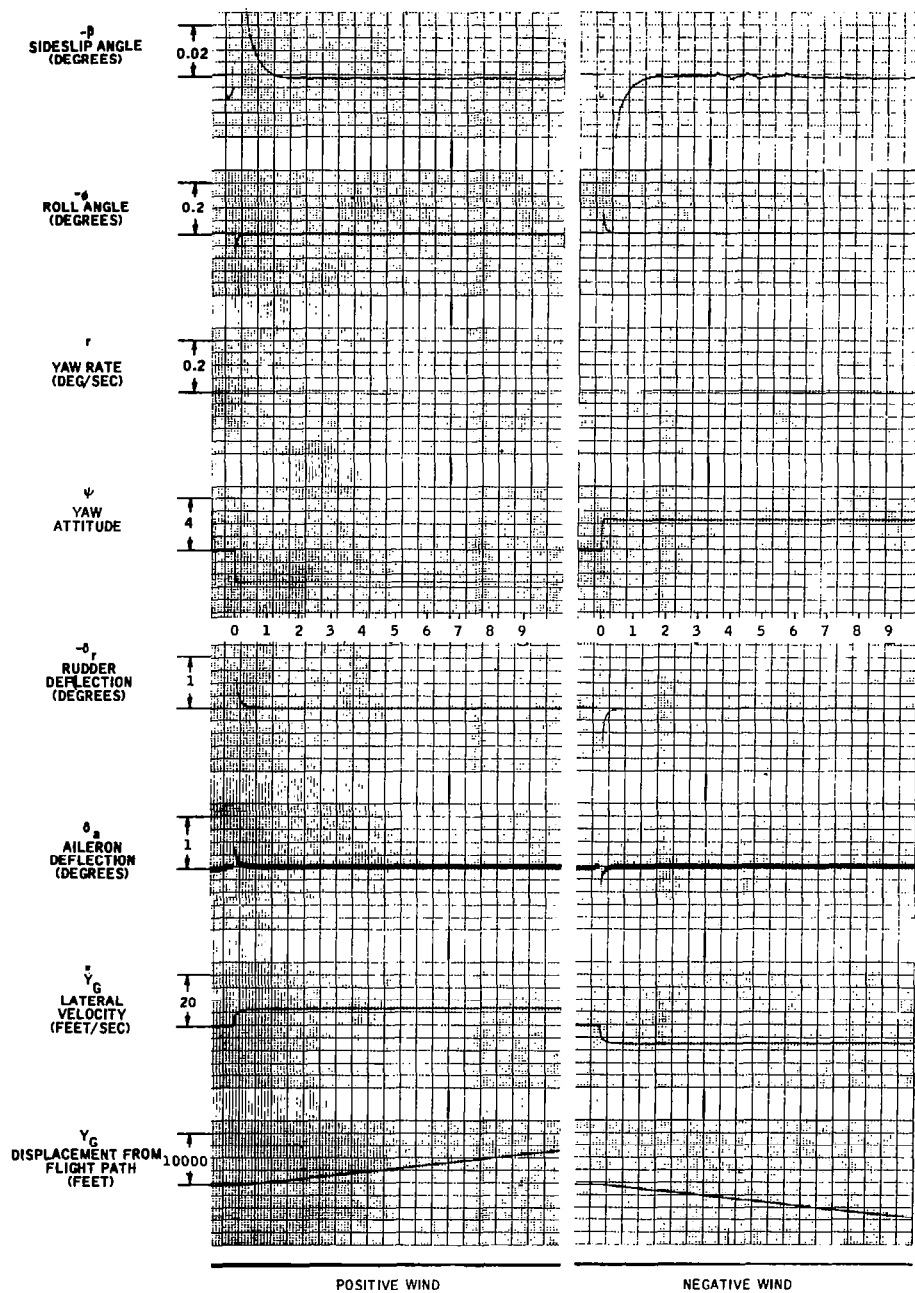
Figure 29. Heading Hold Biased by Integral of Sideslip (C2)
- Response to ±20 fps Lateral Wind Step

In 15 minutes this would yield a lateral deviation of

$$\epsilon_{Y_G} = 5220 \text{ feet}$$

which is unacceptable. The recordings of Figure 29 agree closely with these values.

It is seen that $\dfrac{\delta_{r\psi}}{\delta_{r\beta}}$ should be made as small as possible, to meet flight path control requirements.

DUAL MODES (D)

The "Dual Mode" flight path control configurations provide another way of adding flight path control to an autopilot which also has a heading hold loop.

In the Dual-Mode approach, as in the Biased Heading Hold concepts, a "heading bias" equal to an amount required to compensate for a change in cross-course wind conditions is generated and added to a heading command signal.

The differences are: (1) in the Dual-Mode approach, the required bias is "computed" by letting the airplane weathercock into the wind, when the onset of a wind change is detected, rather by an explicit computation such as is used in the "Biased Heading Hold" concepts; (2) the "computed" bias is "remembered" by means of a heading synchronizer rather than by the use of an integrator. Therefore, the Dual-Mode approach offers alternatives that are perhaps easier to mechanize than the computation and integration employed in the Biased Heading concepts.

A "wind detector" and switching must be provided to switch from a conventional heading mode to a "weathercocking" mode at the onset of a lateral wind change. The switching must also actuate the synchronizer so that the yaw change due to "weathercocking" is stored, and then re-engage the heading mode. A representative dual mode configuration is shown in Figure 30.
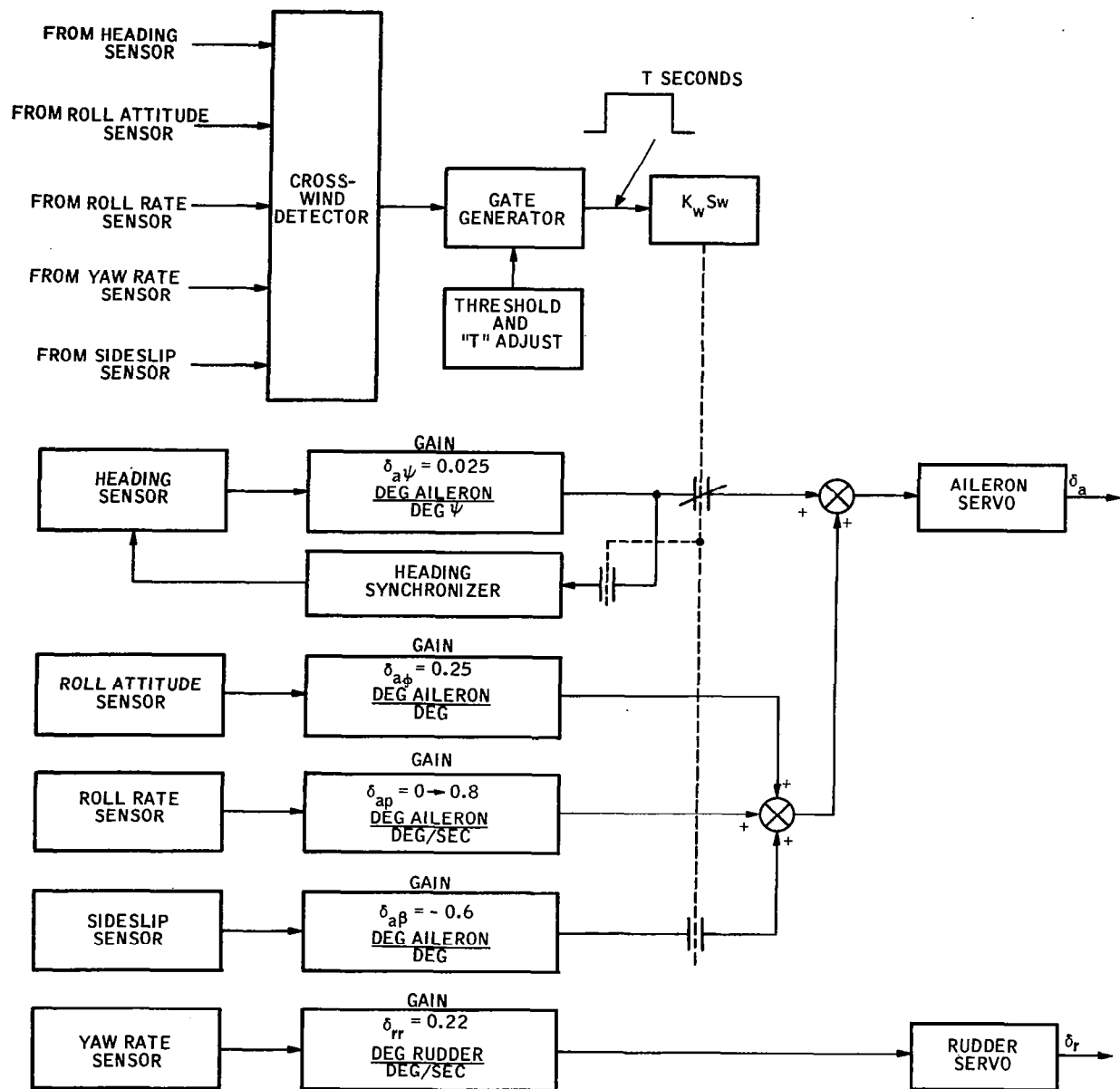
Figure 30. Dual Mode, with Mode Control Shown (D)

A note about the "wind detector": The exact configuration of the wind detector has not been studied, but, in general, we may say that it will merely add sensor outputs already required for the heading loop mode. In addition, we may safely say that it can be allowed much greater gain tolerances and is more tolerable of sensor error sources that the sideslip or side force integrators of the Biased Heading Hold concepts.

In the practical situation, it is expected that there will be the capability to manually vary the "wind detector" threshold and the width of the gate (as indicated in Figure 30) to optimize performance for prevailing wind conditions.

The "weathercocking" mode is one of the single-axis or tight roll configurations discussed under concepts A and B.

The "heading hold" mode used in this study was chosen from the following configurations:

- Heading Loop with Roll Attitude Inner Loop

- Heading Loop with "Wings Leveler" Inner Loop

- Heading Loop with "Wings Leveler" Inner Loop (heading error feedback to rudder)

These are shown in block diagram form in Figures B1, B2, and B3 in Appendix B, Section D.

Appendix B also discusses the performance of each of these loops and indicates the basis used for gain selection. Expressions describing the response of these loops to a lateral wind step are tabulated in Table B1.

59

The four dual-mode configurations discussed in the following subsections are illustrative of many others that can be formed from the three heading loops considered here and the numerous weathercocking modes discussed previously.

The significant factors and potential dual-mode operations are amply demonstrated by combinations chosen, and these represent a gradation in hardware requirements; that is, the first concept requires roll attitude sensor and sideslip sensor, the second dispenses with the roll attitude sensor, and the third with the sideslip sensor.

The success of the dual-mode approach rests on the ability of the weathercocking mode to:

- Cause the proper change in ψ when a step wind occurs

- Maintain this value of ψ until the heading error can be synchronized

In doing this, the weathercocking mode must tolerate:

- A delay of switchover from the heading hold mode

- Initial conditions in ϕ developed by the heading hold mode before switchover

When a "Tight Roll" weathercock mode is employed, the initial condition on ϕ is easily tolerated since the roll attitude loop quickly drives this ϕ to zero without affecting ψ_{ss}.

However, when a weathercocking mode not employing a roll attitude loop is used, then this "initial condition" on ϕ adds directly to the ϕ attained during weathercocking. The rate of change of ψ after the weathercocking transient is proportional to the magnitude of this ϕ. Therefore, when combining a heading mode and a weathercocking mode which does not employ a roll attitude hold loop, the following additional design constants are imposed:

- The heading loop roll response to a wind step input must be minimized (consistent with an acceptable compromise of heading loop response).

- The long-term roll response of the weathercock mode must be made divergent by the appropriate choice of feedback gain effecting spiral divergence criteria.

This will allow the roll angle attained during the weathercock transient to oppose the ϕ developed during the heading hold mode.

In investigating the four dual-mode configurations, a step change in lateral wind was applied to an analog computer simulation which was initially in the heading mode configuration. After a delay, T_D, the configuration is switched to the "weathercock" mode. The delay, T_D represents the time lost in detecting the onset of a lateral wind change in effecting the switchover.

In evaluating the results, we are interested in what the yaw angle or, more directly, the cross-course velocity error $\epsilon_{\dot{Y}_G}$, is at 30 seconds after switchover, since this is a reasonable amount of time to allow for the synchronizer to store the yaw angle change. ($\epsilon_{\dot{Y}_G}$, is much easier to read from the recordings than yaw angle).

For a step in lateral wind, the desired value of Ψ should equal the initial value of sideslip angle, β_o, at the onset of the step change in lateral wind. Maximum acceptable error, for a 20-fps step in lateral wind, in cross-course velocity is $\epsilon_{\dot{Y}_G} = \dfrac{2880 \text{ ft}}{900 \text{ sec}} = 3.2$ fps, since this results in a lateral deviation, ϵ_{Y_G}, of 2880 feet at the end of 15 minutes (see Appendix A).

Dual Mode: Roll Attitude with Sideslip to Aileron (D1)

In this configuration, the heading loop consists of heading error feedback to the aileron with a roll attitude inner loop (such as shown in Figure B1) and a

"weather cocking" mode consisting of roll attitude plus sideslip to aileron (as shown in Figure 18).

This dual-mode configuration is shown in Figure 31. The switching is shown symbolically. The synchronizer, wind detector and gating are not shown. These components are included as shown in Figure 30.
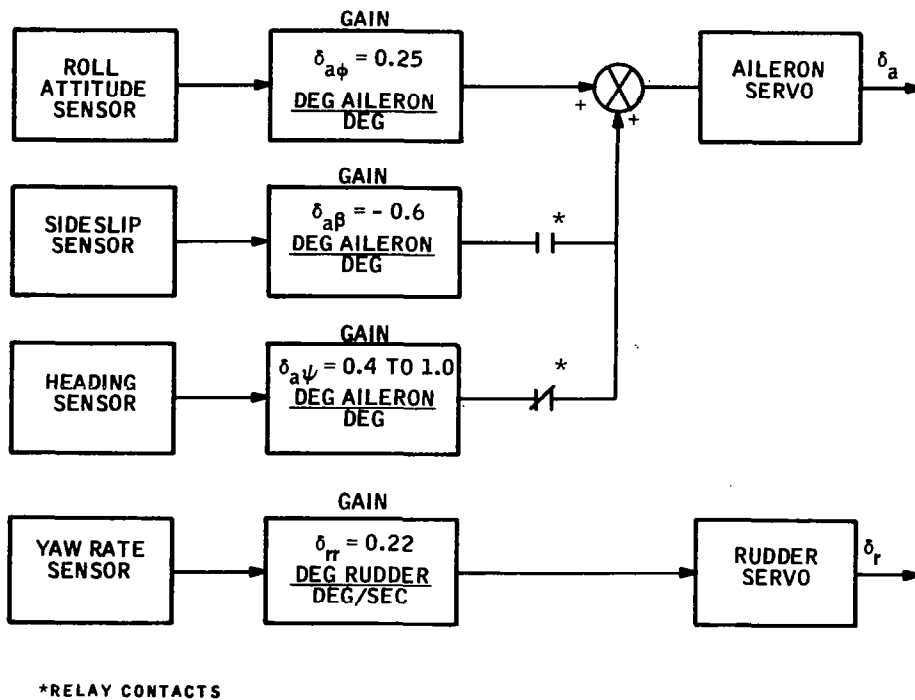
Figure 31.   Dual Mode: Roll Attitude Control with
Sideslip Feedback to Aileron (D1)

Two series of 20-fps step wind response traces were taken for this config-uration with varying delays between the onset of the step and switching to the $\epsilon_{\psi ss}$ weathercock mode. For one set, Figure 32, the heading gain, in degrees of aileron per degree of heading error is $\delta_{a\psi} = 0.4$, and for the second, Figure 33, $\delta_{a\psi} = 1.0$. For both sets, the sideslip feedback gain in degrees of aileron per degree of sideslip angle, is $\delta_{a\beta} = 0.6$, the value
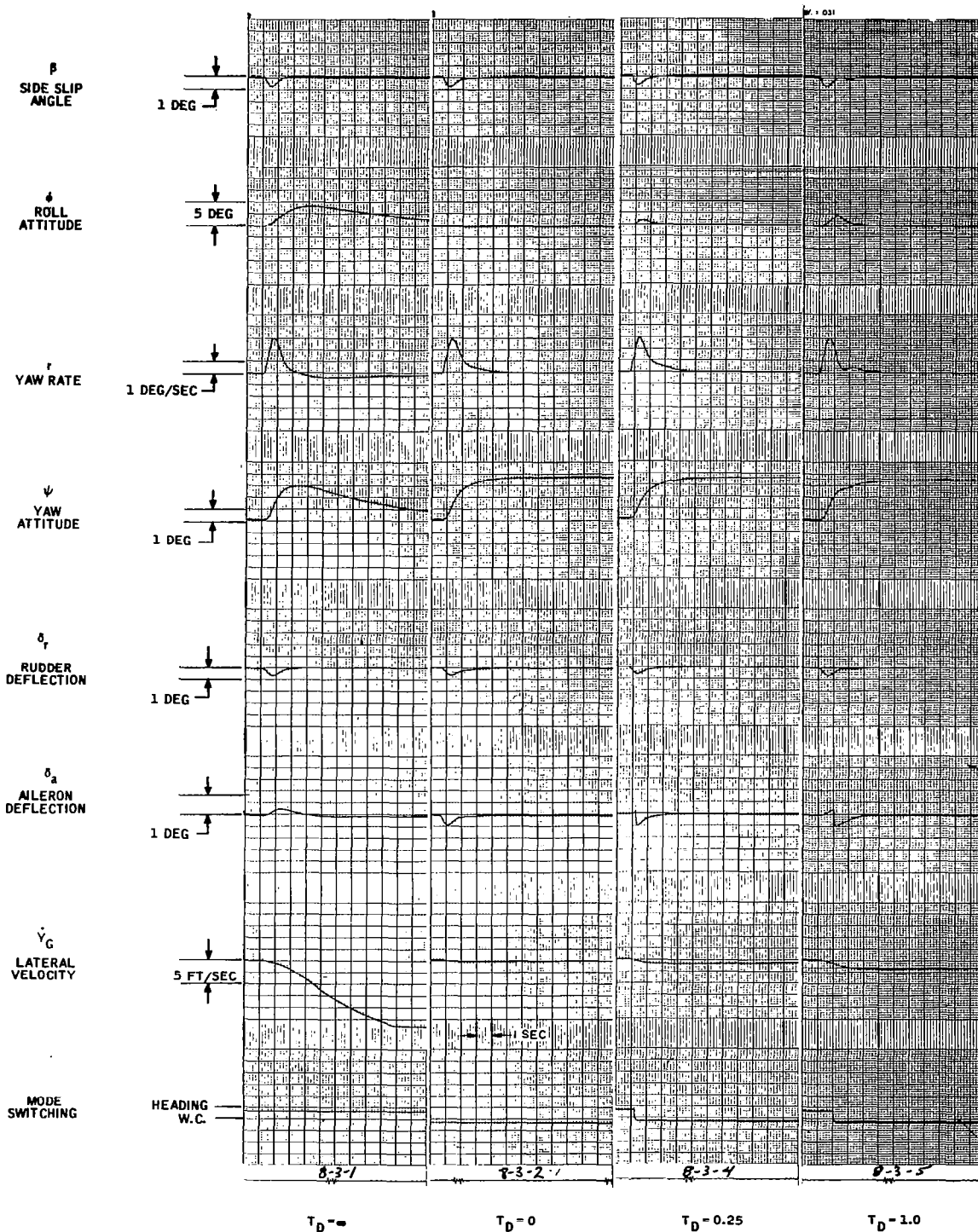
Figure 32. Dual Mode: Roll Attitude Control with Sideslip
Feedback to Aileron (D1) - Response to 20-fps
Step, K_ψ = 4

63
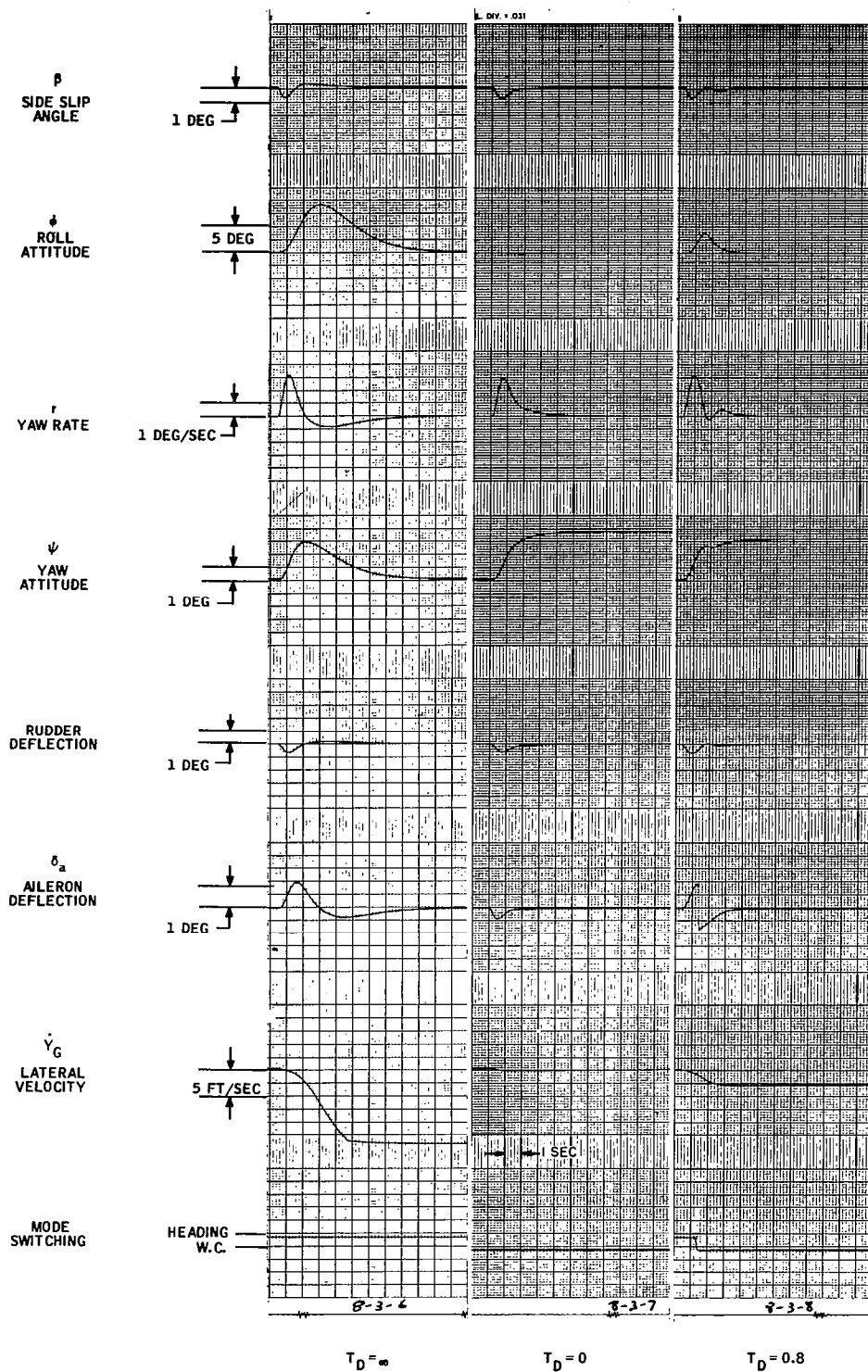
Figure 33. Dual Mode: Roll Attitude Control with Sideslip
Feedback to Aileron (D1) - Response to 20-fps
Step, K_ψ = 10

64

which in the weathercock mode gives an $\epsilon_{\psi_{SS}}$ of zero. The other gains are set at the values shown in Figure 31.

The difference between the series of traces is that, for the larger value of K_ψ, the value of ϕ peak is greater. However, since the weathercock mode contains an attitude hold loop, ϕ, peak is quickly brought to zero without affecting ψ_{SS}.

By interpolating the traces of Figure 32, it can be seen that for 20-fps step, with $T_D = 0.5$, $\epsilon_{\dot{Y}_G}$ at 30 seconds will be about 1-fps.

Extrapolating this error for 15 minutes, by means of,

$$\epsilon_{Y_G} = \epsilon_{\dot{Y}_G} \quad 900,$$

we have

$$\epsilon_{Y_G} = 900 \text{ ft.}$$

Dual Mode: "Wings Leveler" with Sideslip to Aileron (D2)

In this configuration, the heading loop consists of heading error feedbacks to the aileron with a "wings leveler" inner loop. That is, the inner loop consists of yaw rate feedback to the aileron instead of roll attitude feedback. This heading loop is shown by itself in Figure B2 in Appendix B. The weather-cock mode consists of the single-axis flight path configuration A3, (i.e. sideslip to aileron without a roll attitude loop). This dual-mode configuration is shown in Figure 34.
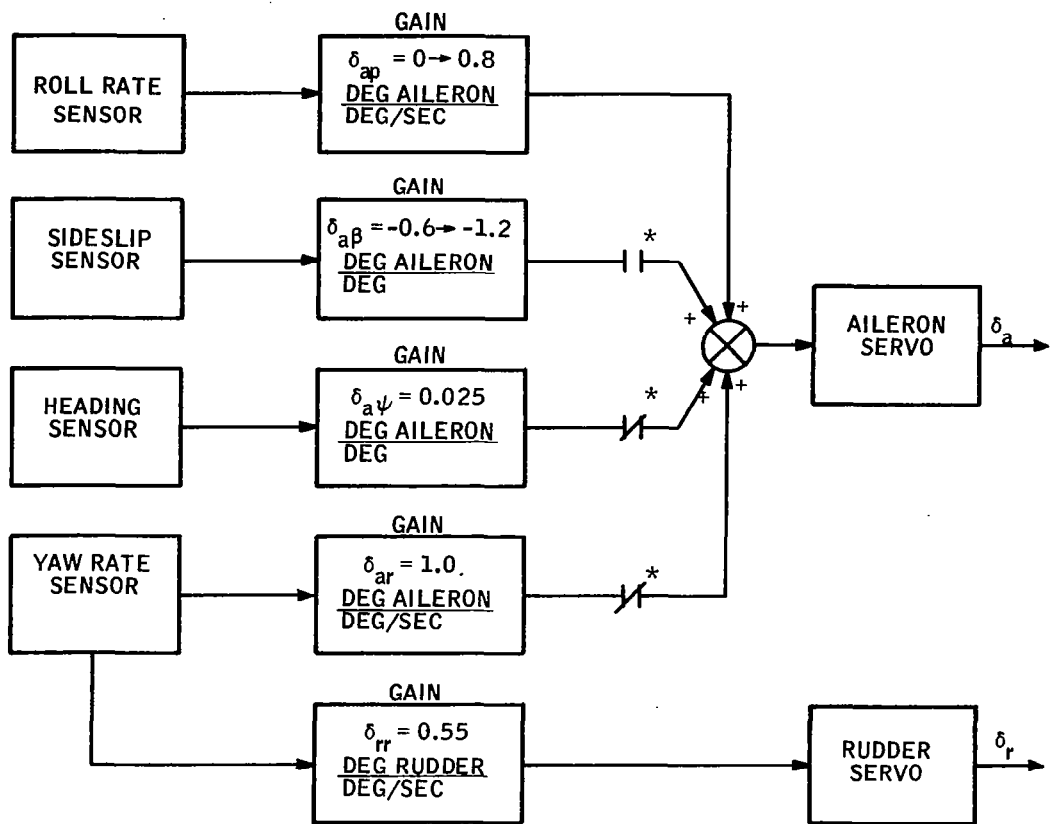
Figure 34. Dual Mode: "Wings Leveler" with Sideslip Feedback
to Aileron (D2)

By means of step response recording, the range of sideslip feedback gain to aileron, $\delta_{a\beta}$ and roll rate gain to aileron, δ_{ap}, necessary for acceptable performance was determined. The tolerance to wind step variation for a given "wind detector" delay was also investigated. These traces are reproduced as Figures 35 through 39.

The first set of gains investigated is based on providing fast heading response in the heading mode and zero roll angle due to weathercocking in the weathercocking mode. Response traces for this configuration, run at various value of delay, are given in Figure 35.

For these traces δ_{ap} = 0 and $\delta_{a\beta}$ = 0.6. From Figure 35, it can be seen that performance is relatively sensitive to switching delay T_D.

By increasing the β feedback, it is possible to use the ϕ attained during the weathercocking mode to cancel ϕ at the time of mode switching and thus reduce the ϕ existing after the weathercock transient. The net result would be to allow longer switching delays, since a large ϕ at switching could be tolerated. This is demonstrated by the traces of Figure 36. In these traces, $\delta_{a\beta}$ has been changed from -0.6 to -1.2., while δ_{ap} = 0, as in Figure 35.

From these traces it is seen that there is a greater tolerance of switching delay.

For the traces of Figures 37 and 38, the roll rate feedback, δ_{ap}, is increased from 0 to 0.8. This increases the roll damping and, for the "wings leveler" heading loops, reduces the amount of roll angle developed before switching (see Appendix B, Table B1). This will result in further increase in tolerance to switching times. The traces of Figures 37 and 38 confirm this expectation. For the traces of Figure 37, $\delta_{a\beta}$ = 0.6, and for Figure 38, $\delta_{a\beta}$ = 1.2.

Figure 35. Dual Mode: "Wings Leveler" with Sideslip Feedback to Aileron (D2) - Response to 20-fps Step; $\delta_{a\beta} = -0.6$, $\delta_{ap} = 0$

68
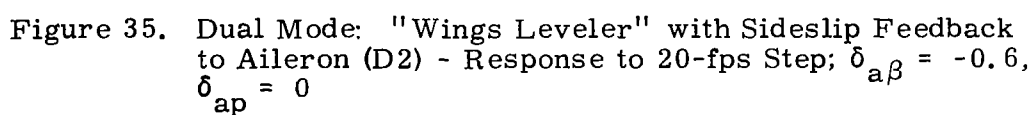
Figure 36. Dual Mode: "Wings Leveler" with Sideslip Feedback to Aileron (D2) - Response to 20-fps Step; $\delta_{a\beta} = 1.2$, $\delta_{ap} = 0$

69
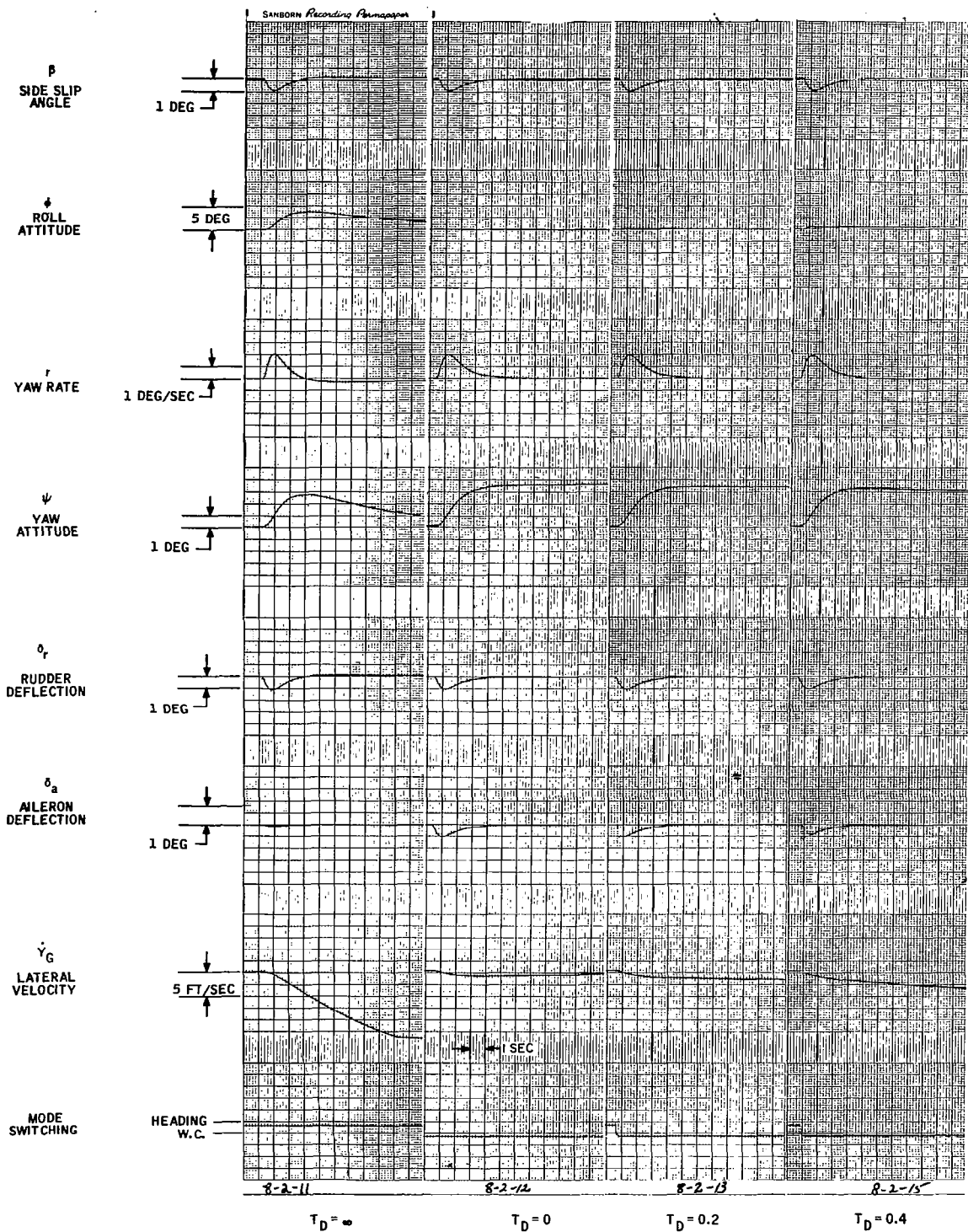
Figure 37. Dual Mode: "Wings Leveler" with Sideslip Feedback
to Aileron (D2) - Response to 20-fps Step; $\delta_{a\beta}$ = -0.6,
δ_{ap} = 0.8

70
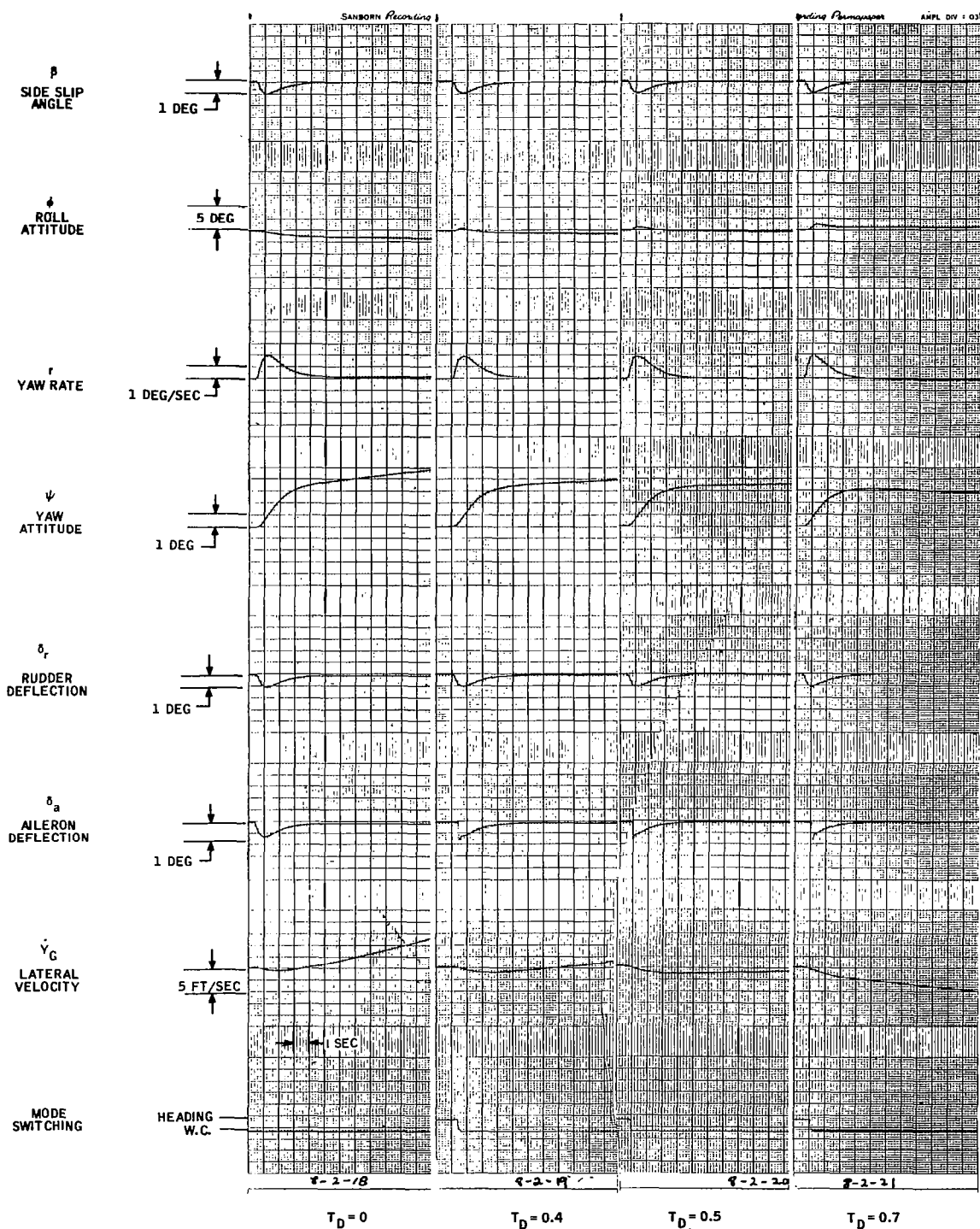
Figure 38. Dual Mode: "Wings Leveler" with Sideslip Feedback to Aileron (D2) - Response to 20-fps Step; $\delta_{a\beta} = -1.2$, $\delta_{ap} = 0.8$

71

In the final set of responses, shown in Figure 39, $\delta_{a\beta}$ = 1.2, δ_{ap} = 0.8 and the switching time, T_D is kept at 0.5 seconds. The step input magnitude is varied rom 10 to 40 fps. The purpose of this series of responses to check the variation in performance due to variation in the size of the lateral wind.

A variation is expected since the both roll angle developed before switching and that compensated for after switching are functions the step input.

From the traces it can be seen that the variation in performance due to changes in wind step magnitude is small.

For comparison of performance with the preceding configuration, we have, using Figure 39, for a step of 20 fps and T_D = 0.5 seconds, $\epsilon_{\dot{Y}_G}$ at 30 seconds is 1.5 fps and ϵ_{Y_G} at the end of 15 minutes is $\epsilon_{Y_G} = \epsilon_{\dot{Y}_G} T$ = 1350 feet.

Dual Mode: Wings Leveler with Yaw Rate to Aileron (D3)

This configuration employs the same heading loop used for concept D2. However, the weathercock mode uses yaw rate feedback to the aileron instead of β feedbacks. This weathercock mode is the single-axis configuration with yaw rate to aileron, concept A4. It will be noted that δ_{ar} is positive in the "heading loop" mode and negative in the "weathercock" mode.

A block diagram for this configuration is shown in Figure 40. In this figure, δ_{ar} is the yaw rate feedback gain employed in the heading mode, and δ_{ar_w} is the gain used in the weathercocking mode.

The first set was taken with heading mode gains which give good heading response and with the weathercock mode yaw rate feedback to ailerons adjusted to hold zero ϕ due to weathercock transient. These are reproduced in Figure 41.
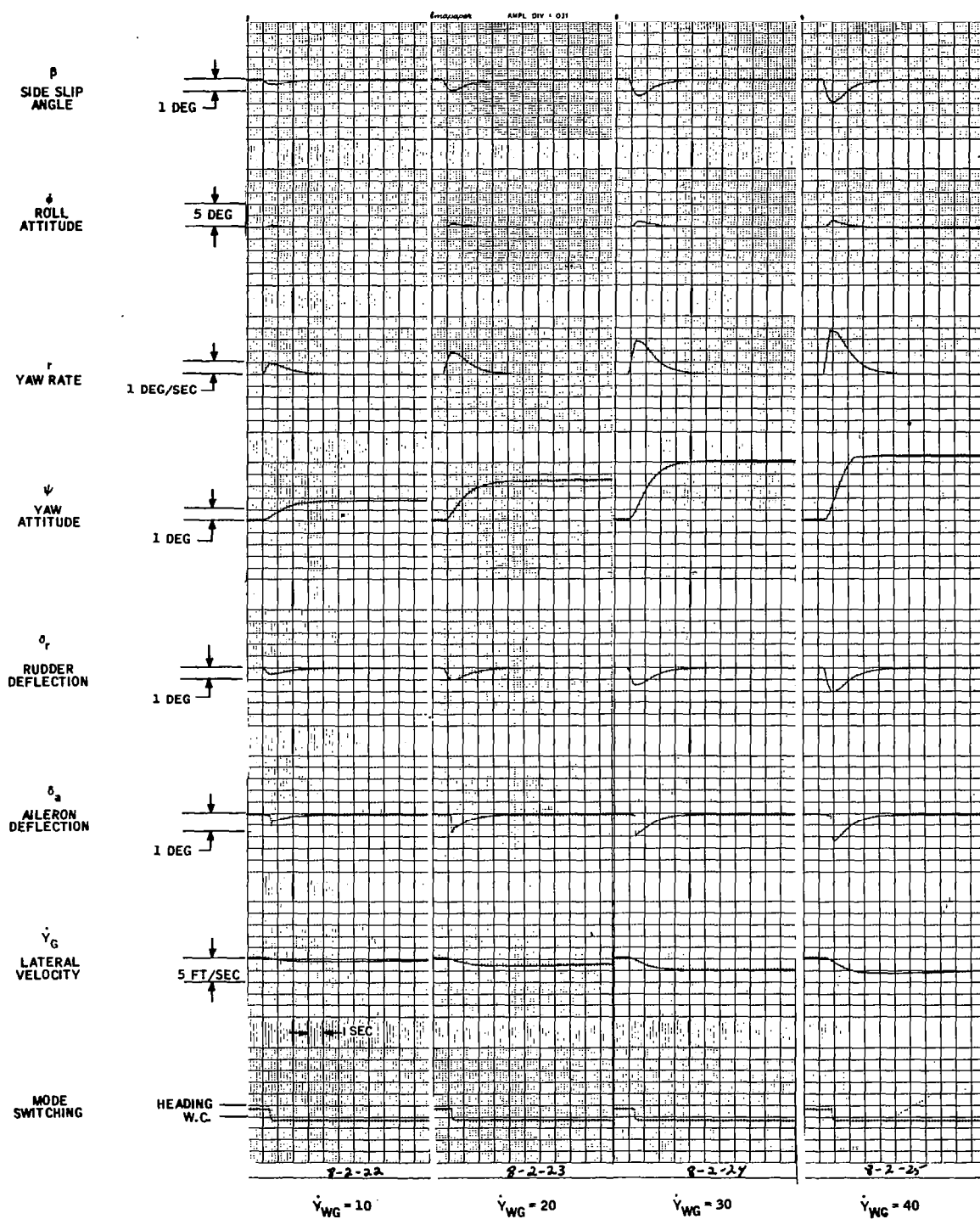
Figure 39. Dual Mode: "Wings Leveler" with Sideslip Feedback
to Aileron (D2) - Response to Varying Step Sizes;
T_D = 0.5 sec, $\delta_{a\beta}$ = -1.2, δ_{ap} = 0.8

73
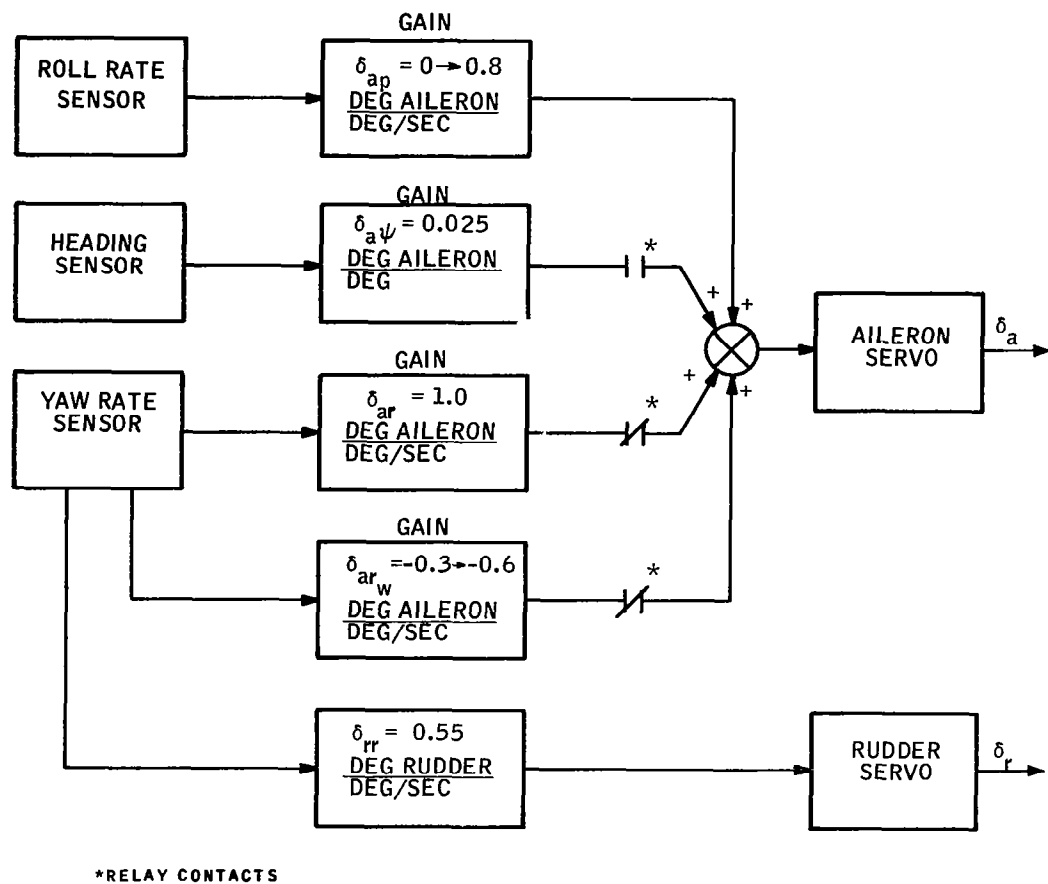
Figure 40. Dual Mode: "Wings Leveler" with Yaw Rate Feedback to Aileron (D3)

74
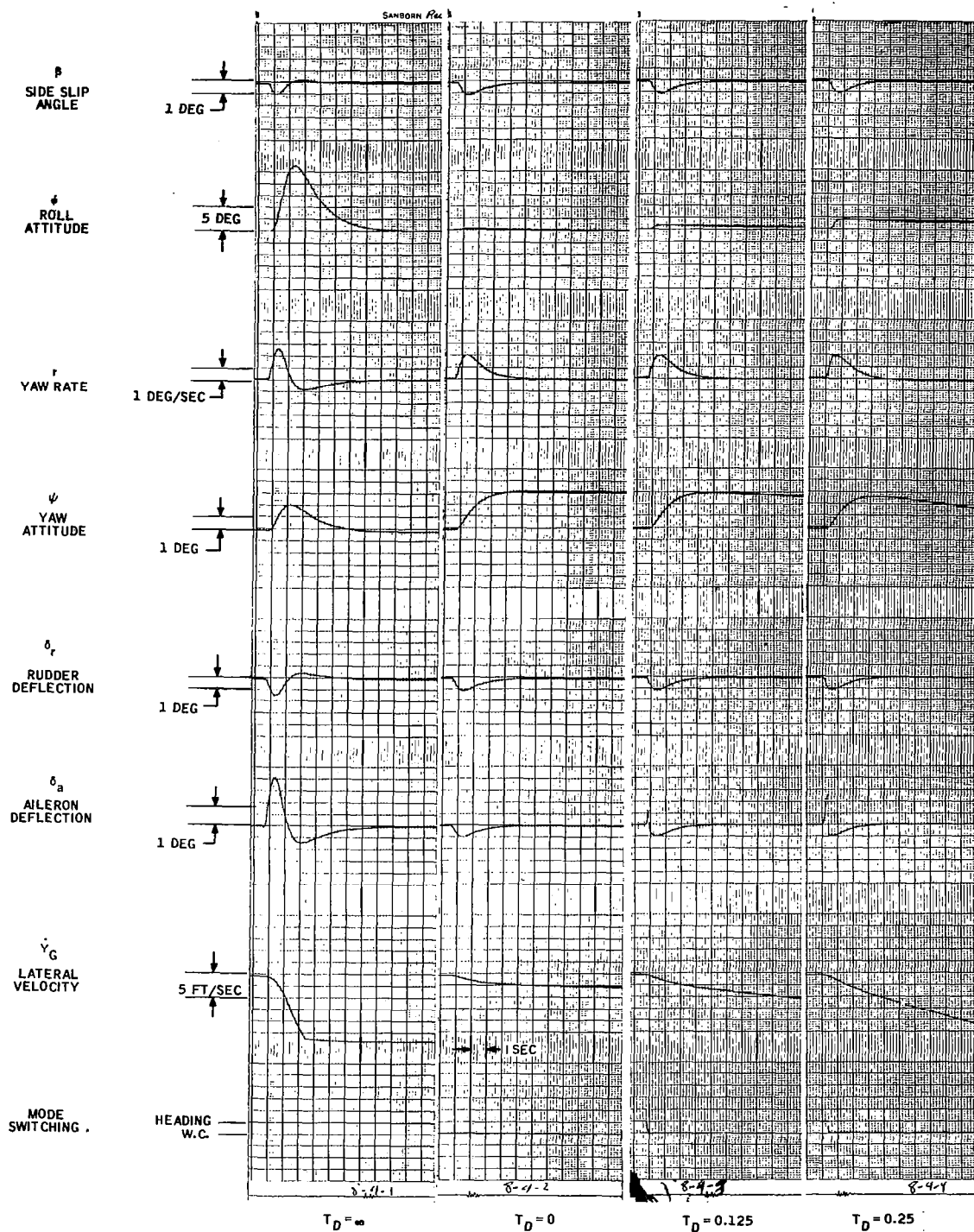
Figure 41. Dual Mode: "Wings Leveler" with Yaw Rate Feedback to Aileron (D3) - Response to 20-fps Step; $\delta_{ar_{WC}} = -0.3$, $\delta_{ap} = 0$

The yaw rate to aileron gain in the weathercocking mode, δ_{ar_w}, and the roll rate gain, δ_{ap}, are set at the following values for the runs of Figure 41:

$$\delta_{ar_w} = -0.3$$

$$\delta_{ap} = 0$$

The traces indicate a relatively large sensitivity to switching delay, T_D.

In the second set, the roll damping was increased to reduce the ϕ present at the time of modal switching for a given delay (see Table B1). This allows longer switching delays for the same flight path performance but makes the heading mode more sluggish. These traces are reproduced in Figure 42. For the responses of Figure 42, $\delta_{ap} = 0.8$ and $\delta_{ar_w} = -0.3$.

These traces show that the roll angle at switchover has decreased and that larger switching delays can be tolerated.

In the third set the yaw rate feedback used in the weathercocking mode is increased to cause ϕ developed during weathercocking to help cancel ϕ present at the time of switching. The increased roll damping of the second set is retained also. This set of traces is reproduced in Figure 43. The gains used for the responses of Figure 43 are $\delta_{ap} = 0.8$ and $\delta_{ar_w} = -0.6$.

The traces of Figure 43 show that increasing the magnitude of δ_{ar_w} has allowed the same performance to be obtained with larger switching delays.

For comparison purposes, the values of ϵ_{Y_G} for 15 minutes for a 20-fps step and $T_D = 0.5$ is determined, based on the recordings of Figure 43, as:

$$\dot{\epsilon_{Y_g}} \text{ at 30 seconds} = 2 \text{ fps}$$

$$\epsilon_{Y_G} = (\dot{\epsilon_{Y_G}})(900) = 1800 \text{ ft.}$$
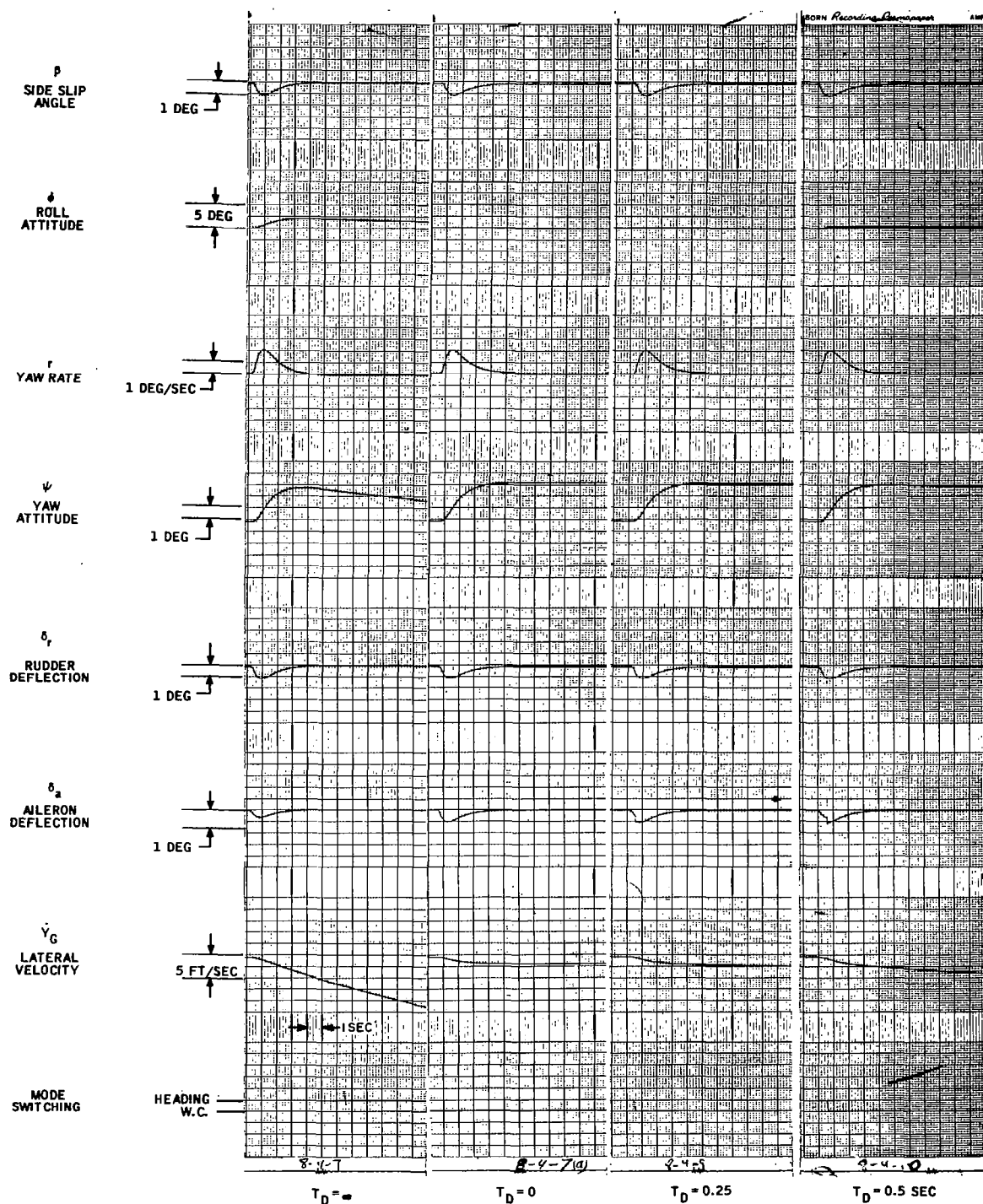
Figure 42. Dual Mode: "Wings Leveler" with Yaw Rate Feedback to Aileron (D3) - Response to 20-fps Step; $\delta_{ar_{WC}}$ = -0.3, δ_{ap} = 0.8

77
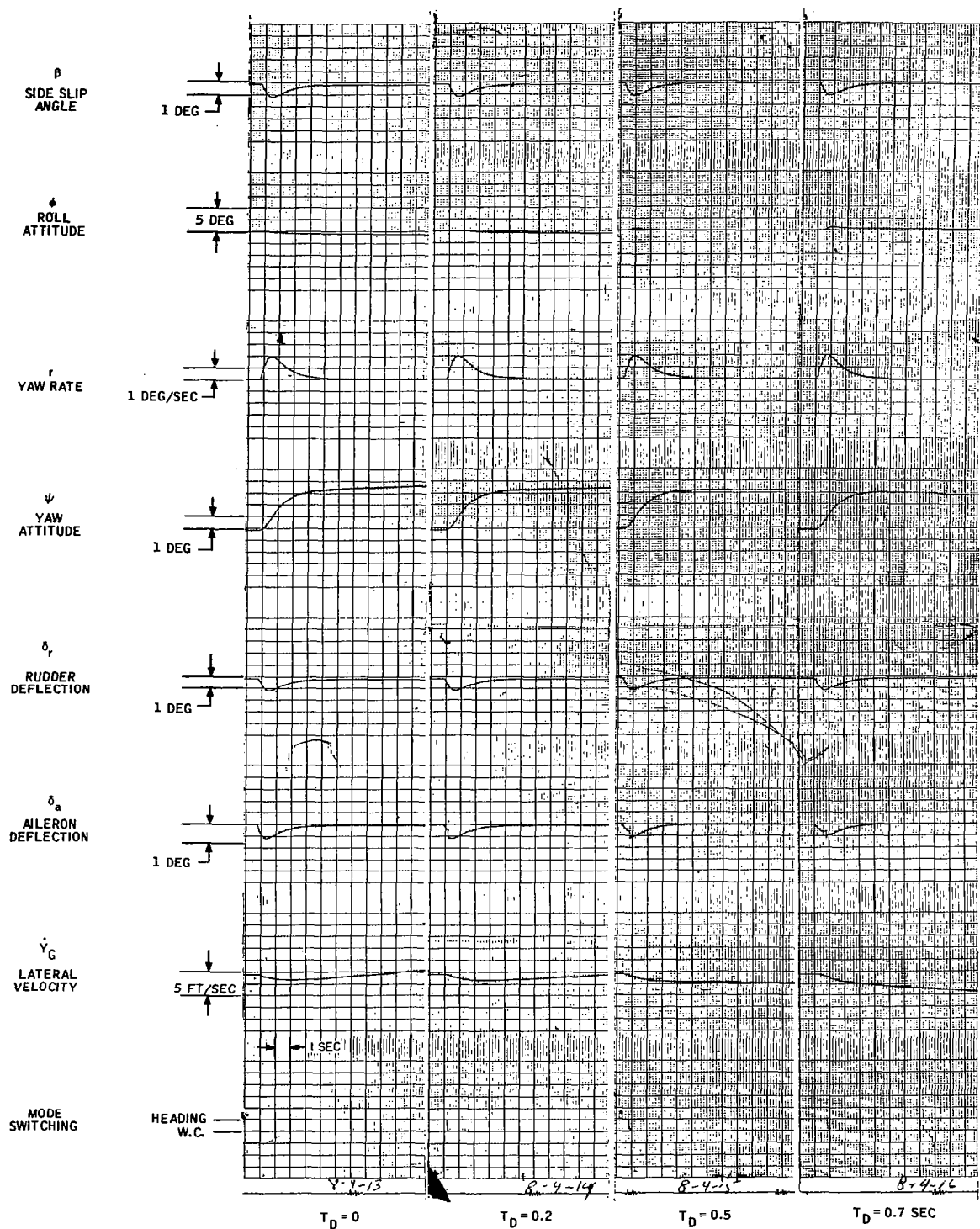
Figure 43. Dual Mode: "Wings Leveler" with Yaw Rate Feedback
to Aileron (D3) - Response to 20-fps Step; $\delta_{ar_{WC}}$ = -0.6,
δ_{ap} = 0.8

78

Dual Mode: Heading to Rudder (Sideslip to Aileron) (D4)

This configuration is the same as concept D2 with the exception that the heading error is fed back to the rudder instead of to the aileron. The block diagram for this configuration is shown in Figure 44.

Heading loop performance with the heading error feedback to the rudder or the aileron is not significantly different, as is demonstrated by Table B1 of Appendix B. In addition, both concept D2 and D4 employ the same weathercock mode configuration. Therefore, it would be expected that the dual-mode operation for both concepts would be similar. This is borne out by the simulator results.

For the configuration under discussion, three sets of lateral wind step responses were recorded as a function switching delay. The first set of recordings is for gains which yield good heading response and nearly zero roll angle due to weathercock in the weathercocking mode. These are shown in Figure 45 and are similar to those obtained in Figure 35 for concept D2. In Figures 45 and 35, $\delta_{ap} = 0$ and $\delta_{a\beta} = -0.6$.

The second set of responses were taken with the roll damping increased to allow larger switching delays to be tolerated. These are reproduced in Figure 46. The results are the same as those obtained for D2 and reproduced in Figure 37. The gains for both Figures 46 and 37 were $\delta_{ap} = 0.8$ and $\delta_{a\beta} = -0.6$.

Finally, the β feedback gain was increased to cancel out the ϕ present at the time of switching with ϕ resulting from weathercocking. These responses are reproduced in Figure 47 and are quite similar to the results obtained for D2 as shown in Figure 38. For Figure 47 and 38 the gains are $\delta_{ap} = 0.8$ and $\delta_{a\beta} = -1.2$.

The performance for $T_D = 0.5$ seconds and a 20-fps step for this configuration is the same as for concept D2; that is, the lateral deviation in 15 minutes would be 1350 feet.
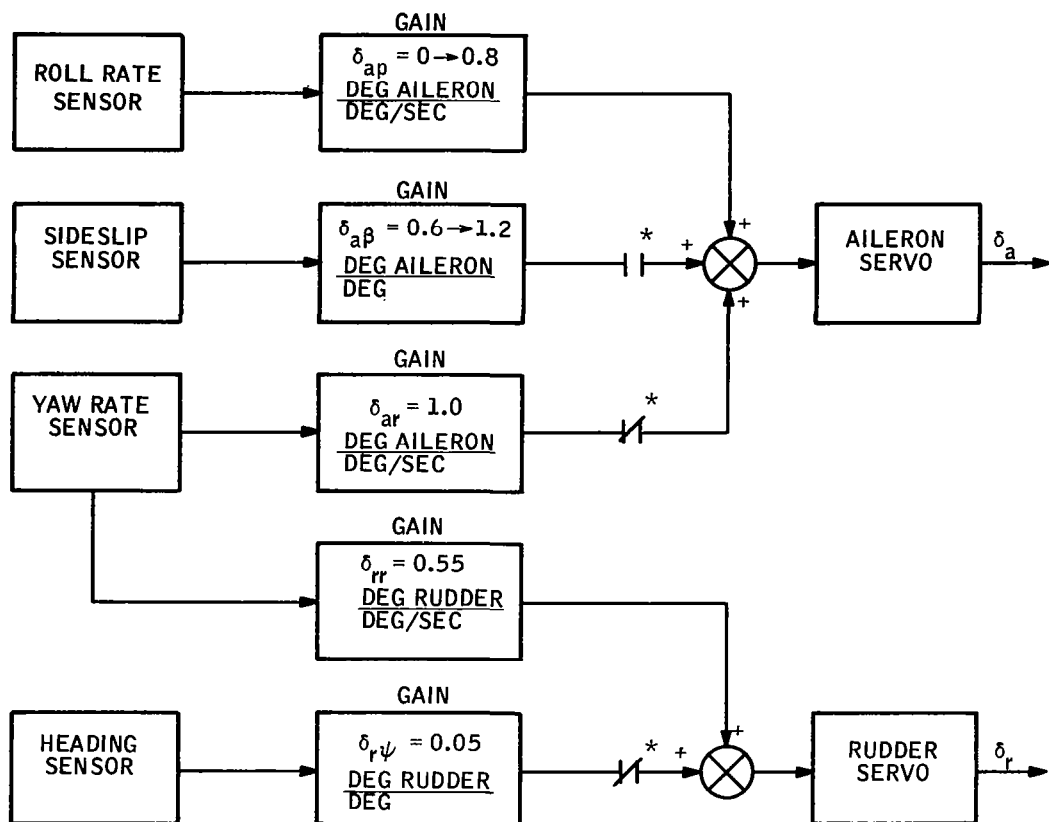
Figure 44. Dual Mode: Heading, "Wings Leveler" and Sideslip Feedback to Aileron (D4)

*RELAY CONTACTS

80
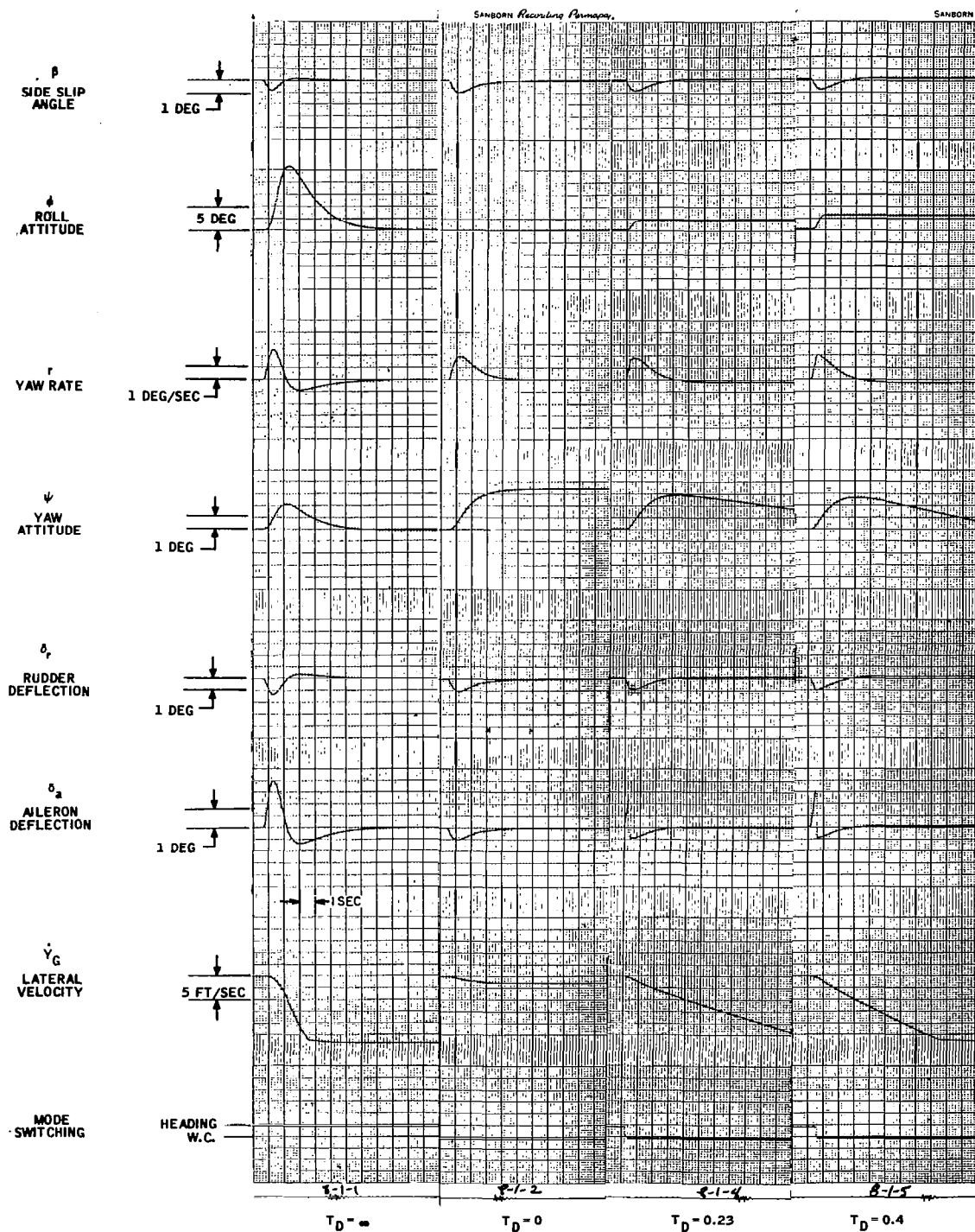
Figure 45. Dual Mode: Heading, "Wings Leveler" and Sideslip
Feedback to Aileron (D4) - Response to 20-fps Step;
$\delta_{a\beta} = -0.6$, $\delta_{ap} = 0$

81
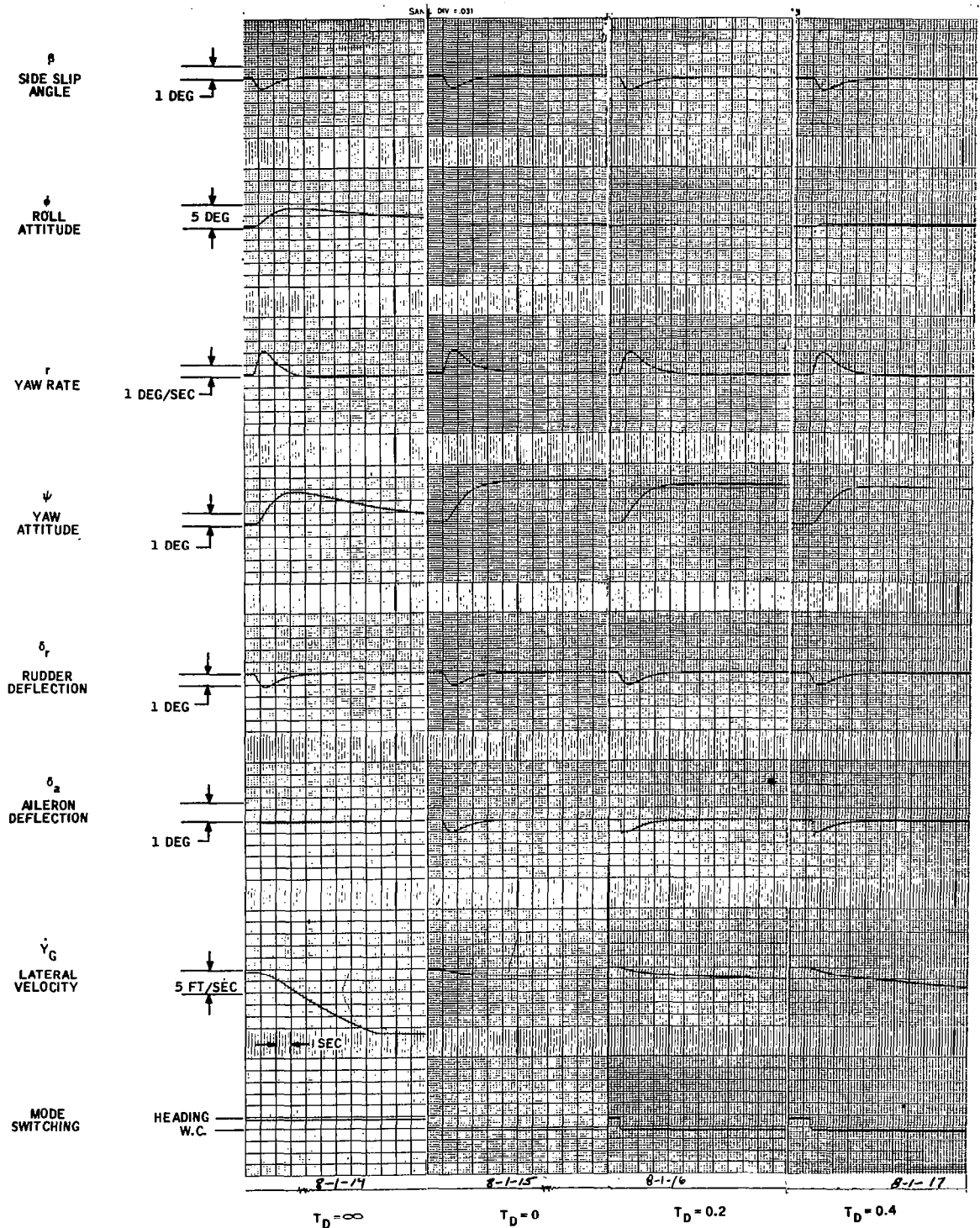
Figure 46. Dual Mode: Heading, "Wings Leveler" and Sideslip
Feedback to Aileron (D4) - Response to 20-fps Step;
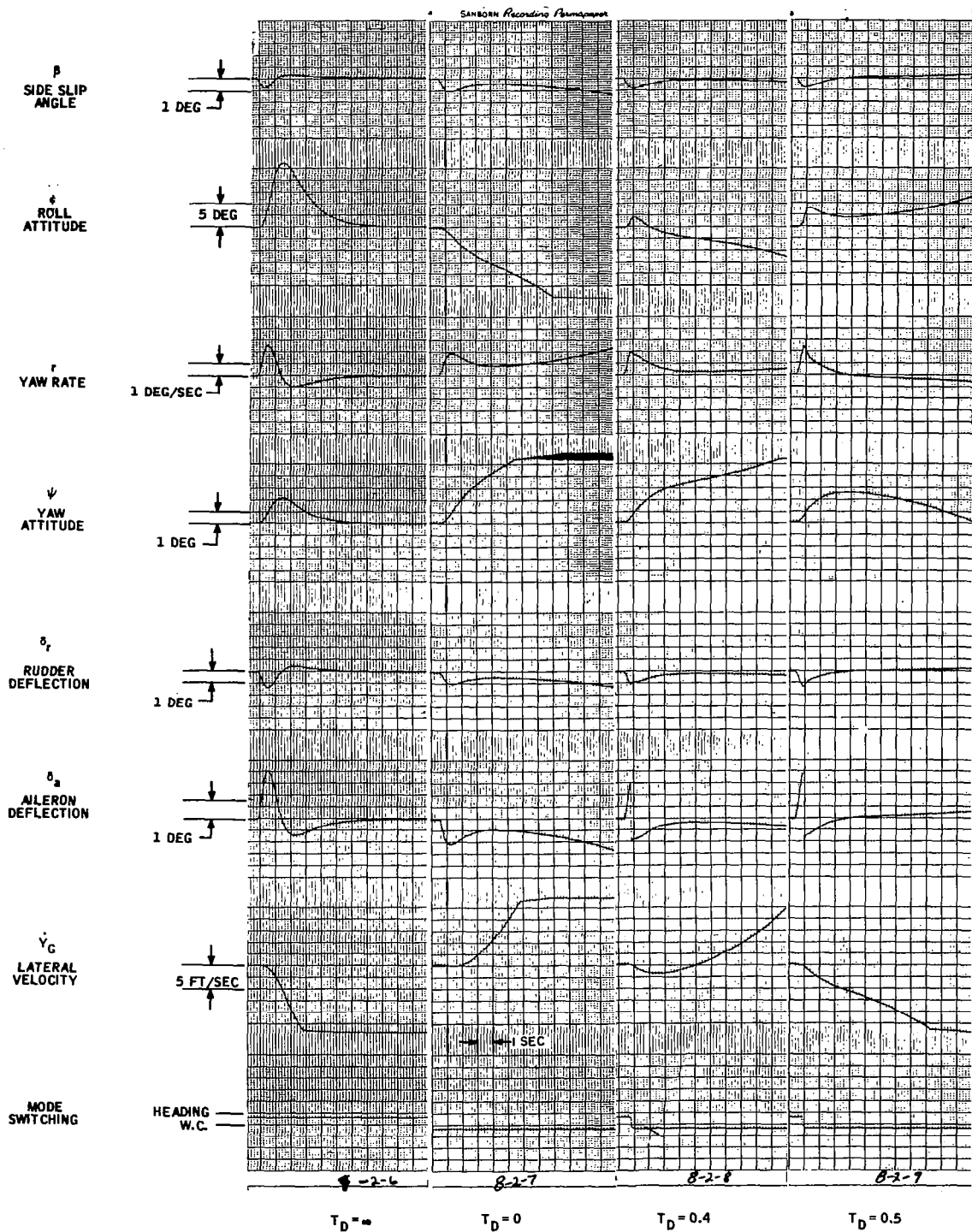$\delta_{a\beta} = -0.6$, $\delta_{ap} = 0.8$
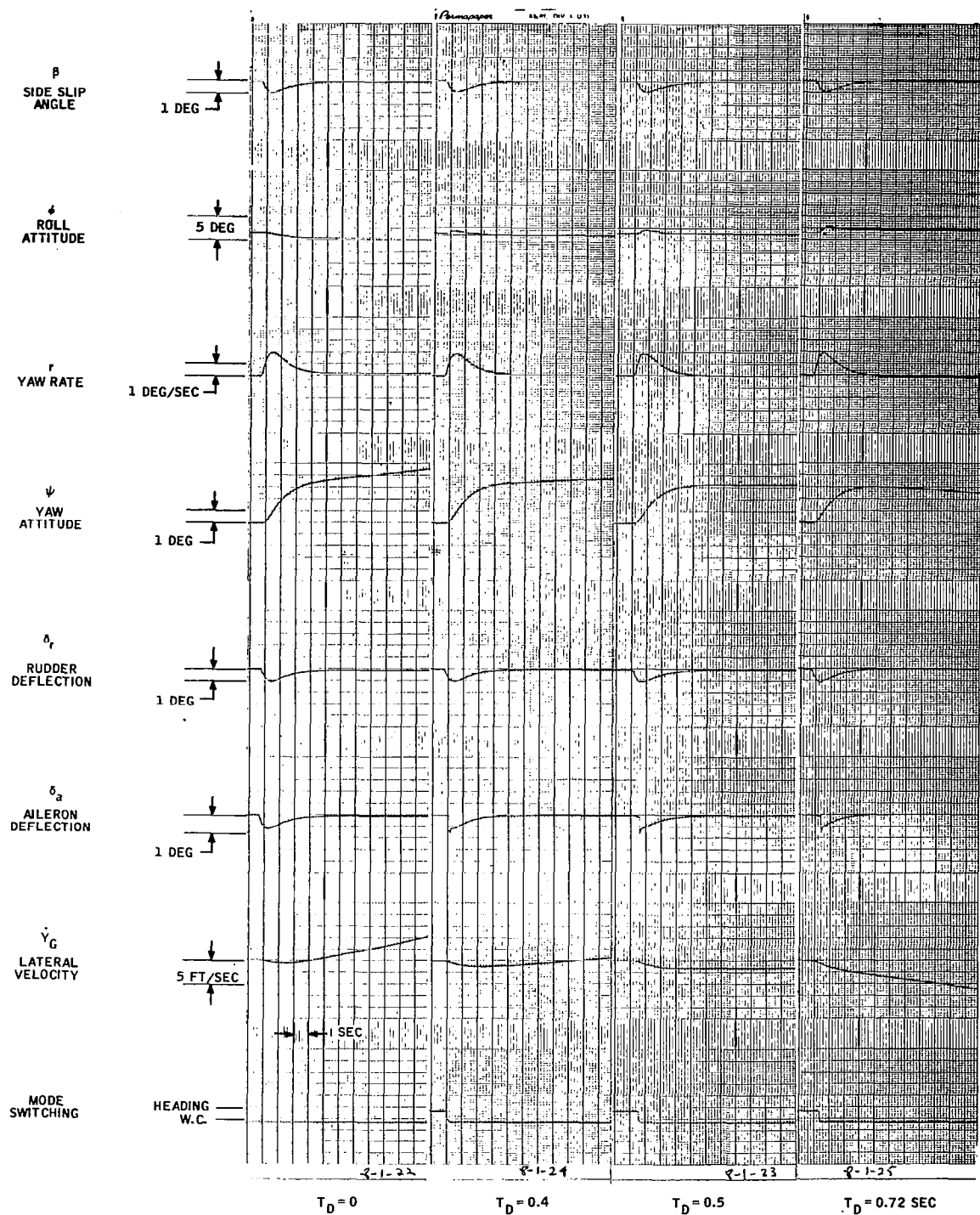
Figure 47. Dual Mode: Heading, "Wings Leveler" and Sideslip
Feedback to Aileron (D4) - Response to 20-fps Step;
$\delta_{a\beta} = -1.2$, $\delta_{ap} = 0.8$

"CONSTANT HEADING" FLIGHT PATH CONTROL (E)

In the previous concepts, the device employed to maintain the flight path unaltered, following a step change in the cross-course wind, was to yaw into the wind by an appropriate amount. A steady-state would then be established in which the wings are level and the sideslip equal to zero.

In the "Constant Heading" Flight Path Control, lateral deviations from the flight path is minimized partially by rolling into the wind to cancel the effects of side force and partially by yawing into the wind. The amount of yaw necessary to effect perfect compensation is smaller for this concept than for the previous ones.

In the steady-state condition, neither sideslip nor the roll angle would be zero. Such an approach, which minimizes the yaw angle response to a wind change, may be advantageous in the landing approach phase.

The name for this configuration derives from the fact that, with high enough heading gain, flight path control is achieved without heading change. This is demonstrated later.

In the particular configuration studied, sideslip is fed back to the aileron (provided with a roll attitude loop) to ensure a roll into the wind, while the yawing moments produced by such a roll are opposed by a heading loop and yaw damper through the rudder. This configuration is shown in Figure 48.
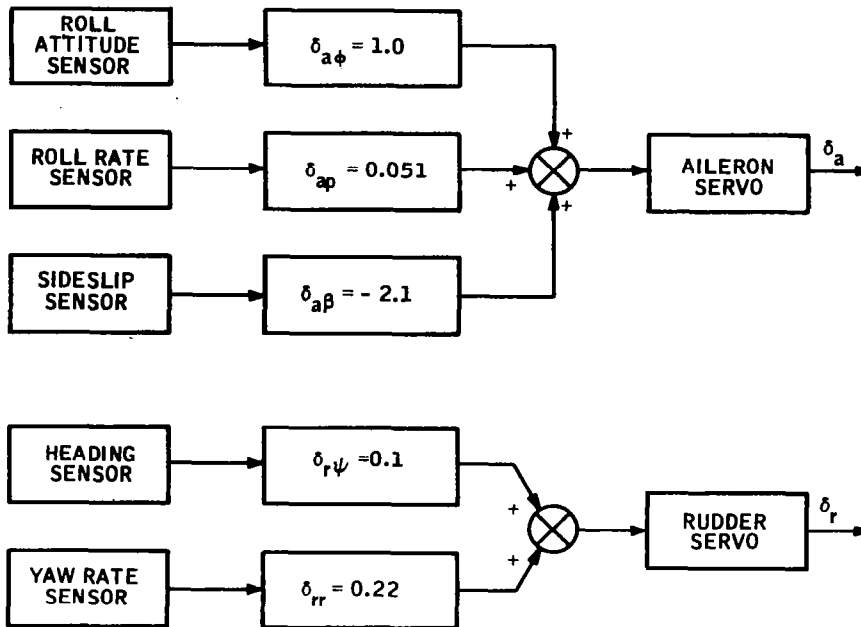
Figure 48. "Constant Heading" Flight Path Control (E)

The short-term response of this configuration to a step in wind is shown in the Appendix B, Section E, to result in a combined value of yaw and sideslip, which results in close to exact compensation for the effect of wind change on the flight path. A roll angle also exists at the end of short-term response.

However, Appendix B also shows that, unless the following condition is satisfied,

$$\underline{L}_\beta g - U_1 Y_V K_\phi = 0,$$

ψ, β and ϕ will, in the steady state, return to zero (if the left hand side is greater than zero) or increase (if it is less than zero). This is analogous

to the spiral mode exhibited by the single-axis systems and represents the physical condition that for only one set of gains and flight conditions will the moments and forces be zero after the short term response.

However, by having $\underline{L}_\beta g - U_1 Y_v K_\phi$, nearly equal to zero, the rate of change from the short-term values of ψ and β can be kept small.

The value of $\underline{L}_\beta$ that satisfies the condition for neutral stability, for cruise conditions and the gains of Figure 48 is

$$\underline{L}_\beta = \frac{U_1 Y_v K_\phi}{g} = 86.0$$

For this $\underline{L}_\beta$: $\delta_{a\beta} = \frac{\underline{L}_\beta - L_\beta}{L_{\delta a}} = \frac{86 + 23.40}{-36.8} = 2.9$

The error in cross-course velocity $\epsilon_{\dot{Y}_G}$ is derived in Appendix B:

$$\epsilon_{\dot{Y}_G} = \frac{\beta_o g N_\beta L_r}{K_\phi (N_\beta - K_\psi)} = 0.0464 \text{ fps} \quad (B64)$$

The lateral flight path error is then

$$\epsilon_{Y_G} = \epsilon_{\dot{Y}_G} \times T$$

where T is the reset interval:

For cruise conditions and a lateral wind step of 20-fps ($\beta_o = 0.064$ rad) and the gains of Figure 48,

$$\epsilon_{Y_G} = 45 \text{ feet}$$

This error is negligible, but it must be remembered that this performance is realized only if F = 0. Otherwise, the condition after the initial transient is not maintained but yaw roll and sideslip angle exponentially drift toward zero (for the dynamically stable case) with a time constant given by Equation (B65).

The step input responses reproduced in Figure 49 are for the configuration shown in Figure 48 under cruise flight conditions, but with $\delta_{a\beta}$ varied. From these traces it is seen that for some value of $\delta_{a\beta}$, in the range

$$-3 < \delta_{a\beta} < -1,$$

a neutrally stable condition is achieved after the short-term response. This agrees with the computed value for $\delta_{a\beta} = -2.9$.

These traces also confirm the computed values of ψ_{ss} and β_{ss}.

Another interesting result is that the amount of ψ_{ss} and β_{ss} can be determined by selecting the value of heading loop gain.

From Equations (B60) and (B61), we have

$$\frac{\psi_{ss}}{\beta_{ss}} = \frac{-N_\beta}{K_\psi} \tag{5}$$

We also have

$$\beta_{ss} + \psi_{ss} \approx \beta_o \tag{6}$$

Combining Equations (5) and (6), we obtain

$$\psi_{ss} = \frac{\dfrac{-N_\beta}{K_\psi} \cdot \beta_o}{1 + \dfrac{-N_\beta}{K_\psi}} \tag{7}$$

$$\beta_{ss} = \frac{\beta_o}{1 \quad \dfrac{-N_\beta}{K_\psi}} \tag{8}$$
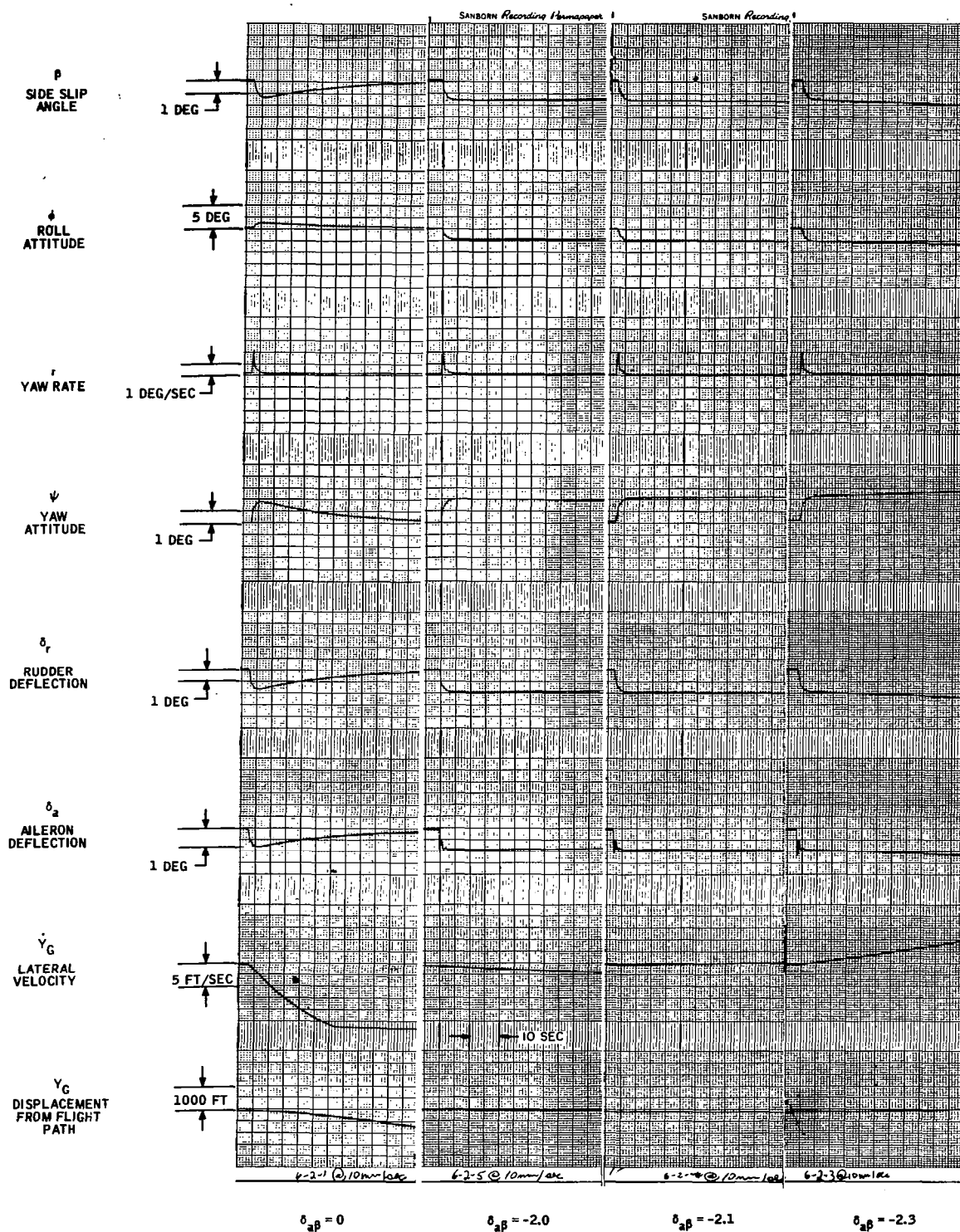
Figure 49. "Constant Heading" Flight Path Control (E) - Response to 20-fps Step

88

From Equations (7) and (8) we see that as $\dfrac{-N_\beta}{K_\psi}$ approaches zero, ψ_{ss} approaches zero and β_{ss} approaches β_o.

This finding is confirmed by the traces of Figure 50. For these runs, the yaw angle was held artifically at zero, simulating infinite yaw gain or $\dfrac{-N_\beta}{K_\psi} = 0$. The traces show that flight path control is maintained solely through a build up of the roll angle and that, in the steady state, the sideslip angle equals the initial value generated at the onset of the wind step. That is

$$\beta_{ss} = \beta_o$$

MISCELLANEOUS CONCEPTS

In addition to the previous concepts, several general approaches were also considered. The concepts all had deficiencies that precluded further study, but, nevertheless, they are listed here.

Fluid Strapdown Navigator (F)

An extensive study was completed on the application of fluid devices to inertial navigation. This study was conducted for the Air Force Avionics Laboratory under Contract No. AF33(657)-11133 (Ref. 4). The final report of that contract states, in essence, that a pure-fluid navigation system with a navigational accuracy of 10 mph would be pushing the state-of-the-art five years from now. The final attainment of this goal will depend on a number of "breakthroughs" in sensor and amplifier technology.

A 10-mph navigation system would, at best, be marginally adequate for fluid flight path control as it is now envisioned. If control system errors are also considered, the error will increase.
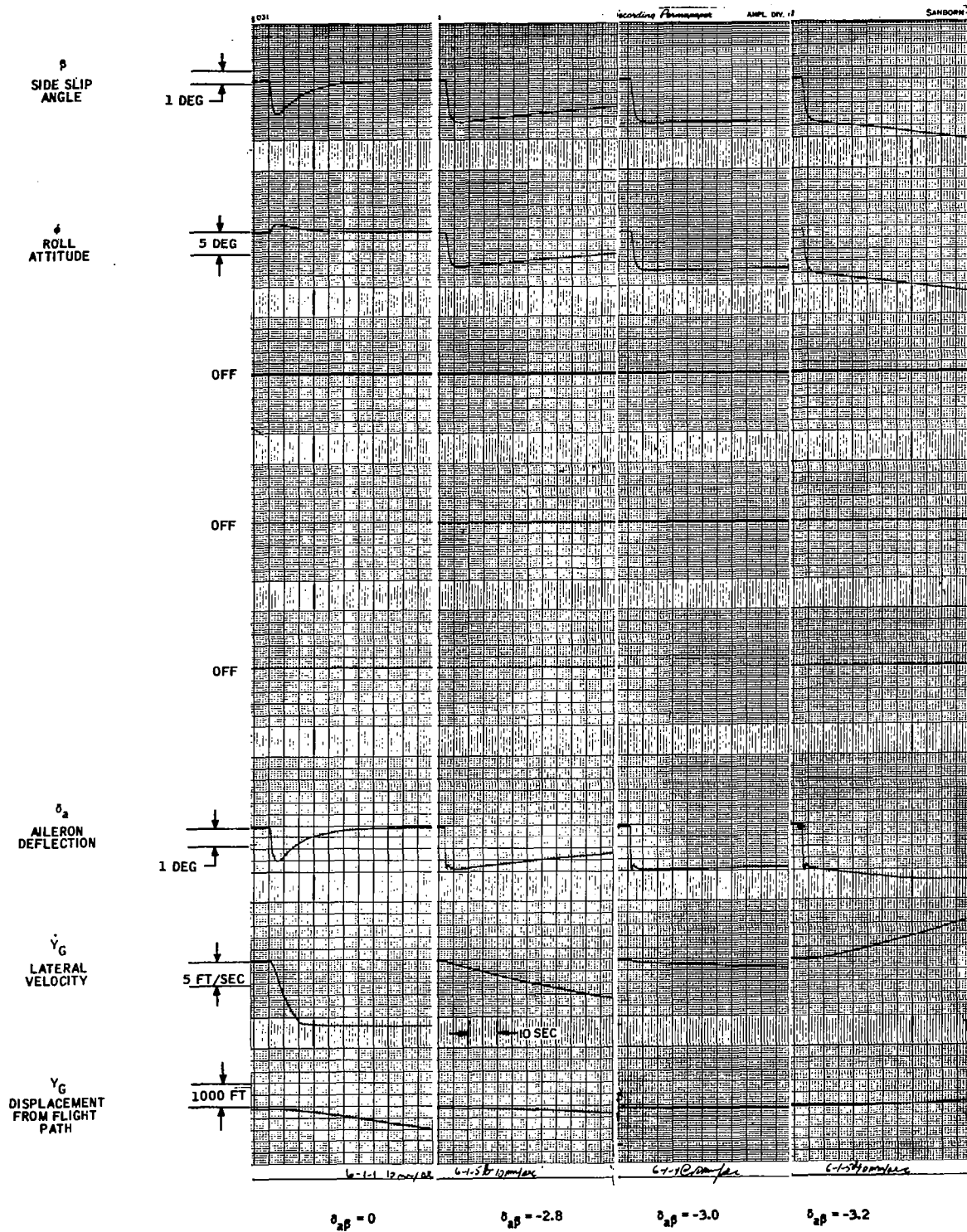
Figure 50. "Constant Heading" Flight Path Control (E), Roll
Channel Only - Response to 20-fps Step

'Since extensive developmental effort is involved in perfecting the fluid strap-down navigator and since its usefulness in this application is doubtful, the concept was dropped from further study.

P-Matrix (G)

P-matrix is a perturbation-type of missile guidance control (Ref. 3). It is specifically oriented toward inertial components which are strapped down to the vehicle. The concept is general enough so that it can be applied to various vehicles. However, since it is specifically oriented to strapped-down inertial components, it must be concluded, for the same reasons cited in the preceding discussion, that its near-term feasibility for fluid flight path control is highly doubtful.

Balanced Attitude Study (H)

This concept is a "loose" form of attitude control. In this case the attitude is used to balance out the effects of a cross-course velocity.

Studies were conducted on two missiles at Honeywell using this system. The results of these studies showed that the system is effective for a very short flight time, measured in seconds. The system works best with a vehicle in which the fore and aft accelerations are high and where the thrust is applied aft of the center of gravity. These conditions are not satisfied by light aircraft.

Even for missile applications, the system leaves a lot to be desired; the results can be compared to a roll attitude hold with large thresholds. As a consequence, the study was dropped from further consideration.

LATERAL FLIGHT PATH CONCEPT COMPARISON AND SELECTION

In this section, the lateral flight path concepts studies are compared, and configurations are selected as possible choices for detailed design, fabrication and flight testing.

Comparison of Concepts

Table 1 compares the performance and characteristics of the lateral flight path control concepts series A through E. Comparisons are made of:

- Qualitative theoretical performance attainable (lateral flight path deviations due to cross-course wind variations)

- Expected performance sensitivity to departure from nominal conditions

- Components required to mechanize each concept

- Comments on relative mechanization complexity

- Critical components

Table 1 does not include the Strapped-Down Navigator, P-Matrix or Balanced Attitude concepts, since these involve distinctly different principles and can be dismissed from further consideration on the basis of complexity and incompatibility with the present state of development of pure-fluid components.

Concept A1 (Free-Airplane-Controls Locked) is omitted from the tabulation, since, even under nominal conditions, it produces an error of 7000 feet -- much in excess of the maximum allowable.

Table 1. Comparison of Lateral Flight Path Concepts

Concept	Theoretical Performance (Lateral Flight Path Error for 20-fps Wind Step)	Performance Sensitivity To Variation From Nominal Condition	Rudder Servo	Aileron Servo	Integrator	Synchronizer	Roll Attitude Sensor	Heading Sensor	Roll Rate Sensor	Yaw Rate Sensor	Sideslip Sensor	Wind Detector	Comments on Mechanization Complexity	Critical Components
A2: Single Axis – Sideslip Feedback to Rudder	430 ft.	No restraint on roll and yaw due to mistrims and biases. Cancellation of spiral mode upset by parameter variations. Both cause rapid increase in rate of flight path error growth.	•							•	•		Simplest concept: No attitude sensors, roll rate sensor or aileron servo. Yaw rate sensor used for damper only – not critical.	Slideslip Sensor
A3: Single Axis – Sideslip Feedback to Aileron	810 ft.	Same as above.	•	•						•	•		Requires an aileron servo in addition to same hardware as A2.	Sideslip Sensor
A4: Single Axis – Yaw Rate Feedback to Aileron	1020 ft.	Same as above.	•	•						•			Requires same hardware as A3, but eliminates slideslip sensor. However, yaw rate sensor must be more precise.	Yaw Rate Sensor
B1: Roll Attitude Control	324 ft.	Roll angles held to zero. Therefore, only yaw mistrims and biases affect error, and spiral mode elimination is independent of parameter variation. Worst effects due to yaw rate thresholds and roll altitude thresholds. Within roll threshold sensitivity is like single axis.	•	•			•		•	•	•		Requires a roll attitude sensor. Roll rate sensor may be required for roll damping.	Roll Attitude Sensor
B2: Roll Attitude Control – Sideslip Feedback to Rudder	77.4 ft.	Same as above.	•	•			•		•	•	•		Requires a sideslip sensor in addition to B1 hardware.	Roll Attitude Sensor and Sideslip Sensor
B3: Roll Attitude Control – Sideslip Feedback to Aileron	0	Same as above.	•	•			•		•	•	•		Same hardware as B2.	Same as B2
B4: Roll Attitude Control – Servoed Sideslip to Aileron	1000 ft (0.02 cps Limit Cycle) 0.10 roll ampl. 0.20 yaw ampl.	A mode of operation is possible which will tolerate a roll sensor threshold. However, accompanying limit cycle in yaw and roll may be objectionable.	•	•			•	•	•	•	•		Same hardware as B2 plus heading sensor. Sideslip sensor is mounted on platform slaved to heading error.	Same as B2 plus Heading Sensor
C1: Heading Hold – Biased with Side Velocity	0	The roll and yaw attitude control loops of this configuration eliminate (or drastically reduce) effects of mistrims and biases. Parameter and sensor variations will cause fixed cross-course velocity errors. Drift of integrator must be kept low.	•	•	•		•	•	•	•	•		Requires both roll and heading attitude sensors. In addition a side-velocity computer (summer plus integrator).	Roll Attitude Sensor, Heading Sensor, Integrator, Sideslip Sensor, Yaw Rate Sensor, Roll Rate Sensor.
C2: Heading Hold Biased with Integral of Sideslip	465 ft. with: $\frac{K_I}{K_\beta} = 0.1$	Same as for C1. However, since bias depends on sideslip sensor only, it is only the variations from norminal of this sensor that effects performance.	•	•	•		•	•	•	•	•		Same as above except that side velocity computer is replaced by sideslip integrator.	Same as C1 except Yaw Rate and Sideslip Sensors are not critical.
D1: Dual Mode – Roll Attitude with Sideslip Feedback to Aileron	900 ft. (T_D = 0.5 Sec)	Same insensitivity to biases and mistrims as C1 and C2. Absence of integrator drift problems and sensitivity of bias comp. to parameter variation replaced by errors produced by switchover delay variations.	•	•		•	•	•		•	•	•	Same roll and yaw attitude hold "inner loop" hardware as C1. Synchroizer replaces integrator. Wind detection and switching logic allows implicit computation of heading bias to replace side-velocity computation of B1.	Roll Attitude Sensor, Heading Sensor, Sideslip Sensor, Wind Detector, Synchronizer.
D2: Dual Mode – "Wings Leveler" with Sideslip to Aileron	1350 ft. (T_D = 0.5 sec)	Absence of roll attitude sensor signal may complicate wind detection problem and introduce delay variations.	•	•		•		•	•	•	•	•	Eliminates the need for roll attitude gyro.	Same as D1. Except eliminate Roll Attitude Sensor and add Yaw Rate Sensor.
D3: Dual Mode – "Wings Leveler" with Yaw Rate to Aileron	1800 ft. (T_D = 0.5 sec)	Absence of sideslip sensor compounds problem of wind-detector. Still larger switch-over delays may be encountered.	•	•		•		•	•	•		•	Eliminates both roll attitude sensor and sideslip sensors. (However sideslip sensor may be required by Wind detector).	Same as D2 Except Sideslip Sensor not critical component.
D4: Dual Mode – "Wings Leveler" with Sideslip to Aileron (Heading Error to Rudder)	1350 ft. (T_D = 0.5 sec)	Same as above.	•	•		•		•	•	•	•	•	Same as for D2.	Same as D2.
E: "Constant Heading" Flight Path Control	45 ft.	Cancellation of a statically unstable mode upset by parameter variations, causing exponentially growing errors.	•	•				•	•	•	•		Same roll and yaw attitude hold hardware as C and D groups, but only sideslip sensor is needed in outer loop.	Roll Attitude Sensor Heading Sensor Sideslip Sensor

The first entry in Table 1 gives the theoretical performance. It represents the lateral flight path deviation developed in 15 minutes, due to a step change in the cross-course wind of 20 fps. The design goal sets a maximum of 2880 feet for this value (see Appendix A, "Concept Performance Evaluation Criteria"). This error is due to the lateral wind change only. All systems listed generate less than the maximum allowable error.

The tabulation of remarks on performance sensitivity are preliminary quantitative observations on expected effects of control surface and thrust mistrims, component thresholds and aircraft aerodynamic variations and variations in flight conditions. These observations are based on the form of the performance equations and the experience obtained on the analog computer with the various configurations studied.

As indicated in the introduction to this section, a detailed study of non-linearities, mistrims and sensitivity to parameter variations was considered outside the scope of this study, as were performance errors due to complex disturbances.

As is noted in Appendix A, the error due to these sources must be substantially less than 5 miles in 15 minutes if any significant over-all flight path improvement over a conventional attitude hold autopilot is to be realized.

In general, the Single-Axis systems will show the greatest sensitivity to mistrims, biases, etc., since the attitude loops are not present to eliminate or limit the roll and heading excursions. Presence of roll and yaw displacements will cause flight path errors which grow at increasing rates. In addition, the cancellation of the spiral response mode occurs only at one set of gains and aircraft parameters. Thus, parameter variations will upset this cancellation and cause an exponentially growing flight path deviation. It is highly doubtful that the flight path error due to these effects will be limited to less than 5 miles in 15 minutes. Therefore, single-axis concepts cannot meet either the primary or secondary goals (discussed in Appendix A).

94

The "Tight Roll" systems will tolerate mistrim, biases, and so forth much better than the single-axis systems because roll is held to zero. The effects of yaw axis mistrim and biases are not reduced, however. Spiral mode elimination depends only on the attitude hold loop and not on obtaining a specific relation between autopilot gains and aircraft dynamic parameters. Therefore, parameter variations will not introduce the spiral mode. Parameter variations will cause a fixed cross-course velocity error to occur. If a roll threshold is present, the performance sensitivity within the sensor threshold boundaries are the same as for the single-axis systems. However, with an appropriate amount of sideslip feedback, to the aileron, the roll threshold can be tolerated at the expense of introducing a limit cycle (see discussion of Concept B4). It is probable that these effects will prevent the primary design goal from being achieved (since the primary design goal was determined on the basis of employing an attitude hold autopilot for an inner loop); however, the secondary design objectives may be within reach with these configurations.

The Biased Heading systems and Dual Mode are expected to show the least sensitivity to mistrim biases, etc., because both roll and yaw excursions are held close to zero. In particular, roll sensor thresholds can be tolerated, since the resulting yaw errors are limited by the heading hold loop. Parameter, gain and switching delay variations are expected to produce constant cross-course velocity errors and therefore linearly changing lateral flight path deviations. These systems are feasible approaches to meeting the primary design goals.

The "Constant Heading Flight Path" control will be quite sensitive to parameter and gain variations since the static stability of the steady state holds for one condition. Variations from this condition would result in an exponentially growing lateral flight path error. In addition, the static stability is achieved at the expense of heading response. Unwanted heading biases are therefore allowed to have a large degrading effect on flight path performance.

Selection of Concept for Development and Flight Testing

It is clear from the previous discussions that the Biased Heading or Dual-Mode concepts are the only feasible approaches (of those studied) to meeting the primary design goal. The Biased Heading concepts are simpler in mechanization than the Dual-Mode and are therefore the better choice for development and mechanization for flight testing.

At this point, the integrated sideslip feedback system is more attractive than the side-velocity feedback, again because of simpler configuration. Therefore, the Heading Hold biased by integrated feedback is the choice for design and mechanization for flight testing, based on meeting the primary design goals.

The possibility of achieving an attractive tradeoff between flight path control performance and hardware simplification with a Tight Roll system should not be overlooked. Including the flight testing of a Roll Attitude Control with Sideslip Feedback to Aileron is therefore also recommended.

It must be noted, however, that certain changes in configuration may occur as a result of the analysis of performance obtainable with these configurations due to:

- Aircraft stability derivative variations

- System mistrims, thresholds and gain variations

- Complex disturbances (i. e. , disturbances other than lateral wind changes, occurring alone or in combination with lateral winds)

- Realistic wind profiles presented on terms of statistical properties

SECTION III
PITCH FLIGHT PATH CONTROL CONCEPTS

GENERAL

The pitch axis computer study was done using a Reac 400 analog computer. The study had two objectives:

- Investigate an altitude hold mode with the conventional pitch autopilot inner loops

- Develop a descent rate mode for use in a landing approach

Pitch axis flight path control during cruise can be obtained by the use of an altitude-hold mode. Vertical gusts or other disturbances are easily corrected since the engaged pressure altitude is maintained. A conventional configuration utilizing altitude error as an outer-loop feedback with pitch attitude and pitch rate inner loops was used for this study. This configuration has been studied on previous programs and required only minor gain tailoring for use on the Cessna 310 simulation.

For the descent rate mode, three concepts were studied:

- Altitude rate feedback

- Altitude rate plus normal acceleration

- Lagged pitch attitude feedback

INNER LOOP CONTROL

A simple attitude and rate type autopilot was used for inner loop control.

The pitch damper gain was first adjusted and then pitch attitude and pitch rate loops were added. The damper gain was set on the basis of the response to a wind gust and provided a well-damped response. This is shown in analog recordings in Figures 51(a) and 51(b) for a free airplane with and without damper. The attitude and rate gains were set on the basis of the response to an attitude step command. The attitude response has less than 10 percent overshoot. No attempt was made to include all the sensor dynamics since the altitude hold mode was of prime interest. The responses to the attitude input can be seen in Figure 51 (c). A block diagram of the system is shown in Figure 52.

ALTITUDE HOLD

For the altitude control mode, an altitude displacement feedback was added to the basic autopilot inner loops.

A static source lag of $1/1 + 0.23 S$ was used in the simulation. For light aircraft, a trapped-air-type altitude controller may be employed. The altitude controller dynamics were simulated with a lag of $1/1 + 0.23 S$ plus a threshold of ± 1.5 feet. This is a reasonable estimate of a controller for the approach condition. Generally, the threshold increases for higher altitude since the controller is essentially a pressure sensing device. An altitude phasing network lag of $1/1 + 0.5 S$ was used to shape the altitude signal. An altitude step command of 40 feet was given to the system. The responses to the altitude input are shown in Figure 51 (d). Typical accuracies expected of this configuration at cruise flight conditions are ± 50 feet in straight and level flight and ± 75 feet in turns.
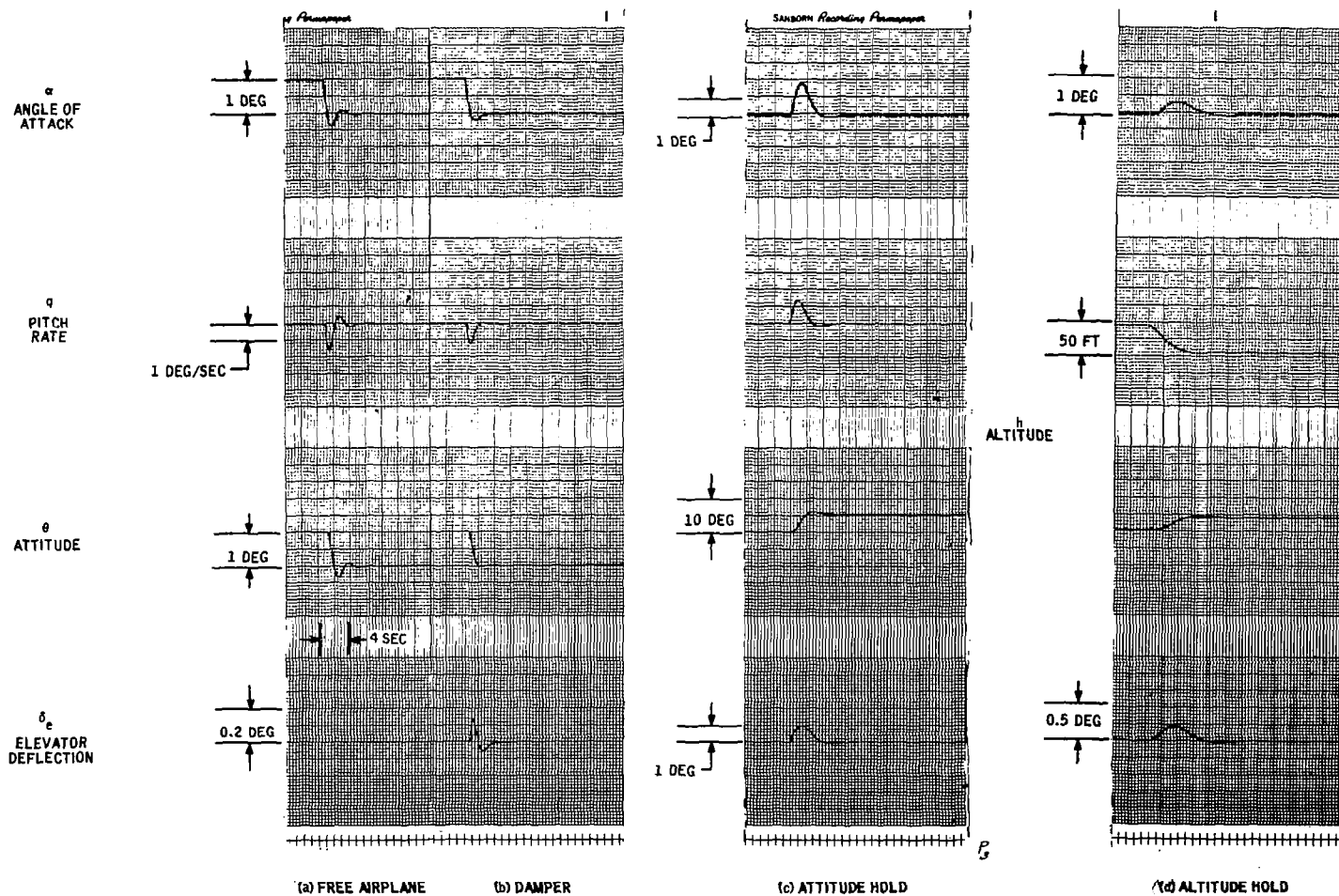
Figure 51. Pitch Axis Cruise Condition
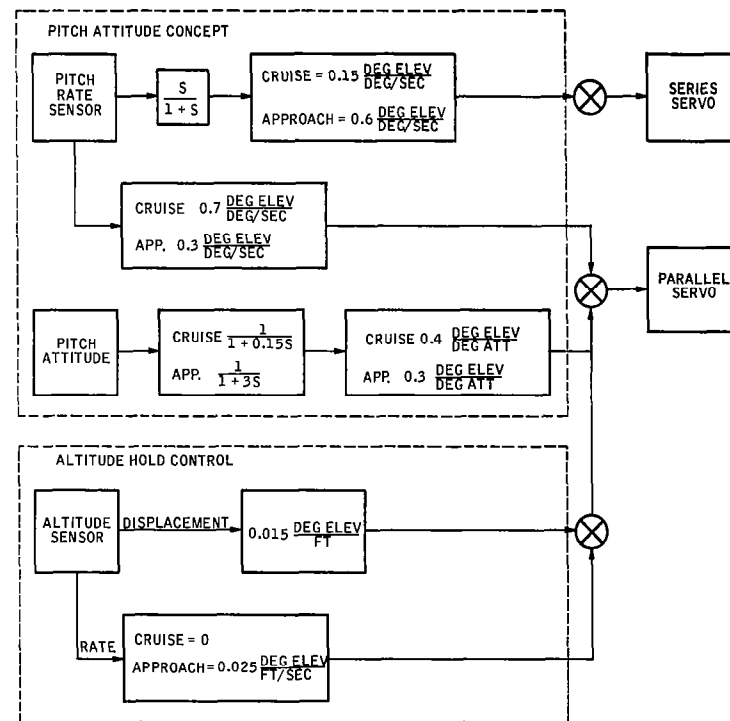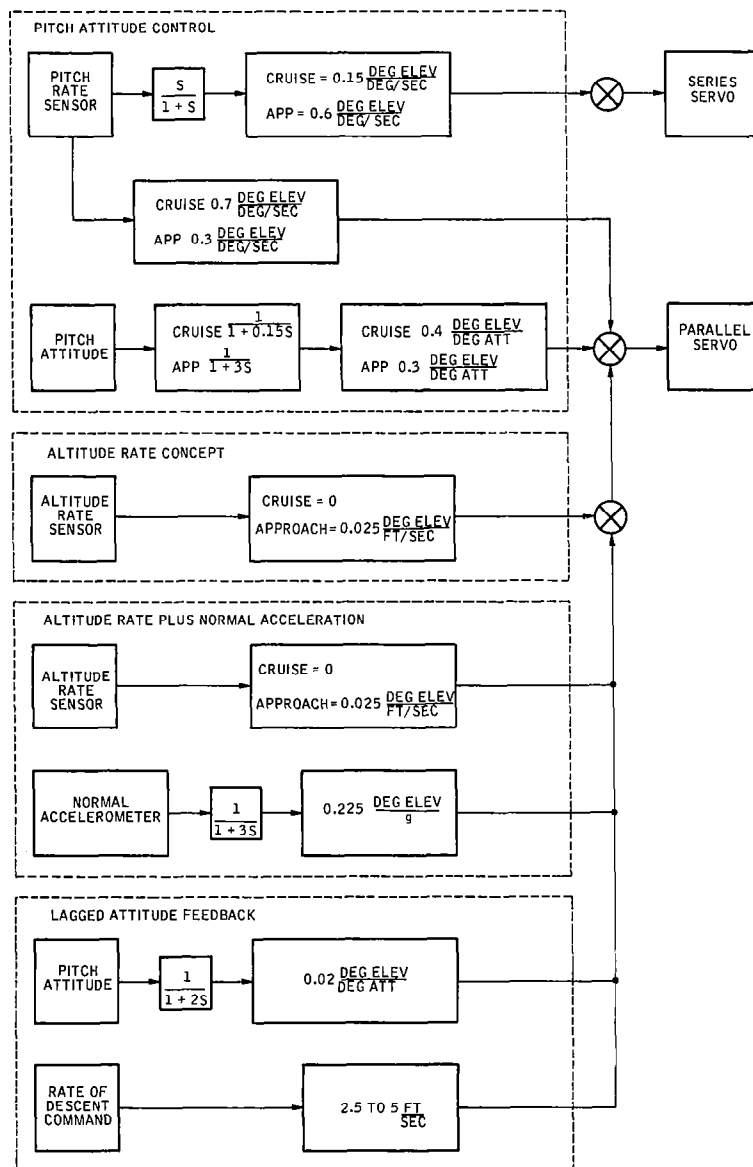
Figure 52. Pitch Axis Block Diagram

DESCENT CONTROL

Several methods of controlling the descent phase were studied. Each of the methods presupposes the pilot is free to command a descent rate through a trim knob on the autopilot function selector. The pilot commands the flight path desired and the autopilot controls to this path.

Altitude Rate

The first of the descent concepts studied uses an altitude rate signal as the feedback for the pilot's input. A block diagram of this mechanization is shown in the dotted portion of Figure 52.

The altitude rate descent mode also requires the inner loop damping and stabilization provided by the pitch attitude and pitch rate feedbacks. The optimum inner loop gains for the descent mode were found to be lower than those for the altitude hold mode. However, the magnitude of the gain change is not such as to prevent selection of an acceptable compromise.

A typical response for this type of descent rate control is shown in Figure 53(a). An altitude rate command of 3.5 ft/sec was used. It can be seen that the response is reasonably fast and well damped.

Altitude Rate Plus Vertical Acceleration

Vertical acceleration can be used in conjunction with an altitude rate signal to provide increased damping to disturbance. This is particularly effective where the generated altitude rate signal is noisy or erratic.
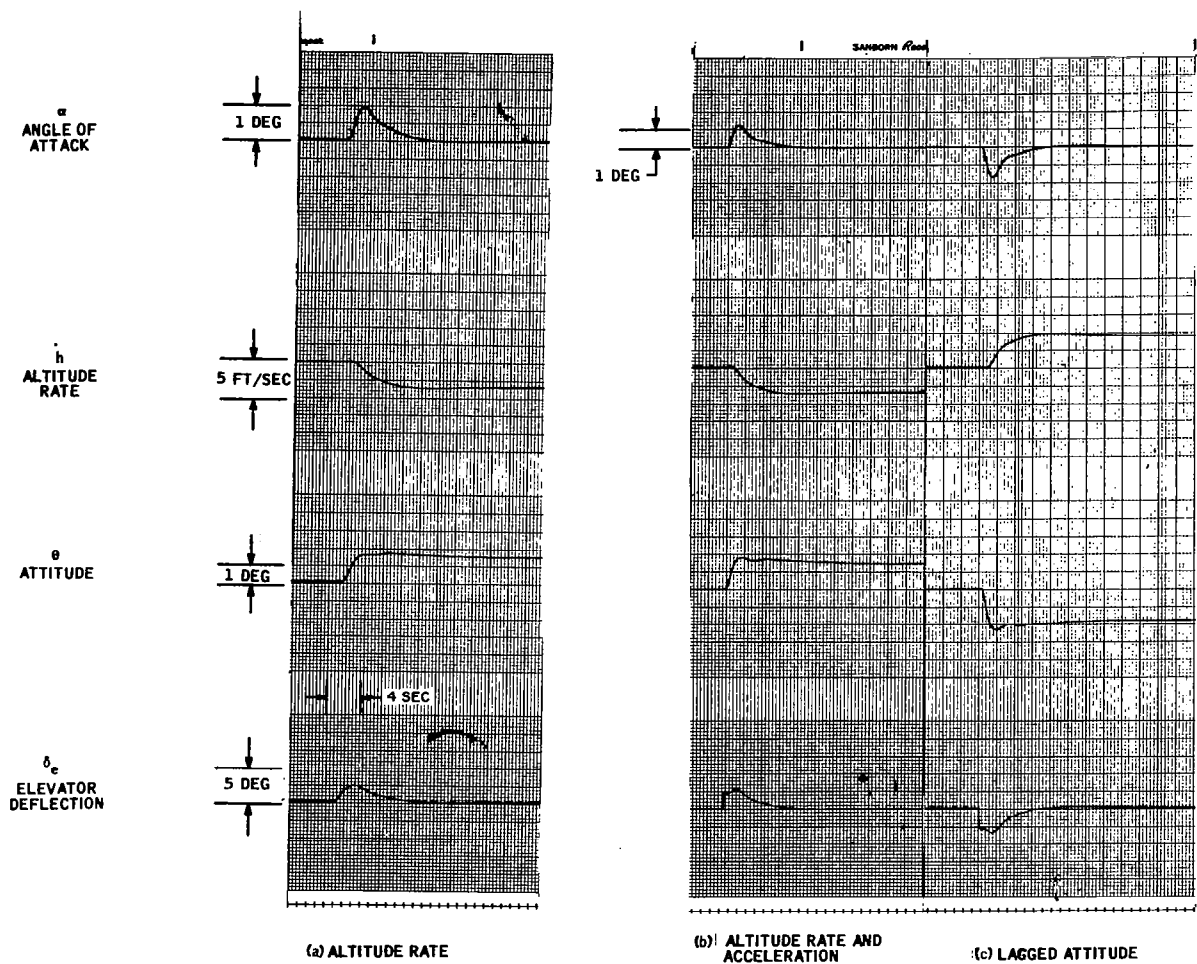
Figure 53. Pitch Axis Approach Condition

Vertical acceleration is most easily obtained by applying a pitch attitude correction or compensation to the output of a normal accelerometer mounted to the airframe. If normal acceleration is used directly, it is destabilizing in one direction due to the pitch attitude effects.

A large lag is usually added to the vertical acceleration signal to give a pseudo-integration. The resulting "rate" signal can then be used to supplement the altitude rate signal.

It was found in this particular simulation that the addition of vertical acceleration feedback improves the response time but not sufficiently to justify its use (see Figure 53(b)). Therefore, this configuration is not recommended for further study.

Lagged Attitude Concept

When pitch attitude is lagged by a time constant equal to the airplane time constant, T_a, the resulting signal approximates flight path attitude. Flight path attitude is the desired pitch control parameter so the use of this type feedback is particularly attractive.

Furthermore, it can be seen that the lagged pitch attitude signal is the equivalent of an altitude rate feedback from the relationship

$$\dot{h} = U_1 \gamma$$

where

U_1 = forward velocity

γ = flight path angle

and

$$\gamma = \theta \frac{1}{1 + T_a S}$$

where

T_a = airplane time constant

In some applications, it may be more desirable to use the pitch attitude signal instead of the altitude rate feedback. Usually the attitude signal has less noise than the altitude rate signal and, in some cases, an altitude rate signal is not readily available.

As can be seen in Figure 52(c), this system gave better performance than the altitude rate configuration.

PITCH FLIGHT PATH CONTROL CONCEPT COMPARISON

The altitude hold mode, as studied, will maintain vertical flight path satisfactorily during cruise. This was expected from previous study results and in-flight demonstrations so that further elaboration is not necessary.

For the "descent rate" mode, two system concepts appear equally satisfactory

- Altitude Rate Feedback
- Lagged Pitch Attitude Feedback

The altitude rate concept offers some advantage in that a desired descent rate may be commanded and maintained without regard to such factors as center-of-gravity position, flap position, and airspeed. However, for the typical light aircraft application, the range of variance of these factors is relatively small.

The lagged pitch attitude concept offers compatible performance for most landing approach situations and has certain mechanization advantages. Altitude rate signals are generally more noisy than pitch attitude signals and frequently are not available in low-cost altitude sensors.

The final choice can be based on the type and quality of sensors available in the aircraft.

SECTION IV
CONCLUSIONS AND RECOMMENDATIONS

CONCLUSIONS

Lateral Flight Path Control

- All configurations studied are theoretically capable of reducing lateral wind effects by considerably more than 85 percent for a given set of conditions, neglecting effects such as system mistrims, biases, drifts, and parameter variations.

- Because of the inevitable presence of system mistrims, biases, etc., configurations employing both roll and heading hold loops are necessary to meet the primary design goal to limit the lateral flight path error to a maximum of 1.3 miles + 0.04 mi/mph of cross-course wind velocity change, in a 15-minute interval.

- Therefore, of the concepts studied, only the Biased Heading Hold and Dual-Mode concepts are capable of meeting the primary design goal. Of these, the Biased Heading Hold concept employing integrated sideslip feedback represents the best compromise of complexity and performance.

- The Tight Roll concepts may reduce the effects of mistrims, biases and so forth, sufficiently to allow the secondary design goal to be achieved. The Roll Attitude Hold with Sideslip Feedback to Aileron configuration is the most promising of the Tight Roll concepts.

(The secondary design goal is to achieve a substantial improvement in flight path control, in the presence of a 20-mph variation in cross-course wind over the performance of the conventional attitude hold autopilot, while attaining a significant reduction in complexity relative to the configuration which is required to meet the primary design goal.)

● Neither the primary nor secondary design goals can be met by the "Single-Axis" concepts or the "Constant Heading Flight Path" concept because of the incapacity of these systems to limit the flight path errors due to mistrims, biases, and parameter variations.

● The general concepts of the strapped-down navigator, the P-matrix, and balanced attitude are not feasible approaches for meeting the design goals because of complexity and incompatibility with the present state of pure-fluid component development.

Pitch Flight Path Control

A conventional-type hold mode is satisfactory for cruise flight path control. The three descent rate control concepts all provide satisfactory control. These concepts are:

● Altitude Rate

● Lagged Pitch Attitude

● Altitude Rate Augmented by Vertical Acceleration

The choice of a simple concept from these three for mechanization and flight testing will be made on the basis of sensor availability and quality.

RECOMMENDATIONS

In order to verify the analytical results obtained in this study, to optimize the configuration design, and to evaluate and demonstrate the performance capabilities of the Fluid Flight Path Control system the following is recommended.

Lateral Flight Path Control

- Design, fabricate and flight test a fluid control system consisting of the "Heading Hold Biased with Integrated Sideslip" configuration.

- Employ the same hardware and test facilities associated with the above recommendation to also evaluate the performance of the "Roll Attitude Control with Sideslip Feedback to Aileron" configuration.

Pitch Flight Path Control

Design, fabricate and flight test a fluid control system consisting of:

- The Altitude Hold Control configuration

- The selected "descent rate control" concept.

REFERENCES

1. "Variation of Strong Wind Speeds with Height from 30 to 500 Feet"
   4th Weather Group pamphlet 105-12-1 February 15, 1962.

2. "An Operational Method of Calculating the Wind Profile in the
   Boundary Layer of the Atmosphere" L. A. Kluichnikova and
   N. Z. Ariel, translated from Glavnovo Geofizicheskovo Obervatoric,
   Trudy No. 94: 39-41, 1960 (American Met. Soc. Translation T-R-381).

3. "P Matrix Guidance" AIAA Paper No. 64-667; presented at Conf.
   Aug. 24-26, 1964, Authors: W.H. Ito and J. E. Tushie

4. "Fluid Navigation Technology Final Report" AFAL-TR-64-287,
   Contract No. AF33(657)-11133, November 1964, CONFIDENTIAL.

.Ɔ

APPENDIX A
SYSTEM EVALUATION CRITERIA AND PROCEDURES

In this appendix the design goals for the Fluid Flight Path Control System are presented. Evaluation criteria, based on these design goals, which were employed to establish the feasibility of proposed concepts are discussed. Proposed procedures to be employed in flight testing are outlined. Finally, a cost and weight comparison of a conventional Honeywell autopilot and a FFPC system is presented.

DESIGN GOALS

Tentative goals for systems considered in this study are expressed in terms of accuracy over a specified reset interval, based on accuracies of conventional control techniques, as well as anticipated pilot preferences. Accuracies of conventional, beam-following systems (Omni, ILS) are regarded as upper accuracy limits. These conventional, beam-following systems are closed-loop systems inherently more accurate than any self-contained, open-loop fluid system.

Lower accuracy limits are those of conventional aircraft attitude control systems. Reasonable goals for the fluid flight path system should lie between the upper and lower extremes selected.

The accuracies of the "beam following" systems and conventional aircraft attitude control systems are discussed and expected flight path accuracies for specific flight conditions and reset intervals given below are tabulated. The accurancy goal of Fluid Flight Path Control System is also determined and entered into this tabulation for comparison.

Initial estimates of reset intervals were made for the various flight conditions, based on past experience and discussions with several private pilots. The values tabulated below are not necessarily optimum at this point. However, they are considered to be realistic and "in the ball park" of what would be acceptable to the pilots. The final values will probably be a compromise between pilot desires and accuracy considerations. They could, therefore, differ somewhat from the following.

Flight Condition	Reset Interval
Cruise	15 minutes
Descent	3 minutes
Climbout	5 minutes
Approach	20 seconds

Flight conditions selected are:

Flight Condition	Speed	Altitude
Cruise	180 mph	10K ft
Descent	180 mph	2000 ft/min.
Climbout	122 mph	1000 ft/min.
Approach	94 mph	500 ft/min.

(These flight conditions are representative for the Cessna 310)

The Cessna 310 light twin aircraft was chosen as a representative airplane on which to base the study program. This selection is partially influenced by the

fact that Honeywell has had considerable experience with this aircraft and has aerodynamic data available.

The lateral flight path capabilities of "beam-follower" systems are as follows:

Lateral Cruise Control-Omni

- Accuracy - ±1 degree steady-state beam following error
- Residual oscillations - no periodic flight path oscillations
- Roll axis activity - less than 2 degrees roll attitude activity on beam (exclusive of bracketing maneuver)
- Range - up to 100 miles

Lateral Approach Control - ILS (localizer)

- Accuracy - ±0.5 degree steady-state beam following error
- Residual oscillations - no periodic oscillation
- Roll activity - less than 2 degrees roll attitude activity on beam
- Range - ≈15 miles

A conventional "heading hold" mode of a representative autopilot has the following capabilities:

Lateral Cruise Control With Heading Hold Mode

- Heading -- This mode is assumed to be a tie-in to a conventional, non-slaved, directional gyro as found on most light aircraft. It is not a true flight path control, since it controls aircraft rather than flight path heading. The mode, however, is often used as an approximation to lateral flight path control.

-A3-

- Accuracy --
    (a) Directional gyro drift - 0.2 deg/min (typical)
    (b) Autopilot error - 0.5 degree
    (c) Wind error - equal to cross-course component of wind

For the pitch axis, "beam-follower" systems have these capabilities:

Vertical Cruise Control - Altitude Hold

- Accuracy - ±20 feet in straight and level flight
           - ±60 feet in turns
- Oscillations - no residual oscillations
- Overshoot - one overshoot for 100 feet overpower

Vertical Approach Control - ILS (Glideslope)

- Accuracy - ±0.1 degree steady-state beam-following error
- Oscillations - no residual oscillation
- Range - 5-10 miles (normal lock-on point)

The Fluid Flight Path Control System (lateral) accuracy goals are based on the following error sources:
    (a) 0.2 deg/min drift in heading reference
    (b) 0.5 degree autopilot mechanization error
    (c) 0.16-mph cross course velocity/mph crosswind or .039 mi crosswind error/mph crosswind

It is assumed that the configuration is a Heading Hold system biased by a signal that continously compensates for cross-course wind changes. Thus error components (a) and (b) have been chosen on the basis of a conventional heading loop.

The reduction of the effect of a crosswind, (c), on the flight path performance is the major contribution of the "Flight Path Control System." As a goal, an 84 percent reduction in the effect of cross wind is selected.

The cross-course error for a 15-minute reset interval at 180-mph cruise speed is computed below:

Gyro drift 0.2/57.3 x 180 x 15 x 0.25 = 1.18 mi

Heading bias error 0.5/57.3 x 180 x 0.25 = 0.39 mi

Control error 0.5/57.3 x 180 x 0.25 = 0.39 mi

Crosswind error = 0.039 mi/mph Δcrosswind

Total fixed error (RSS) = 1.3 mi + 0.039 mi/mph crosswind

proportional error

Total error would be the RSS of the fixed and proportional errors. For crosswind changes up to 20 mph, the cross course deviation between resets would be less than 1.5 miles. This appears to be satisfactory from a pilot acceptance standpoint.

This is therefore selected as the primary design goal. However, any configuration which provides significantly better lateral flight path performance in the presence of lateral wind variations of 20 mph, deserves further consideration, provided it also offers significant hardware simplication possibilities over a configuration which may perform more accurately. Achieving such a configuration is a secondary design goal.

Accuracy goals for the other flight conditions were calculated in a similar manner and are given in Table A1, which also presents, in comparison, deviation data for conventional system.

Vertical flight path accuracy goals are estimates based on what experience suggests would be acceptable to pilots. They do not necessarily reflect present hardware capabilities.

Table A1. Accuracy Goals Proposed for Fluid Flight Path
Control versus Accuracies of Conventional Systems

Flight Condition	Reset Interval	Goals for Lateral Flight Path Accuracy (Miles cross-course deviation in reset interval)	Goals for Vertical Flight Path Accuracy (Altitude error in feet or altitude rate error in ft/min)	Conventional Flight Path Control Accuracy		Conventional Heading Control (Miles cross-course deviation in reset interval)
				Lateral (miles cross-course deviation in reset interval)	Vertical (altitude or altitude rate error)	
Cruise 10K feet 180 mph	15 minutes	1.3 miles +0.04 mi/mph Δ crosswind	±50 ft.	Omni 0.8 miles	Barometric alt. hold ±20 ft	1.24 miles +0.25 mi/mph Δ crosswind
Descent 2000 ft/min 180 mph	3 minutes	0.144 miles +0.008 mi/mph Δ crosswind	100 ft/min	Omni 0.16 miles	-	0.091 miles +0.05 mi/mph Δ crosswind
Climbout 1000 ft/min 122 mph	5 minutes	0.153 miles +0.009 mi/mph Δ crosswind	100 ft/min	Omni 0.175	-	0.1245 miles +0.0 mi/mph Δ crosswind
Approach 500 ft/min 94 mph	20 seconds	0.0065 miles +0.00046 mi/mph Δ crosswind	50 ft/min	ILS 0.0046 miles	ILS 15 ft/min	0.0046 miles +0.0055 mi/mph Δ crosswind

CONCEPT PERFORMANCE EVALUATION CRITERIA

The approach employed in evaluating the performance of proposed concepts is described in this subsection. It is simplified, in accordance with the scope of the study, to allow the survey of a relatively large number of configurations.

Evaluation of the lateral axis performance is based on the extent to which its employment reduces the effect of cross-course wind on the lateral deviation under ideal conditions with crosswind variation restricted to steps and ramps.

The lateral deviation of the flight path due to these crosswinds are computed analytically for each system and are also determined from analog computer simulation recordings.

The computation neglects effects of lateral flight path deviations due to mistrims, biases and thresholds. The analogue computer determination of lateral deviation is also "trimmed" to produce no lateral deviation under no-wind conditions.

Therefore for 20 fps, the lateral deviation in 15 minutes should be no more than 2880 feet. This value is based on the crosswind effect only and is arrived at as follows:

> Lateral deviation without Flight Path Control:
>> 20 fps x 900 sec = 18,000 feet

> Design goal is to reduce this figure by 84 percent or:
>> 0.16 x 18,000 = 2,880 feet

In addition, a qualitative comparison is made with respect to the tolerance of each proposed configuration to mistrims, biases and parameter variations based on the analytical performance equations and analogue computer experience.

A quantitative analysis of sensivities to mistrims, biases, thresholds and parameter variations as well as more complex lateral wind profiles and other disturbances are considered necessary before a final configuration is determined.

The flight path deviation generated by a given configuration as a result of these effects must be considerably smaller than the deviation due to the uncompensated effect of nominal lateral wind variations between resets, if the FFPC is to have any significant effect -- that is, if it is to show a substantial improvement over the performance of a conventional attitude hold configuration in the presence of large lateral wind variations.

Thus, the flight path error in a 15-minute interval due to effects other than the lateral wind variation must be significantly less than:

$$20 \text{ mph} \times 0.25 \text{ hrs.} = 5 \text{ miles}$$
(based on the effect of a 20-mph step change in lateral wind magnitude)

This figure can be used as a criterion to judge the acceptability of the errors produced by a given configuration as a result of mistrims, biases, etc. (i. e., all effects other than those due to lateral wind variations).

Evaluation of proposed pitch axis configuration is based on analogue computer results satisfactory performance is determined by comparison of these results with design goals for Vertical Flight Path accuracy listed in Table A1.

FLIGHT EVALUATION PROCEDURES

A procedure to be employed for flight testing a Fluid Flight Path Control system is outlined:

(1) Initially align the airplane's actual ground track to a aesired flight path. This can be done by the use of a drift

meter* or, more desirably, by means of "Omni" lateral course error indicator, installed for test purposes. If the drift meter is used, then all test flight paths should be chosen to intercept two readily identifiable landmarks, 15 minutes apart.

(2) Engage the Fluid Flight Path System when the first landmark is intercepted. (Up to this point the flight path is maintained manually, through drift meter observations or observations of the "Omni" lateral course deviation indicator.).

(3) After 15 minutes establish aircraft position and compute lateral deviation.

It is suggested that the use of a tracking radar and plotting board would immeasurably expedite flight path control evaluation. Employment of a tracking radar with suitable range and accuracy obviates the necessity for instrumentation of the test vehicle with a drift meter or an "Omni" facility, since a 15-minute run could start at any time, without the necessity of establishing any particular flight path with precision.

A relatively large number of runs at different bearings with respect to the prevailing wind, and under different wind conditions, would be necessary to support any conclusions.

---

* A drift meter to align the aircraft to a desired flight path need not be a precision device, and offers a simple on-board means for re-alignment at preset intervals (every 15 minutes, for example) in the operational situation. From the drift meter, the pilot reads the drift angle, ψ_d, with respect to his heading, ψ_H. This angle plus the magnetic heading equals his actual flight path bearing, ψ_{FP}. The re-alignment procedure is to manual steer until $\psi_H + \psi_d = \psi_{FP \ des.}$, where $\psi_{FP \ des}$ is the desired flight path bearing. At that time, the FFPC is re-engaged.

If runs under FFPC are alternated with runs under Heading Hold control,
(if available), a direct measure of improvement over the conventional attitude
hold approach can be obtained. In addition, if the flight path of the airplane
under Heading Hold Control is plotted, a means is provided for gaging the wind
conditions over the test course.

An inertial reference package should be installed on board to record in-flight
attitude accurately. All sensor outputs as well as control surface (or control
surface actuator inputs) should be recorded.

Evaluation of the aircraft pitch axis is simpler. Since the control is a
barometric altitude type, the altitude error is available for direct recording.

COST AND WEIGHT COMPARISON

An estimated cost and weight tabulation of one of the more complex Fluid
Flight Path Control System mechanizations studied is given in Table A2.
This is a Heading Hold Biased with Integral of Sideslip. Weight and cost for
a pure-fluid system mechanization is compared with a mechanization using
H-14 system type components.

Table A2. Cost and Weight Comparison – Conventional
and Fluid Component Mechanization

Element	Conventional Mechanization (H14 Type)		Pure-Fluid Components	
	Weight (lbs)	Cost	Weight (lbs)	Cost
1. Rate Sensor 3 required	1.7 each 5.1	$ 250.00 each 750.00	0.3 each 0.9	$ 52.00 each 156.00
2. Attitude Sensor	3	477.00	0.75	203.00
3. Altitude Sensor	1.4	370.00	1.25	350.00
4. Computer	7	1,033.00	0.93	890.00
5. Servos 3 required (conv.) 4 required (fluid)	5.8 each 17.4	198.00 each 594.00	4 each 16	134.00 each 536.00
6. Directional Gyro	3.0	477.00	3	585.00
7. Sideslip Sensor	1.5	515.00	1.5	500.00
8. Sideslip Transmitter	4.5	1,800.00	(Not required)	(Not required)
9. Integrator	0.25	100.00	0.1	55.00
10. Function Selector	1.0	368.00	1.0	69.00
TOTAL	44.15	$6,484.00	25.43	$3,344.00

APPENDIX B
LATERAL FLIGHT PATH CONCEPT ANALYSIS

GENERAL

In this appendix the performance of the various lateral flight path control configurations listed in the body of this report are investigated mathematically, and relationships between parameters and performance are developed.

EQUATIONS OF MOTION

The equations of motion with the terms normally considered are:

$$\dot{p} = L_p p + L_r r + L_\beta \beta + L_{\delta a}\delta_a + L_{\delta r}\delta_r$$

$$\dot{r} = N_p p + N_r r + N_\beta \beta + N_{\delta a}\delta_a + N_{\delta r}\delta_r \qquad \text{(B1)}$$

$$U_1\dot{\beta} = Y_p p + g\phi + (Y_r - U_1)r + Y_v\beta U_1 + Y_{\delta r}\delta_r$$

These equations are approximated by the following:

$$\dot{p} = L_p p + L_r r + L_\beta \beta + L_{\delta a}\delta_a$$

$$\dot{r} = N_r r + N_\beta \beta + N_{\delta r}\delta_r \qquad \text{(B2)}$$

$$U_1\dot{\beta} = Y_v\beta U_1 + g\phi - U_1 r$$

These approximations will not change the general form of response and are believed adequate to screen concepts before undertaking more detailed study.

Stability derivatives for the "cruise condition" are used.

In addition, the following kinematical relations are used:

$$
\begin{bmatrix} \dot{U} \\ \dot{V} \\ \dot{W} \end{bmatrix} = \frac{1}{m} \begin{bmatrix} F_x \\ F_y \\ F_z \end{bmatrix} - \begin{bmatrix} O & -r & q \\ r & O & -p \\ -q & p & O \end{bmatrix} \begin{bmatrix} U \\ V \\ W \end{bmatrix} + a \begin{bmatrix} O \\ O \\ q \end{bmatrix}
$$

$$
\begin{bmatrix} \dot{X}_G \\ \dot{Y}_G \\ \dot{Z}_G \end{bmatrix} = (a)^{-1} \begin{bmatrix} U \\ V \\ W \end{bmatrix}
$$

$$
\begin{bmatrix} U_a \\ V_a \\ W_a \end{bmatrix} = -(a) \begin{bmatrix} \dot{X}_{WG} \\ \dot{Y}_{WG} \\ \dot{Z}_{WG} \end{bmatrix} + \begin{bmatrix} U \\ V \\ W \end{bmatrix}
$$

$$
(a) = \begin{bmatrix} a_{11} & a_{12} & a_{13} \\ a_{21} & a_{22} & a_{23} \\ a_{31} & a_{32} & a_{33} \end{bmatrix} = \begin{bmatrix} (c\theta c\psi) & (c\theta s\psi) & -s\theta \\ (s\phi s\theta c\psi - c\phi s\psi) & (s\phi s\theta s\psi + c\phi c\psi) & s\phi c\theta \\ (c\phi s\theta c\psi + s\phi s\psi) & (c\phi s\theta s\psi - s\phi c\psi) & c\phi c\theta \end{bmatrix}
$$

Restricting ϕ and ψ to small angles and keeping $\dot{X}_{WG} = \dot{Z}_{WG} = 0$, the kinematic equations reduce to:

$$\dot{Y}_G = U_1 \psi + V \tag{B3}$$

$$V_a = -\dot{Y}_{WG} + V \tag{B4}$$

In addition, for small values of angle of attack and sideslip, the sideslip angle can be expressed as

$$\beta = \frac{V_a}{U_1} \qquad\qquad\qquad \text{(B4a)}$$

Combining with the reduced expressions for $\dot{Y}_G$ and V_a, we have:

$$\dot{Y}_G - \dot{Y}_{WG} = U_1(\psi + \beta) \qquad\qquad \text{(B5)}$$

This last relationship is used to establish the initial value of sideslip angle, β_o, for a step change in the cross-course component of wind (i.e., step in lateral wind), $\dot{Y}_{WG_o}$.

Assuming: $\dot{Y}_G = \dot{Y}_{WG} = \psi = \beta = 0$ at t_o^-. Then, when:

$$\dot{Y}_{WG} \text{ at } t_o^+ = \dot{Y}_{WG_o}$$

Since

$$\psi \text{ at } t_o^+ = 0$$

$$\dot{Y}_G \text{ at } t_o^+ = 0$$

We have:

$$\beta \text{ at } t_o^+ \triangleq \beta_o = \frac{-\dot{Y}_{WG_o}}{U_1} \qquad\qquad \text{(B6)}$$

From Equation (B5)

$$\dot{Y}_G = U_1 (\psi + \beta) + \dot{Y}_{WG} \qquad\qquad \text{(B7)}$$

Following a step in wind, Y_{WG_o}, the steady state can be expressed as:

$$\dot{Y}_{G_{ss}} = U_1 (\psi_{ss} + \beta_{ss}) + \dot{Y}_{WG_o} \qquad\qquad \text{(B8)}$$

For the wings level solution to the flight path control problem, we desire:

$$\dot{Y}_{G_{ss}} = 0$$

and

$$\beta_{ss} = 0$$

Substituting in Equation (B8), we have:

$$O = U_1 (\psi_{ss_{des.}} + O) + \dot{Y}_{WG_o}$$

or

$$\psi_{ss_{(des.)}} = \frac{-\dot{Y}_{WG_o}}{U_1}$$

On combining with Equation (B6)

$$\psi_{ss_{(des.)}} = \beta_o \tag{B9}$$

A SINGLE-AXIS CONCEPT

A1 Free Airplane - Controls Locked

For this condition $\delta_r = -\delta_{a} = 0$, and the equations of motion, in matrix form become for a step input of Y_{WG_o}

$$
\begin{bmatrix}
-S + L_p & L_r & L_\beta \\
0 & -S + N_r & N_\beta \\
\dfrac{g}{S} & -U_1 & U_1(-S + Y_v)
\end{bmatrix}
\begin{bmatrix}
p \\
r \\
\beta
\end{bmatrix}
=
\begin{bmatrix}
0 \\
0 \\
-U_1 \beta_o
\end{bmatrix}
\qquad (B10)
$$

The solution for $\psi(S)$ is found to be

$$
\psi = \frac{1}{S} r = \frac{-\beta_o \left[-N_\beta S + N_\beta L_p \right]}{\left[AS^4 + BS^3 + CS^2 + DS + E \right]}
\qquad (B11)
$$

where

$A = 1$

$B = -\left[N_r + Y_v + L_p \right] = 8.02$

$C = +\left[N_\beta + Y_v(N_r + L_p) + L_p N_r \right] = 26.81$

$$D = -\left[N_\beta L_p + Y_v L_p N_r\right] - g\frac{L_\beta}{U_1} = 124$$

$$E = -\frac{g}{U_1}\left[N_\beta L_r - L_\beta N_r\right] = 0.916$$

(Coefficients were evaluated using the cruise condition stability derivations.)

Applying the final value theorem to Equation (B11), we obtain:

$$\lim_{t \to \infty} \psi(t) = \lim_{S \to 0} S\psi(S) = 0$$

However the denominator of Equation (B11) contains a real root that is much smaller than the remaining roots and can therefore be factored out approximately, as follows:

$$(AS^3 + BS^2 + CS + D)(S + a) = AS^4 + (B + aA)S^3$$
$$+ (C + aB)S^2 + (D + aC)S + E \qquad (B12)$$
$$\approx AS^4 + BS^3 + CS^2 + DS + E$$

Since $aA \ll B$
$aB \ll C$
$aC \ll D$

Using Equation (B12), Equation (B11) can be written as:

$$\psi(S) \approx \frac{-\beta_o\left[-N_\beta S + N_\beta L_p\right]}{\left[AS^3 + BS^2 + CS + D\right]\left[S + a\right]}$$

By comparing terms in Equation (B12), we obtain:

$$a = \frac{E}{D} = \frac{0.916}{124} = 0.0074 \qquad \text{(B13)}$$

Corresponding to a time constant of 135 secs.

The presence of this real root indicates that a stable condition is not reached at the end of the weathercocking activity (i. e., at the end of the initial transient). It will be shown that the amount of Roll attitude that exists at the end of the initial transient is proportional to the magnitude of "a".

The sign of "a" also determines whether $\psi_{(t)}$ converges or diverges. For a < 0, $\psi_{(t)}$ diverges. The unstable response is generally referred to as "Spiral Divergence." It will be shown later that the Roll Angle attained at the end of the initial transient changes sign as this mode goes from the convergent to the divergent region.

The remaining three roots of the denominator of Equation (B11) determine the initial transient. The value of heading at the end of this initial transient, $\psi^*_{(t)}$ (i. e., at the end of the weathercocking action) can be found by applying a modified form of the Final Value Theorem to Equation (B13).

Thus,

$$\psi^*_{(t)} = \lim_{S \to \xi} s\psi_{(S)}$$

Where ξ is much larger than "a" but much smaller than the smallest of the three remaining roots. Such a value of ξ exists since there is a large separation between the initial response time and the slowest response time.

Applying the modified Final Value Theorem to Equation (B11), we obtain:

$$\psi^*_{(t)} = \lim_{S \to \dot{\xi}} S\psi_{(S)} = \frac{-\beta_o N_\beta L_p}{D}$$

$$= \frac{-\beta_o N_\beta L_p}{-N_\beta L_p - Y_v L_p N_r - g \frac{L_\beta}{U_1}} = \beta_o \frac{120}{124} = +0.97 \beta_o \qquad (B14)$$

Equation (B14) indicates that, after the initial transient, ψ has changed an amount which compensates for 97 percent of the effect of the wind step. ψ_{ss} does not equal β_o because during the time the airplane yaws to a zero sideslip attitude it has achieved a small velocity in the direction of the cross wind.

However, the decaying response introduces an additional error, since ψ decays from the correct value to zero. This error is found as follows:

$$Y_G = \int_o^T \dot{Y}_G dt = \int_o^T U_1 \beta_o (1 - e^{-at}) dt$$

$$= U_1 \beta_o \left(t + \frac{1}{a} e^{-at} \right) \Big|_o^T$$

Therefore,

$$Y_G = U_1 \beta_o \left[T - \frac{1}{a} \left(1 - e^{-aT} \right) \right] \qquad (B15)$$

Equation (B15) yields an error of about 7000 feet at the end of one time constant. It is clear that, for the flight path application, the slow return of ψ to its initial value must either be eliminated or the time constant made larger than 900 seconds (based on a 15-minute reset interval). In addition, the difference between aircraft yaw after the initial transient and β_o must be reduced.

It will now be shown that the slow response mode is related to the roll angle accumulated during the initial transient.

Solving Equation (B10) for $p_{(S)}$, we obtain:

$$p = \frac{-U_1 \beta_o \left[L_r N_\beta - L_\beta (-S + N_r) \right]}{\dfrac{-U_1}{S} \left[AS^4 + BS^3 + CS^2 + DS + E \right]} \tag{B16}$$

Or, using the results expressed in Equation (B12)

$$p = \frac{-\beta_o \left[L_r N_\beta - L_\beta (-S + N_r) \right]}{\dfrac{-1}{S} \left[AS^3 + BS^2 + CS + D \right] \left[S + a \right]} \tag{B17}$$

ϕ_{ss} can be shown to be zero (for a stable system) by application of the Final Value Theorem:

$$\phi_{ss} = \lim_{S \to 0} S\, \phi_{(S)} = \lim_{S \to 0} S \left[\frac{1}{S} P_{(S)} \right] = 0$$

To find $\phi^{*}_{(t)}$ ($\phi_{(t)}$ at end of the initial transient) the modified final value theorem is applied to Equation (B17).

$$\phi_{(t)}^{*} = \lim_{S \to \xi} S\left[\frac{1}{S} P_{(S)}\right]$$

$$= \frac{+\beta_o\left[L_r N_\beta - L_\beta N_r\right]}{D}$$

$$= \frac{+\beta_o\left[L_r N_\beta - L_\beta N_r\right]}{-N_\beta L_p - Y_v L_p N_r - g\dfrac{L_\beta}{U_1}} \tag{B18}$$

In terms of the coefficient of the characteristic equation:

$$\phi_{(t)}^{*} = \frac{+\beta_o\left(\dfrac{U_1}{g}\right)\ (E)}{D} \tag{B19}$$

but $a = \dfrac{E}{D}$.

$$\therefore \qquad \phi_t^{*} = -\beta_o\, a\, \frac{U_1}{g} \tag{B20}$$

Equation (B19) demonstrates the proportionality between the time constant $1/a$ and the roll angle attained at the end of the initial transient.

A2 Single-Axis with Sideslip Feedback to Rudder

The free airplane was seen to reach a yaw angle at the end of the initial transient of:

$$\psi^*_{(t)} = \frac{-\beta_o N_\beta L_p}{-N_\beta L_p - Y_v L_p N_r - g \frac{L_\beta}{U_1}} \qquad (B21)$$

And an exponential decay away from this value with a time constant of:

$$\tau = \frac{1}{a} = \left[\frac{D}{E}\right] = \frac{-N_\beta L_p - Y_v L_p N_r - g \frac{L_\beta}{U_1}}{-\frac{g}{U_1}\left[N_\beta L_r - L_\beta N_r\right]} \qquad (B22)$$

For β feedback to the rudder, the control equation becomes:

$$\delta_r = \delta_{r\beta}\beta + \delta_{rr}\, r$$

$$\delta_a = 0.$$

And matrix Equation (B10) is modified only by changing N_β to $\underline{N}_\beta$ where

$$\underline{N}_\beta = N_{\delta r}\,\delta_{r\beta} + N_\beta \qquad (B23)$$

Equations (B14) and (B13) become:

$$\psi^*_t = \frac{-\beta_o \underline{N}_\beta L_p}{-\underline{N}_\beta L_p - Y_v L_p N_r - g \frac{L_\beta}{U_1}} \qquad (B24)$$

and

$$a = \frac{E}{D} = \frac{-\frac{g}{U_1}\left[\underline{N}_\beta L_r - L_\beta N_r\right]}{-\underline{N}_\beta L_p - Y_v L_p N_r - g \frac{L_\beta}{U_1}} \qquad (B25)$$

To improve the flight path control, we wish to approach:

$$\psi^*_t = \beta_o$$

and

$$a = 0$$

The error in $\psi^*_{(t)}$, $\epsilon_{\psi^*_{(t)}}$, can be expressed as:

$$\epsilon_{\psi^*_{(t)}} = \beta_o \left[\frac{Y_v L_p N_r - g \frac{L_\beta}{U_1}}{\underline{N}_\beta L_p} \right] \tag{B26}$$

The major contribution to the flight path control error results from a non-zero "a".

Selecting $\underline{N}_\beta$ to make "a" = 0, we have, from Equation (B25):

$$\underline{N}_\beta = \frac{L_\beta N_r}{L_r} \tag{B27}$$

and from Equation (B23):

$$\delta_{r\beta} = \frac{\underline{N}_\beta - N_\beta}{N_{\delta r}}$$

Therefore, for the cruise flight condition, $\underline{N}_\beta$ and $\delta_{r\beta}$ for "a" = 0 are

$$\underline{N}_\beta = \frac{(-23.4)\,(-1.06)}{0.892} = 27.8$$

$$\delta_{r\beta} = \frac{27.8 - 17.84}{-14.24} = -0.698$$

With the addition of a yaw damper to give 0.32 damping ($\delta_{rr} = 0.15$), N_r is replaced by $\underline{N}_r = N_{\delta r}\delta_{rr} + N_r$ and equals -3.2, and $\underline{N}_\beta$ and $\delta_{r\beta}$ for "a" = 0 become:

$$\underline{N}_\beta = \frac{(-23.4)\ (-3.2)}{0.892} = 83.8$$

$$\delta_{r\beta} = \frac{83.8 - 17.84}{-14.24} = -4.63$$

The corresponding errors in $\psi^*_{(t)}$ are from Equation (B26)

(a) Without damper $(\delta_{rr} = 0,\ \underline{N}_r = N_r = -1.06)\ \dot{\underline{N}}_\beta = 27.8$

$$\epsilon_{\psi^*_{(t)}} = -0.00371\ \beta_o$$

(b) With damper $(\delta_{rr} = 0.15,\ \underline{N}_r = -3.2,\ \underline{N}_\beta = 83.8)$

$$\epsilon_{\psi^*_{(t)}} = 0.00488 \beta_o$$

A3 Single-Axis with Sideslip Feedback to Aileron

The constant "a" can also be made zero by an appropriate change in the effective L_β. In this case the control equation becomes

$$\delta_a = \delta_{a\beta}\beta$$

$$\delta_r = \delta_{rr}r$$

and Equations (B10), (B14), (B21), (B25), and (B26) hold, with L_β changed to $\underline{L}_\beta$ where:

$$\underline{L}_\beta = L_{\delta a}\,\delta_{a\beta} + L_\beta \tag{B28}$$

To make "a" zero, it can be seen from Equation (B25) that:

$$\underline{L}_\beta = \frac{N_\beta L_r}{N_r} \tag{B29}$$

For cruise flight conditions, $\underline{L}_\beta$ and $\delta_{a\beta}$ for zero "a", are:

$$\underline{L}_\beta = \frac{17.84\,(0.892)}{-1.06} = -15.01$$

$$\delta_{a\beta} = \frac{\underline{L}_\beta - L_\beta}{L_{\delta a}} = \frac{-15.01 - (-23.4)}{-36.8} = -0.228$$

With a yaw damper added, such that $\delta_{rr} = 0.15$ and $\underline{N}_r = -3.2$:

$$\underline{L}_\beta = \frac{(17.84)\,(0.892)}{-3.2} = -4.96$$

$$\delta_{a\beta} = \frac{-4.96 - (-23.4)}{-36.8} = -0.5.$$

Without damper:

$$(N_r = -1.06, \underline{L}_\beta = -15.01)$$

$$\epsilon_{\psi^*(t)} = 0.000141 \, \beta_o$$

With damper:

$$(\underline{N}_r = -3.2, \underline{L}_\beta = -4.96)$$

$$\epsilon_{\psi^*(t)} = -0.045 \, \beta_o$$

A4 Single-Axis with Yaw Rate Feedback to Aileron

Finally, "a" can be made equal to zero by changing the effective value of L_r. In this case the control equation becomes:

$$\delta_a = \delta_{ar} r$$

$$\delta_r = \delta_{rr} r$$

and Equations (B10), (B14), (B21), and (B23) hold with L_r changed to $\underline{L}_r$ where:

$$\underline{L}_r = L_{\delta a} \delta_{ar} + L_r \tag{B29a}$$

From Equation (B25), it is seen that for "a" = 0, $\underline{L}_r$ is:

$$\underline{L}_r = \frac{L_\beta N_r}{N_\beta}$$

Therefore, for cruise conditions for "a" = 0, we have

$$\underline{L}_r = \frac{(-23.4)(-1.06)}{17.84} = 1.392$$

$$\delta_{ar} = \frac{\underline{L}_r - L_r}{L_{\delta a}} = \frac{1.392 - 0.892}{-36.8} = -0.0136$$

With dampers ($\delta_{rr} = 0.15$, N_r is replaced by $\underline{N}_r = -3.2$).

$$\underline{L}_r = \frac{(-23.4)(-3.2)}{17.84} = 4.2$$

$$\delta_{ar} = \frac{4.2 - 0.892}{-36.8} = -0.0899$$

The corresponding errors in $\psi^*_{(t)}$ are from Equation (B26):

Without dampers: $\quad \epsilon_{\psi^*_{(t)}} = 0.00579 \beta_o$

With dampers: $\quad \epsilon_{\psi^*_{(t)}} = -0.0365 \beta_o$

₃ TIGHT ROLL CONTROL CONCEPTS

The purpose of this set of configurations is to eliminate the long-term response by preventing a roll angle from occurring at the time the "weathercocking" activity ends. This is accomplished by adding a roll attitude hold loop. In addition, by various usages of β and r feedbacks the steady-state value of $\psi_{(t)}$ can be made equal to β_o.

B1   Roll Attitude Control (Plus Yaw Damper)

In this configuration the control equation becomes:

$$\delta_r = \delta_{rr} \cdot r$$

$$\delta_a = \delta_{a\phi} \frac{p}{s} + \delta_{ap} p$$

Combining these with the vehicle equation of motion, we have in matrix form, for a step input of $\dot{Y}_{WG_o}$:

$$
\begin{bmatrix}
-S + \underline{L}_p + \dfrac{K_\phi}{S} & L_r & L_\beta \\
0 & -S + \underline{N}_r & N_\beta \\
\dfrac{g}{S} & -U_1 & U_1(-S + Y_v)
\end{bmatrix}
\cdot
\begin{bmatrix}
p \\
r \\
\beta
\end{bmatrix}
=
\begin{bmatrix}
0 \\
0 \\
-U_1 \beta_o
\end{bmatrix}
\tag{B30}
$$

where

$$K_\phi = L_{\delta a} \delta_{a\phi}$$

$$\underline{N}_r = N_r + N_{\delta r} \delta_{rr}$$

$$\underline{L}_p = L_{\delta a} \delta_{ap} + L_p$$

Solving Equation (B30) for $\psi_{(S)}$, we obtain:

$$\psi_{(S)} = \frac{1}{S}r_{(S)} = \frac{-\frac{1}{S}\beta_o U_1\left[-SN_\beta + N_\beta \underline{L}_p + \frac{N_\beta K_\phi}{S}\right]}{\frac{U_1}{S}\left[AS^4 + BS^3 + CS^2 + DS + E\right]} \qquad (B31)$$

where

$$A = 1$$

$$B = -\left[N_r + Y_v + \underline{L}_p\right]$$

$$C = \left[N_\beta + Y_v(\underline{N}_r + \underline{L}_p) + L_p \underline{N}_r - K_\phi\right]$$

$$D = -\left[N_\beta \underline{L}_p + Y_v \underline{L}_p \underline{N}_r - K_\phi(\underline{N}_r + Y_v)\right] - g\frac{L_\beta}{U_1}$$

$$E = \frac{-g}{U_1}\left[N_\beta L_r - L_\beta \underline{N}_r\right] - (N_\beta + \underline{N}_r Y_v)K_\phi$$

Applying the final value theorem, we get:

$$\psi_{ss} = \lim_{t \to \infty} \psi_{(t)} = \lim_{S \to o} S\,\psi(S) = \frac{-\beta_o N_\beta K_\phi}{E}$$

$$\psi_{ss} = \frac{-\beta_o N_\beta K_\phi}{\frac{-g}{U_1}\left[N_\beta L_r - L_\beta \underline{N}_r\right] - (N_\beta + \underline{N}_r Y_v)K_\phi} \qquad (B32)$$

Equation (B32) indicates that the slow return of ψ to initial value has been eliminated.

Typically, δ_{a_ϕ} is about 1.00, giving $K_\phi = -36.8$ at cruise conditions. Using this value and cruise condition values for the stability derivatives (also assuming $\underline{N}_r = N_r$, no yaw damper, we have for ψ_{ss}) from (B32):

$$\psi_{\tilde{s}\tilde{s}} = 0.982 \, \beta_o.$$

For the numbers used, it is seen that the disturbing effect of the wind step is reduced by 98.2 percent. Again, as discussed, before ψ_{ss} does not equal β_o, because the airplane has achieved some velocity in the cross-wind direction, while it weathercocked.

Dividing the numerator and denominator of Equation (B32) by $N_\beta K_\phi$, subtracting β_o from the resultant expression, and dropping second-order terms gives the steady-state yaw angle error, we obtain:

$$\epsilon_{(\psi_{\tilde{s}\tilde{s}})} \approx \frac{-\beta_o \left[\underline{N}_r K_\phi Y_v + \frac{g}{U_1} \left(N_\beta L_r - L_\beta \underline{N}_r \right) \right]}{N_\beta K_\phi} \tag{B33}$$

B.2 Roll Attitude Control with Sideslip Feedback to the Rudder

In this configuration the control equation becomes (assuming a yaw damper):

$$\delta_a = \delta_{a\phi}\phi + \delta_{ap}p$$

$$\delta_r = \delta_{rr}r + \delta_{r\beta}\beta$$

Equations (B30) and (B33) hold for this configuration, with N_β replaced by $\underline{N}_\beta$, where:

$$\underline{N}_\beta = N_{\delta r}\delta_{r\beta} + N_\beta$$

Equation (B33) becomes:

$$\epsilon_{\psi_{(ss)}} \approx \frac{-\beta_o\left[\underline{N}_r \cdot K_\phi Y_v + \frac{g}{U_1}\left(\underline{N}_\beta L_r - L_\beta \underline{N}_r\right)\right]}{N_\beta K_\phi}$$

It is clear that the error can be reduced by increasing $\underline{N}_\beta$, but completely eliminated for finite values.

B3 Roll Attitude Control with Sideslip Feedback to Aileron

In this configuration the control equations are:

$$\delta_a = \delta_{a\phi}\phi + \delta_{a\beta}\beta + \delta_{ap}p$$

$$\delta = \delta_{rr}r \qquad \text{(yaw damper)}$$

Equations (B30) and (B33) remain valid, with L_β replaced by $\underline{L}_\beta$, where:

$$\underline{L}_\beta = L_{\delta a}\delta_{a\beta} + L_\beta$$

Equation (B33) becomes:

$$\epsilon_{\psi_{(ss)}} \approx \frac{-\beta_o\left[\underline{N}_r \cdot K_\phi Y_v + \frac{g}{U_1}\left(\underline{N}_\beta L_r - L_\beta \underline{N}_r\right)\right]}{N_\beta K_\phi}$$

To make: $\epsilon_{\psi_{(ss)}} = 0$, we must have:

$$L_\beta \approx \frac{K_\phi Y_v U_1}{g} + \frac{N_\beta L_r}{\underline{N}_r}$$

For cruise conditions and with $\delta_{a\phi} = 1$ ($\therefore K_\phi = -36.8$) and $\underline{N}_r = -3.2$

$$\underline{L}_\beta = 85.6$$

$$\therefore$$

$$\delta_{a\beta} = \frac{\underline{L}_\beta - L_\beta}{L_{\delta a}} = \frac{85.6 + 23.4}{-36.8} = -2.96$$

for zero error in ψ_{ss}.

B4 Roll Attitude Control with "Servoed β" Feedback to Aileron

This configuration was originally conceived as employing a β sensor continuously aligned to the flight path. The servoed β sensor signal is summed with ψ and fedback to the aileron. This is shown in the block diagram of Figure 22.

The aileron control equation for this configuration is:

$$\delta_a = \delta_{a\phi}\phi + \delta_{a\beta_s}\beta_s + \delta_{a\psi}\psi + \delta_{ap}p$$

where β_s is the output of the platform mounted β sensor and $\beta_s = \beta + \psi$.

Therefore, the control equation becomes:

$$\delta_a = \delta_{a\phi}\frac{p}{S} + \delta_{a\beta_s}\beta + \delta_{a\beta_s}\psi + \delta_{a\psi}\frac{r}{S} + \delta_{ap}p$$

Combining this control equation with the equations of motion, for a step input of $\dot{Y}_{WG}$, we have:

$$
\begin{bmatrix}
-S + \underline{L}_p + \dfrac{K_\phi}{S} & L_r + \dfrac{K_\psi}{S} & \underline{L}_\beta \\[3mm]
0 & -S + \underline{N}_r & N_\beta \\[3mm]
\dfrac{g}{S} & -U_1 & U_1(-S + Y_v)
\end{bmatrix}
\cdot
\begin{bmatrix}
p \\[3mm] r \\[3mm] \beta
\end{bmatrix}
=
\begin{bmatrix}
0 \\[3mm] 0 \\[3mm] -U_1\beta
\end{bmatrix}
\qquad \text{(B34)}
$$

where

$$K_\phi = L_{\delta a}\,\delta_{a\phi}$$

$$K_\psi = L_{\delta a}\left(\delta_{a\beta_s} + \delta_{a\psi}\right)$$

$$\underline{L}_\beta = L_{\delta a}\,\delta_{a\beta_s} + L_\beta$$

$$\underline{L}_p = L_{\delta a}\,\delta_{ap} + L_p$$

When the gains are adjusted so that

$$K_\psi = 0,$$

and

$$\delta_{a\beta_s} = -\delta_{a\psi},$$

this configuration is exactly the same as configuration (B3) as can be seen from a comparison of Equation (B34) with Equation (B30). Simulation results bear this out.

When

$$\delta_{a\beta_s} > \delta_{a\psi},$$

we have a heading hold loop via the ailerons with β feedback to ailerons.

Thus, unless $\delta_{a\beta_s} = -\delta_{a\psi}$ the configuration tends to maintain the initial heading rather than adjust heading to compensate for the step in the cross-flight path wind component.

A unique mode of operation is noted if a roll attitude sensor threshold is introduced. In this case, we have, for roll angles within the roll attitude sensor threshold, a mode of operation equivalent to "Single Axes with Side-slip Feedback to Aileron", (see Section A3). For the gains employed:

$$L_\beta N_r < N_\beta L_r$$

which corresponds to the spiral divergence case. Therefore, in this region the roll angle is driven away from zero until the roll angle exceeds the roll threshold. At that time, the roll attitude feedback drives the angle back to zero. With the gains and inertias of the system, the roll angle is apparently returned past the zero point and the divergent characteristic carries it to the opposite roll limit, and the process continues. The average roll angle over a cycle, is from the traces, close to zero since the airplane net yaw rate over a cycle is also close to zero.

Thus, the yaw angle generated during the initial response to the wind step is maintained. The amount of yaw error at the end of the short-term transient can be found from Equation (B26).

This mode of operation seems to tolerate the roll threshold without drastic degradation of the accuracy of performance relative to the roll attitude with sideslip to aileron; however, it does introduce a limit cycle that may be unacceptable to a pilot.

C BIASED HEADING CONCEPTS

C1 Heading Hold Biased by Side Velocity

The block diagram for this system is given in Figure 26.

The control equations are:

$$\delta_a = \delta_{a\phi}\frac{p}{S} + \delta_{ap}p$$

$$\delta_r = \delta_{r\psi}\frac{r}{S} + \delta_{rv}V + \delta_{rr}r$$

V can be expressed as:

$$V = V_a + \dot{Y}_{WG} = U_1(\beta + \frac{\dot{Y}_{WG}}{U_1}) \left[\text{See Equations (B4) and (B4a)}\right]$$

Substituting for V, δ_r becomes

$$\delta_r = \delta_{r\psi}\frac{r}{S} + \delta_{rv}U_1(\beta - \frac{\dot{Y}_{WG}}{U_1}) + \delta_{rr}r$$

In addition, for a step in $\dot{Y}_{WG} = \dot{Y}_{WG_o}$

$$\mathcal{L}(\dot{Y}_{WG}) = \frac{\dot{Y}_{WG_o}}{S} = -\frac{U_1\beta_o}{S}; \left[\text{see Equation (B6)}\right]$$

Combining the control equations with the vehicle equations of motion and expressing the result in matrix form, we have for a step in $\dot{Y}_{WG}$:

$$
\begin{bmatrix}
-S + \underline{L}_p + \dfrac{K_\phi}{S} & L_r & L_\beta \\[12pt]
0 & -S + \underline{N}_r + \dfrac{K_\psi}{S} & \underline{N}_\beta \\[12pt]
g/S & -U_1 & U_1(-S+Y_v)
\end{bmatrix}
\cdot
\begin{bmatrix}
p \\[12pt] r \\[12pt] \beta
\end{bmatrix}
=
\begin{bmatrix}
0 \\[12pt] N_{\delta r}\delta_{rv}U_1\dfrac{\beta_o}{S} \\[12pt] -U_1\beta_o
\end{bmatrix}
\qquad (B35)
$$

where

$$\beta_o = -\frac{\dot{Y}_{WG_o}}{U_1}$$

$$\underline{L}_p = L_{\delta a}\delta_{ap} + L_p$$

$$K_\phi = L_{\delta a}\delta_{a\phi}$$

$$K_\psi = N_{\delta r}\delta_{r\psi}$$

$$\underline{N}_\beta = N_{\delta r}\delta_{rv}U_1 + N_\beta$$

$$\underline{N}_r = N_{\delta r}\delta_{rr} + N_r$$

$$S = \text{Laplace Operator}$$

Solving for $r(S)$ we obtain:

$$
r = \frac{+N_{\delta r}\delta_{rv}U_1\dfrac{\beta_o}{S}\left[U_1(-S+Y_v)(-S+L_p+\dfrac{K_\phi}{S}) - L_\beta\, g/S\right]}{\Delta} \qquad (B36)
$$

$$
+ \frac{+U_1\beta_o\,\underline{N}_\beta\,(-S+L_p+\dfrac{K_\phi}{S})}{\Delta}
$$

where

$$\Delta = -\frac{U_1}{S^2} [AS^5 + BS^4 + CS^3 + DS^2 + ES + F]$$

$$A = 1$$

$$B = -[\underline{N}_r + Y_v + \underline{L}_p]$$

$$C = \underline{N}_r Y_v + \underline{L}_p (Y_v + N_r) + \underline{N}_\beta - K_\psi - K_\phi$$

$$D = -[\underline{L}_p (\underline{N}_r Y_v + \underline{N}_\beta) - K_\psi (\underline{L}_p + Y_v) - K_\phi (Y_v + \underline{N}_r)] - \frac{gL_\beta}{U_1}$$

$$E = -\frac{g}{U_1} [\underline{N}_\beta L_r - L_\beta N_r] - (\underline{N}_r Y_v - K_\psi + \underline{N}_\beta) K_\phi$$

$$F = \frac{gL_\beta K_\psi}{U_1} - K_\phi Y_v K_\psi$$

$\psi(S)$ is obtained from:

$$\psi = \frac{1}{S} r$$

Applying the Final Value Theorem, we obtain:

$$\psi_{ss} = \lim_{S \to 0} S\psi(S) = \lim_{S \to 0} r(S)$$

$$\psi_{ss} = \frac{+N_{\delta r} \delta_{rv} U_1 \beta_o}{K_\psi} = \frac{\delta_{rv} U_1 \beta_o}{\delta_{r\psi}} \tag{B37}$$

With

$$\delta_{rv} = \frac{\delta_{r\psi}}{U_1}$$

we obtain:

$$\psi_{ss} = \beta_o$$

which, as shown previously in Equation (B9), satisfies the flight path problem.

C2 Heading Loop Hold Biased the Integral of Sideslip

This configuration is represented by the block diagram of Figure 28.

The control equations are:

$$\delta_a = \delta_{a\phi}\phi + \delta_{ap}p$$

$$\delta_r = \delta_{r\psi}\psi + \frac{1}{S}\left[\delta_{r\beta}\beta\right] + \delta_{rr}r$$

Combining the control equations with the vehicle equations of motion and expressing the results in matrix form, we have for a step input in $\dot{Y}_{WG}$:

$$\begin{bmatrix} -S + \underline{L}_p + \dfrac{K_\phi}{S} & L_r & L_\beta \\ 0 & -S + \underline{N}_r + \dfrac{K_\psi}{S} & N_\beta + \dfrac{K_\beta}{S} \\ g/S & -U_1 & U_1(-S+Y_v) \end{bmatrix} \cdot \begin{bmatrix} p \\ r \\ \beta \end{bmatrix} = \begin{bmatrix} 0 \\ 0 \\ -U_1\beta_o \end{bmatrix} \quad (B38)$$

where

$$\beta_o = \frac{-\dot{Y}_{WG_o}}{U_1}$$

$$\underline{L}_p = L_{\delta a}\delta_{ap} + L_p$$

$$K_\phi = L_{\delta a}\delta_{a\phi}$$

$$K_\psi = N_{\delta r}\delta_{r\psi}$$

$$K_\beta = N_{\delta r}\delta_{r\beta}$$

$$\underline{N}_r = N_{\delta r}\delta_{rr} + N_r$$

The solution for r is:

$$r = \frac{+U_1\beta_o \left(-S + \underline{L}_p + \frac{K_\phi}{S}\right)\left(N_\beta + \frac{K_\beta}{S}\right)}{\frac{-U_1}{S^2}[AS^5 + BS^4 + CS^3 + DS^2 + ES + F]}$$

(B39)

where:

$A = 1$

$B = -[Y_v + \underline{N}_r + \underline{L}_p]$

$C = \underline{N}_r Y_v + \underline{L}_p (Y_v + N_r) - K_\psi - K_\phi + N_\beta$

$D = -[\underline{L}_p (\underline{N}_r Y_v + N_\beta) - K_\psi(\underline{L}_p + Y_v) - K_\phi (\underline{N}_r + Y_v) - K_\beta + \frac{gL_\beta}{U_1}]$

$E = -\frac{g}{U_1} [L_r N_\beta - L_\beta \underline{N}_r] - K_\phi [\underline{N}_r Y_v - K_\psi + N_\beta] - \underline{L}_p K_\beta - Y_v K_\psi \underline{L}_p$

$F = -K_\phi [K_\psi Y_v + K_\beta] - \frac{g}{U_1} [L_r K_\beta - K_\psi L_\beta]$

$\psi_{(S)}$ is obtained from:

$$\psi = \frac{1}{S} r$$

Substituting for r and applying the Final Value Theorem, we have:

$$\psi_{ss} = \lim_{S \to 0} S\psi(S) = \lim_{S \to 0} S \left[\frac{1}{S} r(S)\right] = \lim_{S \to 0} r(S)$$

$$\psi_{ss} = \frac{\beta_o K_\phi K_\beta}{+K_\phi \left[K_\psi Y_v + K_\beta\right] + \frac{g}{U_1} \cdot \left[L_r K_\beta - K_\psi L_\beta\right]}$$

(B40)

The flight path control condition is satisfied if $\psi_{ss} = \beta_o$, or

$$\frac{K_\phi K_\beta}{K_\phi [K_\psi Y_v + K_\beta] + \frac{g}{U_1} [L_r K_\beta + K_\psi L_\beta]} = 1 \qquad \text{(B41)}$$

This suggests three approaches to selecting gains to eliminate or minimize the flight path error:

1. Choose $\dfrac{K_\psi}{K_\beta}$ to satisfy Equation (B41) exactly:

   In this case:

   $$\frac{K_\psi}{K_\beta} = \frac{-g L_r}{(K_\phi Y_v - \frac{g}{U_1} L_\beta) U_1}$$

   Evaluating this ratio for cruise conditions and $\delta_{a\phi} = 1$, we obtain:

   $$\frac{K_\psi}{K_\beta} = \frac{\frac{-32.2}{313}(0.892)}{(-36.8)(-0.24) - \frac{32.2}{313}(-23.42)} = -0.009$$

2. Choose $\dfrac{K_\psi}{K_\beta}$ to make:

   $$L_r K_\beta - K_\psi L_\beta = 0$$

   For cruise conditions, therefore:

   $$\frac{K_\psi}{K_\beta} = \frac{L_r}{L_\beta} = \frac{.892}{23.40} \approx -0.0381$$

   and ψ_{ss} becomes:

and

$$\psi_{ss} = \beta_o \frac{K_\beta}{\left[\frac{L_r}{L_\beta} Y_v + 1\right] K_\beta} = 0.99 \beta_o$$

3. Let $K_\psi = 0$,

Then

$$\psi_{ss} = \frac{\beta_o K_\phi K_\beta}{K_\phi K_\beta + \frac{g}{U_1} L_r K_\beta} = \frac{\beta_o K_\phi}{K_\phi + \frac{g}{U_1} L_r}$$

$$= \beta_o \left[\frac{-36.8}{-36.8 + \frac{32.2}{313}(0.892)}\right] \approx \beta_o \left(1 - \frac{32.2(0.892)}{(313)(368)}\right)$$

$$= 0.998 \beta_o$$

For the last case ($K_\psi = 0$), the integral of β is forced to equal zero in the steady state.

This leads to the conclusion that a control system that forces the integral of β to zero in the steady state also forces a steady state yaw for a cross-course step wind input that results in little cross-course velocity change.

The addition of the ψ feedback serves merely to make a small additional correction

Therefore, with ψ feedback used for attitude hold (necessary to combat mistrims and other nonlinearities), K_β must be quite large (relative to K_ψ) to achieve the proper ψ_{ss}.

) HEADING LOOPS FOR DUAL MODES

In the dual mode concepts described in the body of this report, a heading loop
is combined with a weathercock mode to provide flight path control. In this
appendix, the response parameters of three heading loops used as part of
dual-mode configurations are determined.

The heading loops analyzed here are illustrated in Figures B1, B2 and B3. It
will be seen from these diagrams that only the first employs a roll attitude
inner loop, while the other two employ yaw rate feedback to the aileron to
provide the inner loop. The yaw rate feedback to aileron has been referred to
as the "wings leveler" roll control.

For the purposes of flight path control, we are most interested in the heading
loop response to a step in the lateral wind component. The important modes
of response are recorded in Figures B4 through B9. The response relation-
ship determined in this analysis is summarized in Table B1.

D1 Heading Loop with Attitude Hold Inner Loop

This configuration is shown in Figure B1.

The control equations are:

$$\delta_a = \delta_{ap}\, p + \delta_{a\phi}\, \phi + \delta_{a\psi}\, \psi$$

$$\delta_r = \delta_{rr}\, r$$
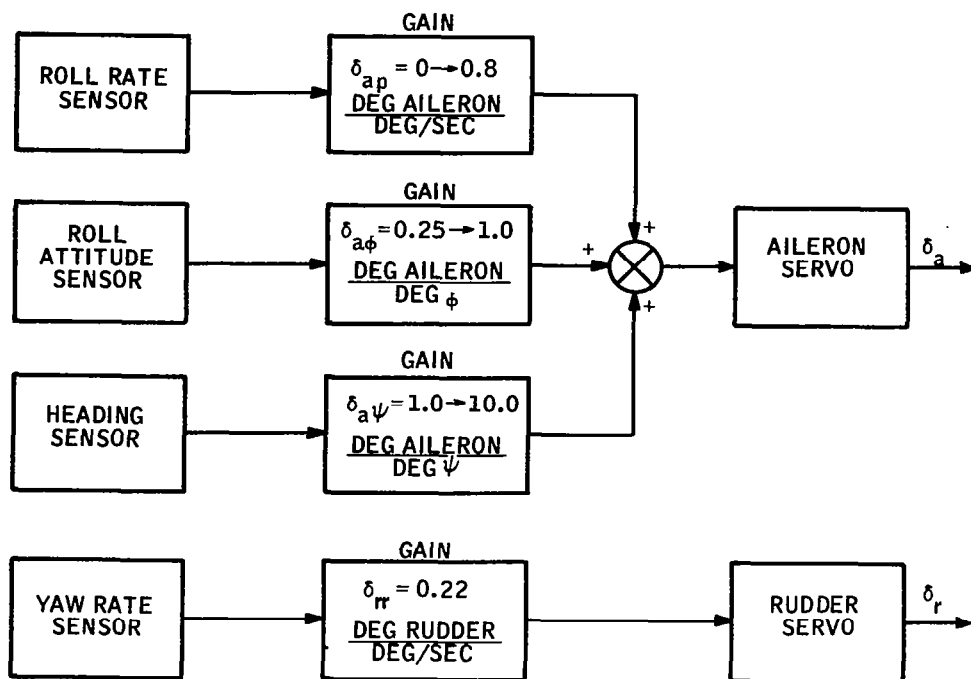
Figure B1. Heading Loop with Roll Attitude Control
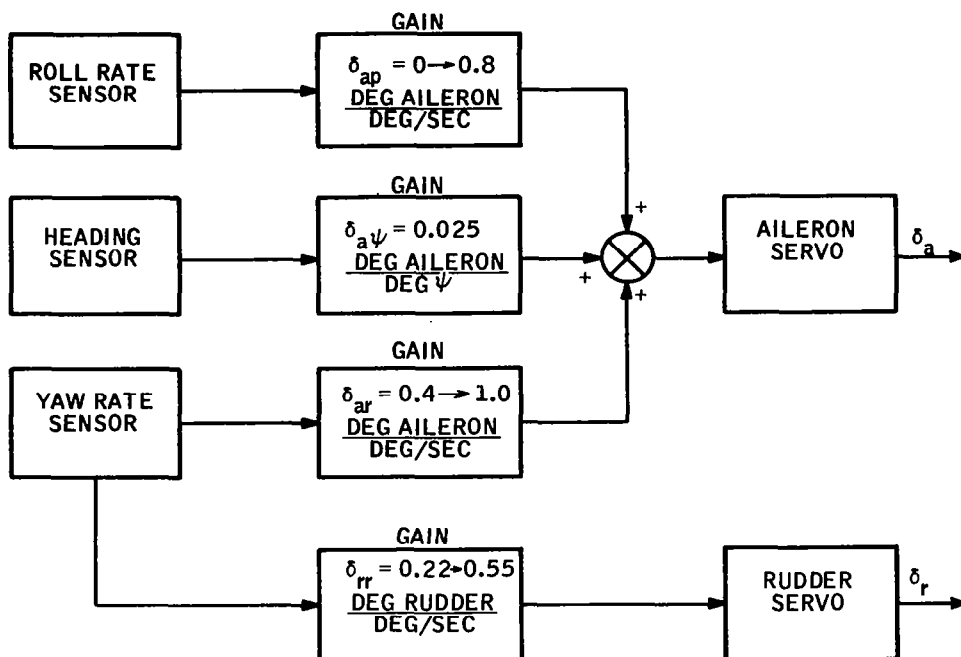
Figure B2. Heading Loop with "Wings Leveler"

GAIN

ROLL RATE SENSOR

$\delta_{a_p} = 0 \rightarrow 0.8$
$\dfrac{\text{DEG AILERON}}{\text{DEG/SEC}}$

AILERON SERVO

δ_a

+
+

GAIN

YAW RATE SENSOR

$\delta_{ar} = 1.0$
$\dfrac{\text{DEG AILERON}}{\text{DEG/SEC}}$

GAIN

$\delta_{rr} = 0.55$
$\dfrac{\text{DEG AILERON}}{\text{DEG/SEC}}$

RUDDER SERVO

δ_r

+
+

GAIN

HEADING ERROR

$\delta_{r\psi} = 0.05$
$\dfrac{\text{DEG RUDDER}}{\text{DEG } \psi}$
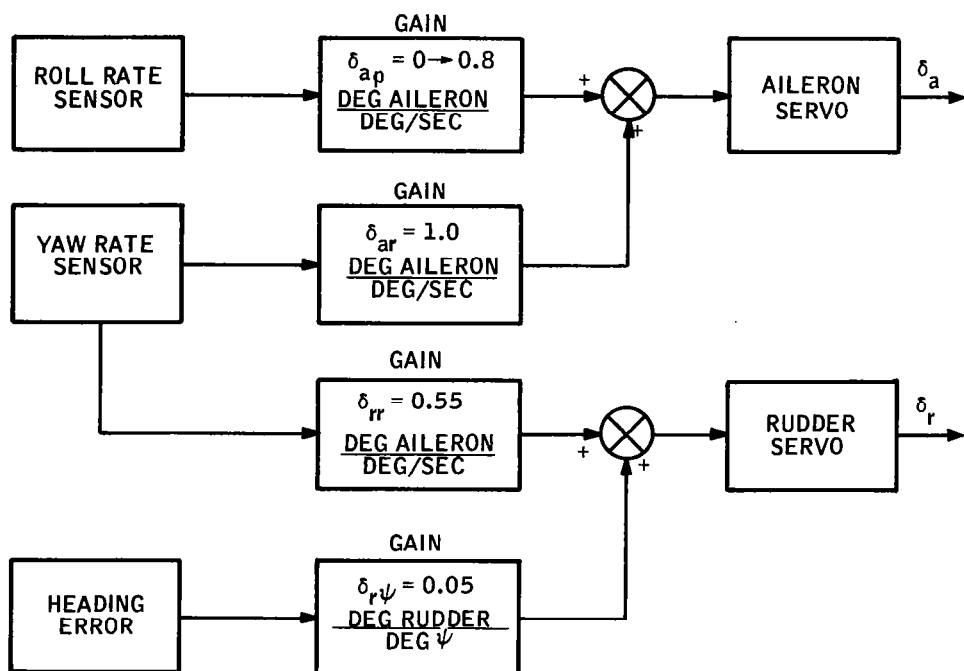
Figure B3. Heading Loop with "Wings Leveler" - Heading Error Feedback to Rudder
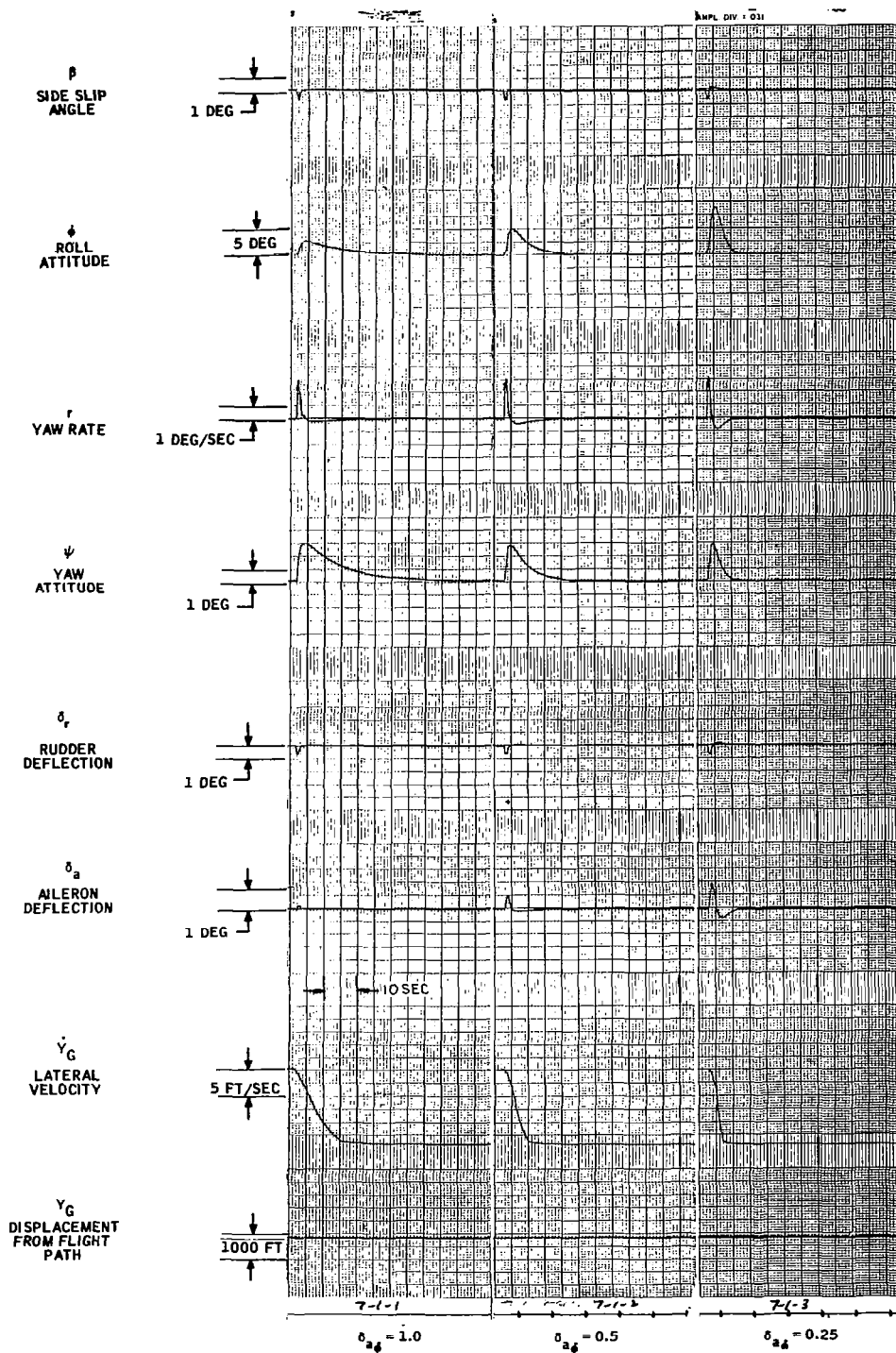
Figure B4. Heading Loop with Roll Attitude Inner Loop
- Response to 20-fps Lateral Wind Step
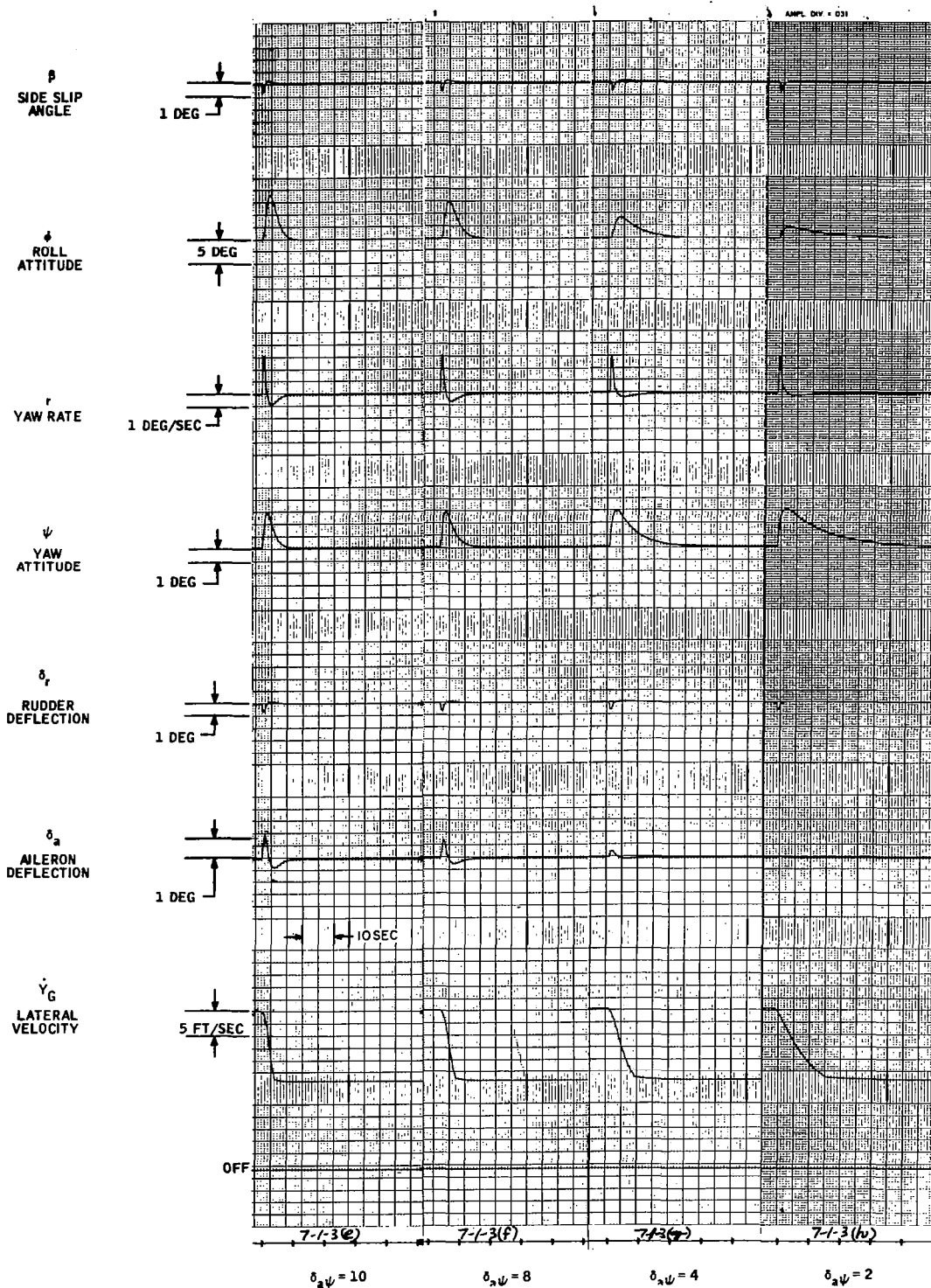
Figure B5. Heading Loop with Roll Attitude Inner Loop - Response to 20-fps Lateral Wind Step (with δ_{ap} varied)
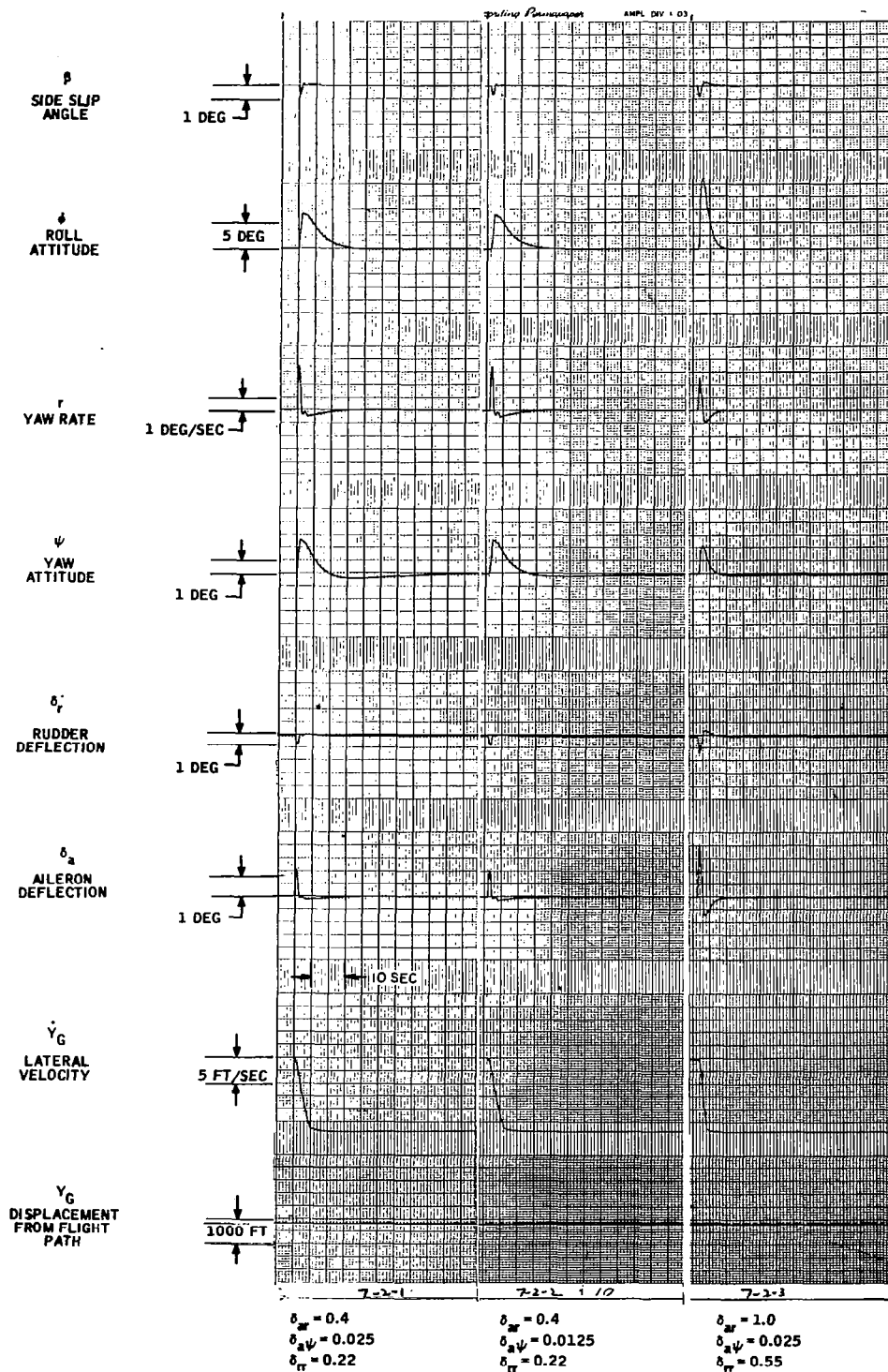
Figure B6. Heading Loop with "Wings Leveler" Inner Loop
- Response to 20-fps Lateral Wind Step
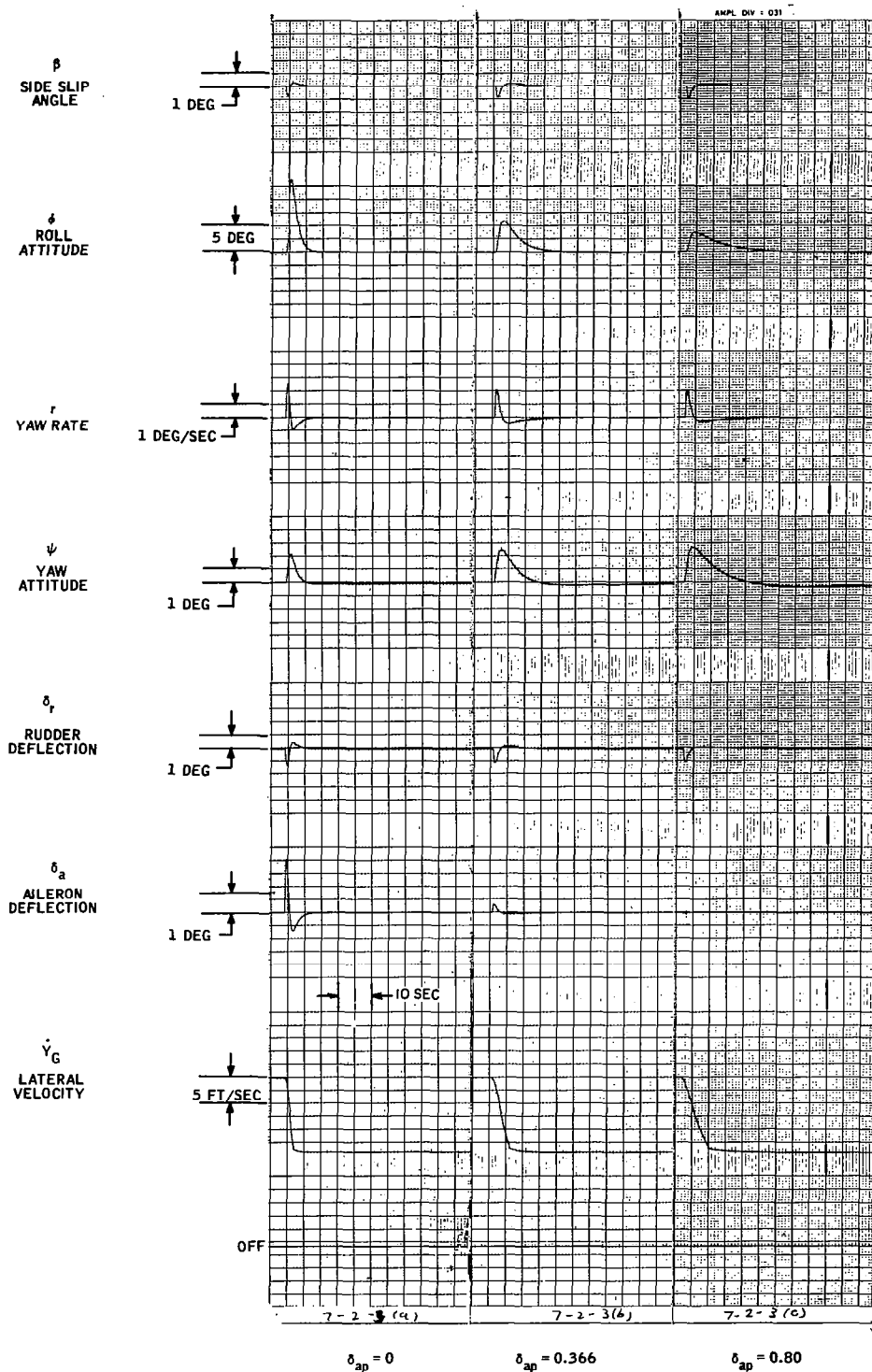
Figure B7. Heading Loop with "Wings Leveler" Inner Loop
- Response to 20-fps Lateral Wind Step (with
δ_{ap} varied)
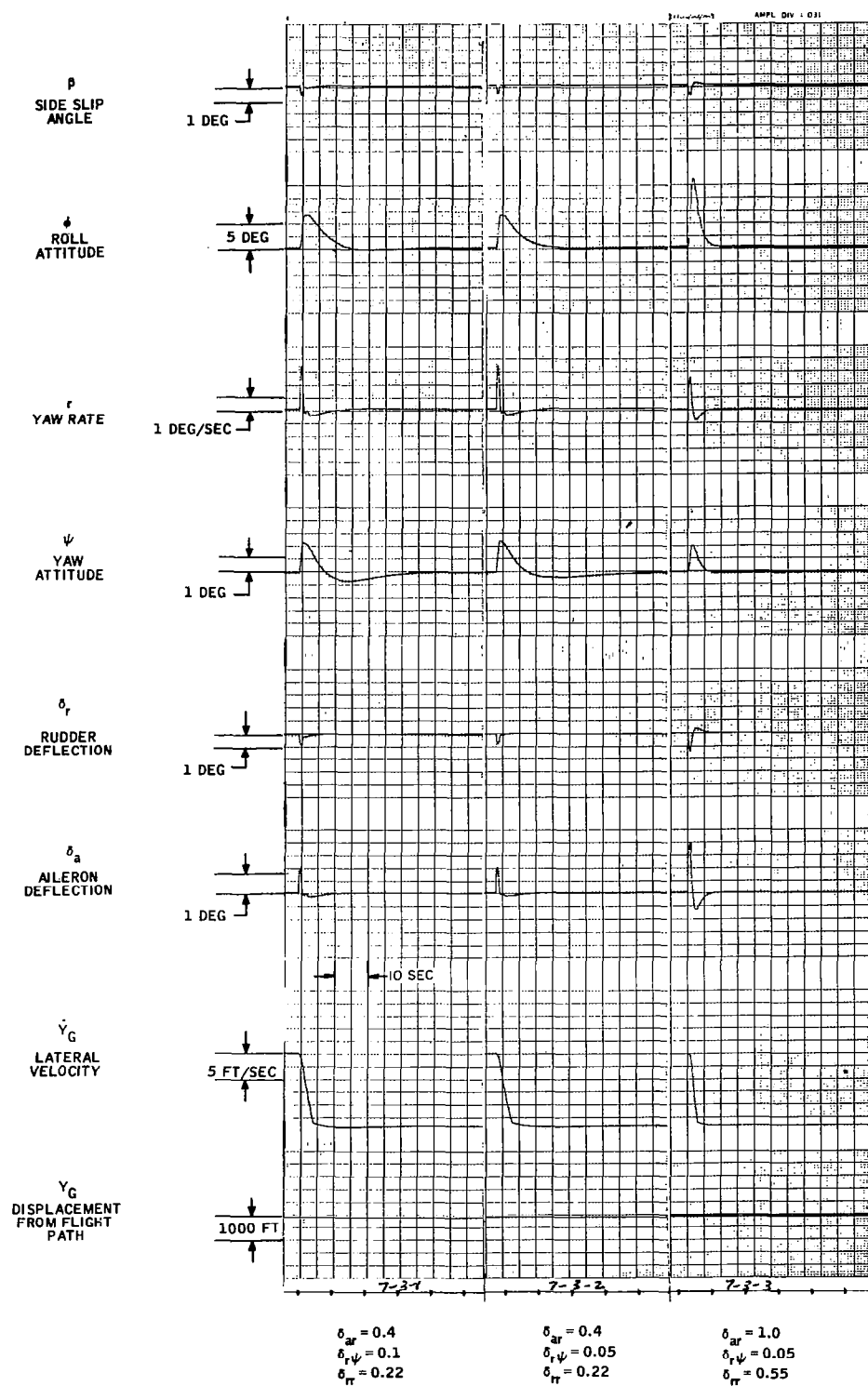
Figure B8. Heading Loop with "Wings Leveler" Inner Loop,
Heading Error Feedback to Rudder - Response to
20-fps Lateral Wind Step
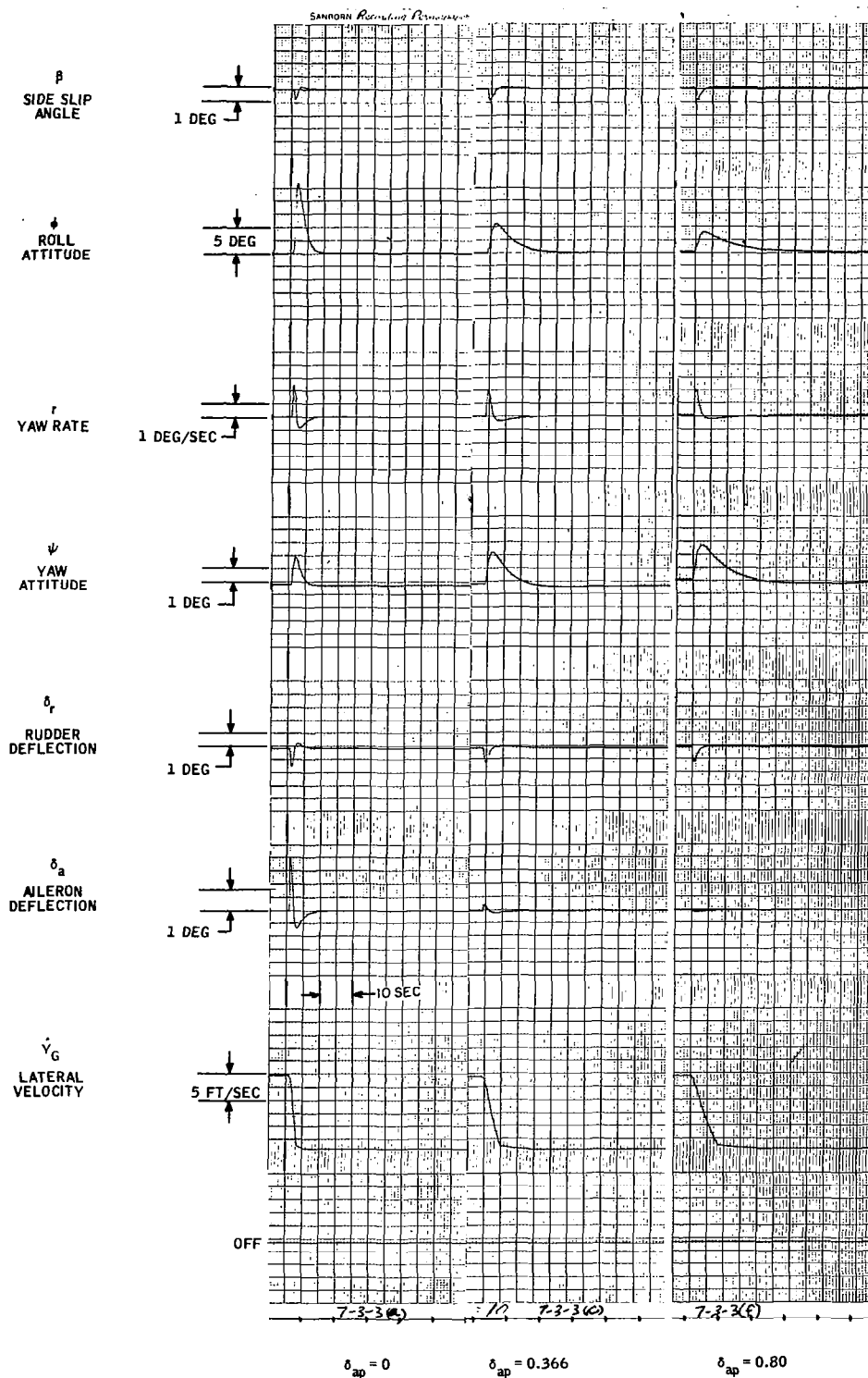
Figure B9. Heading Loop with "Wings Leveler" Inner Loop, Heading Error Feedback to Rudder - Response to 20-fps Lateral Wind Step (with δ_{ap} varied)

Table B1. Response of Heading Loops to Step Change in Lateral Wind

Parameter	Attitude Hold Inner Loop	"Wings Leveler" Inner Loop	"Wings Leveler" Inner Loop (Heading Error to Rudder)
ω_n	$\sqrt{K_\phi - \dfrac{L_r g}{U_1}}$	$\sqrt{\dfrac{L_r g}{U_1}}$	$\sqrt{\dfrac{L_r g}{U_1}}$
ζ	$\dfrac{-L_p}{2\sqrt{\omega_n}}$	$\dfrac{-L_p}{2\sqrt{\omega_n}}$	$\dfrac{-L_p}{2\sqrt{\omega_n}}$
$\tau_{HLT} = 1/a$	$\dfrac{U_1 K_\phi}{g K_\psi}$	$\dfrac{N_\beta L_r - L_\beta N_r}{N_\beta K_\psi}$	$\dfrac{N_\beta L_r - L_\beta N_r}{L_\beta K_\psi}$
ϕ_{peak}	$\approx \dfrac{K_\psi}{K_\phi}\beta_o$	$\approx \dfrac{\beta_o[N_\beta L_r - L_\beta N_r]}{-L_p N_\beta}$	$\approx \dfrac{\beta_o[N_\beta L_r - L_\beta N_r]}{-L_p N_\beta}$

ω_n, ζ = the natural frequency and damping of the short term transient response in heading, respectively.

τ_{HLT} = the long term response in heading.

ϕ_{peak} = the value of the roll angle at the end of the short term heading transient.

Combining these equations with the vehicle equations of motion and expressing the result in matrix form, we have:

$$
\begin{bmatrix}
-S + \underline{L}_p + \dfrac{K_\phi}{S} & L_r + \dfrac{K_\psi}{S} & L_\beta \\[2em]
0 & -S + \underline{N}_r & N_\beta \\[2em]
g/S & -U_1 & U_1(-S + Y_v)
\end{bmatrix}
\cdot
\begin{bmatrix}
p \\[1em] r \\[1em] \beta
\end{bmatrix}
=
\begin{bmatrix}
i_{(S)}
\end{bmatrix}
\qquad (B42)
$$

where

$$\underline{L}_p = L_{\delta a} \, \delta_{ap} + L_p$$

$$K_\phi = L_{\delta a} \, \delta_{a\phi}$$

$$K_\psi = L_{\delta a} \, \delta_{a\psi}$$

$$\underline{N}_r = N_{\delta r} \delta_{rr} + N_r$$

and

$$i(S) = \left\{ \frac{K_\psi \psi_{io}}{S}, \ 0, \ 0 \right\} \quad \text{for a step } \psi_{io} \text{ in heading}$$

or

$$i(S) = \left\{ 0, \ 0, \ -U_1 \beta_o \right\} \quad \text{for a step } \dot{Y}_{WG_o} \quad \text{in lateral wind, where}$$

$$\beta_o = \frac{-\dot{Y}_{WG_o}}{U_1}$$

Response to Step Change in Heading -- With $i_{(S)}$ equal to $\left(\dfrac{K_\psi \psi_{io}}{S}\right)$, we find from Equation (B42) to be:

$$r_{(S)} = \frac{K_\psi \psi_{io}/S \left[N_\beta \, g/S\right]}{\dfrac{-U_1}{S^2}\left[AS^5 + BS^4 + CS^3 + DS^2 + ES + F\right]}$$

where

$$A = 1$$

$$B = -(\underline{N}_r + Y_v + \underline{L}_p)$$

$$C = \left[\underline{N}_r \, Y_v + N_\beta + \underline{L}_p \, (\underline{N}_r + Y_v) - K_\phi\right]$$

$$D = -\left[-K_\phi(\underline{N}_r + Y_v) + \underline{L}_p \, (\underline{N}_r Y_v + N_\beta)\right] - \frac{g \, L_\beta}{U_1}$$

$$E = \frac{-g}{U_1}\left[N_\beta L_r - L_\beta \underline{N}_r\right] - K_\phi \, (\underline{N}_r Y_v + N_\beta)$$

$$F = \frac{-g}{U_1} \, N_\beta K_\psi$$

It is assumed that $\psi(S) = \frac{1}{S} r(S)$, so that the steady state response of $\psi(S)$ can be found by applying the Final Value Theorem to $\frac{1}{S} r(S)$, or

$$\psi_{ss} = \lim_{S \to 0} S\psi(S) = \lim_{S \to 0} \frac{S \, r(S)}{S} = \lim_{S \to 0} r(S)$$

$$\psi_{ss} = \frac{K_\psi \psi_{io} N_\beta g}{-U_1 [F]} = \frac{K_\psi N_\beta g \psi_{io}}{-U_1 \left[-\frac{g}{U_1} N_\beta K_\psi\right]}$$

$$\psi_{ss} = \psi_{io}$$

The response modes can be found directly by evaluating the coefficients and determining the roots of the characteristic equation. Our purpose, however, is to express the response modes in terms of the autopilot gains and the airplane stability derivatives. This can be done by approximate factoring of the characteristic equation.

The accuracy of the approximation depends on the spread between the critical frequencies of the responses represented by the polynomial factors. However, even when the approximations are poor because the critical frequencies are not spread far enough apart, these factors will offer valid indications of which parameters affect the separate response modes and allow a first cut at a selection of parameter values.

In the heading loop investigation discussed in this section, relationships indicated by the approximate factors were confirmed by simulation results.

The fifth order characteristic equation can be factored into two quadratic and one first order polynomials, such as:

$$(S^2 + b'S + c') (S^2 + bS + c) (S + a) \tag{B42a}$$

To find approximate expressions for these coefficients in terms of autopilot gains and aircraft stability derivatives, we proceed as follows:

> Step 1 -- Try to factor the fifth order into a fourth order and a first order polynomial such as:

$$(AS^4 + BS^3 + CS^2 + DS + E) (S + a) \tag{B43}$$

By multiplying out we see that this is approximately true when

$$a = \frac{F}{E}$$

and the following inequalities are satisfied:

$$B \gg aA$$

$$C \gg aB$$

$$D \gg aC$$

$$E \gg aD$$

Evaluating A through F at the representative A/P gains of $\delta_{a\phi} = 1$, $\delta_{a\psi} = 1$ and $\delta_{rr} = 0.22$ and using cruise condition stability derivatives, we have:

$$A = 1$$

$$B = 11.14$$

$$C = 85.4$$

$$D = 315$$

$$E = 827$$

$$F = 67.5$$

$$a = F/E = -0.082$$

For these values the inequalities are seen to hold.

Thus, in Equation B43:

$$a \approx \frac{F}{E}$$

and

$$AS^4 + BS^3 + CS^2 + DS + E$$

is an approximate factor.

Step 2 -- The next step is to try to identify one of the quadratics of the fourth order factor of Equation (B43). Experience has shown that the roll response is relatively independent. That is the decoupled roll response (β held equal to zero) to a roll rate disturbance is almost the same as the coupled response (β allowed to vary).

This implies that the decoupled roll response characteristic polynomial is a factor of the coupled characteristic polynomial. Therefore, we will find the decoupled roll response quadratic and test to determine whether it is indeed a factor of the fourth order polynomial of Equation (B43).

With $\beta = 0$, and opening the outer loop (i.e., letting $K_\psi = 0$), Equation (B42) becomes:

$$\begin{bmatrix} -S + \underline{L}_p + \dfrac{K_\phi}{S} & L_r \\[2em] g/S & -U_1 \end{bmatrix} \begin{bmatrix} p \\[2em] r \end{bmatrix} = \begin{bmatrix} i(S) \\[2em] \end{bmatrix} \tag{B44}$$

The characteristic equation for the system of Equation (B44) is, therefore:

$$S^2 - \underline{L}_p S - \left(K_\phi + \dfrac{L_r g}{U_1} \right) = 0$$

We will, therefore, assume, for the moment, that $S^2 + bS + c$ is a factor of the fourth order polynomial of Equation (B43).

Where
$$b = -\underline{L}_p$$

and
$$c = -K_\phi - \dfrac{L_r g}{U_1}$$

Dividing the fourth order polynomial by $S^2 + bc + c$, we obtain:

$$\frac{AS^4 + BS^3 + CS^2 + DS + E}{S^2 + bS + c} = S^2 + b'S + c' \frac{r_1 S + r_2}{S^2 + bS + c} \tag{B45}$$

where

$$A = 1$$

$$b' = B - b \tag{B45a}$$

$$c' = C - c - b'b \tag{B45b}$$

$$r_1 = D - cb' - bc'$$

$$r_2 = E - cc'$$

Both $S^2 + bS + c$ and $S^2 + b'S + c'$ are approximate factors of the fourth order polynomial if the remainder is negligible. To determine the conditions which make the remainder negligible, multiply both sides of Equation (B45) by $S^2 + bS + c$. We obtain:

$$(S^2 + b'S + c'_2)(S^2 + bS + c) + r_1 S + r_2 = AS^4 + BS^4 + CS^2 + DS + E$$

Therefore:

$$(S^2 + b'S + c')(S^2 + bS + c) = AS^4 + BS^3 + CS^2 + (D-r_1)S + (E - r_2)$$

If:

$$|r_1| << D \text{ and } |r_2| << E$$

Then:

$$(S^2 + b'S + c')(S^2 + bS + c) \approx AS^4 + BS^3 + DS + E$$

Evaluating r_1, r_2, D and E for cruise conditions and for $\delta_{rr} = 0.22$, $\delta_{a\phi} = 1.0$ and $\delta_{a\psi} = 1.0$, we have:

$$\underline{N}_r = -4.2 \qquad\qquad D = 315$$

$$K_\phi = -36.8 \qquad\qquad E = 827$$

$$r_1 = 25.3 \qquad\qquad K_\psi = -36.8$$

$$r_2 = 132$$

It is clear that the inequalities are satisfied.

Thus, Equation (B43) can be factored into:

$$(S^2 + b'S + c') (S^2 + bS + c) (S + a)$$

where

$$b' = -(\underline{N}_r + Y_r), \text{ from Equation (B45a)}$$

$$c' = N_r Y_v + N_\beta + \frac{L_r g}{U_1} \quad \text{ from Equation (B45b)}$$

$$b = -L_p$$

$$c = -K_\phi - \frac{L_r g}{U_1}$$

$$a = \frac{F}{E} \approx \frac{g}{U_1} \frac{K_\psi}{K_\phi}$$

The natural frequency of the first quadratic, which we may refer to as the yaw response, as suggested by the dependency of its coefficients on the yaw axis stability derivatives, is:

$$\omega_{nr} = \sqrt{c'} = \sqrt{\underline{N}_r Y_v + N_\beta + \frac{L_r g}{U_1}}$$

and the damping factor is

$$\zeta_{nr} = \frac{b'}{2\sqrt{c'}}$$

For the roll response:

$$\omega_{np} = \sqrt{c} = \sqrt{-K_\phi - \frac{L_r g}{U_1}}$$

$$\zeta_{np} = \frac{b}{2\sqrt{c}}$$

The first-order term constitutes a break frequency at $a = \dfrac{F}{E}$.

Evaluating at cruise conditions, with

$$\delta_{a\phi} = 1, \; \delta_{a\psi} = 1, \; \delta_{rr} = 0.22, \text{ and } \delta_{ap} = 0$$

we have:

$$\omega_{nr} = 4.35 \text{ radians/sec}$$

$$\zeta_{nr} = 0.55$$

$$\omega_{np} = 6.06 \text{ radians/sec}$$

$$\zeta_{np} = 0.51$$

$$a = 0.08 \text{ radian/sec}$$

<u>Roll Response to Lateral Wind Step Input</u> -- We are now ready to determine the roll response of this heading loop to a wind step.

With i(S) equal to $\left[0,\ 0,\ -U_1\beta_0\right]$, we find p(S) from Equation (B42) to be:

$$p(S) = \frac{-U_1\beta_0\left[\left(L_r + \dfrac{K_\phi}{S}\right)(N_\beta) - L_\beta(-S + \underline{N}_r)\right]}{\dfrac{-U_1}{S^2}\left[AS^5 + BS^4 + CS^3 + DS^2 + ES^2 + F\right]}$$

and

$$\phi_{(S)} = \frac{1}{S}\,p(S)$$

Applying the Final Value Theorem, we find that:

$$\phi_{ss} = 0$$

However, we are more interested in the initial transient of the roll response, since switchover to the weathercocking mode will take place in less than one second. The roll angle at switchover will depend on the actual switching delay as well as the peak in the roll angle response if switching did not occur.

The value of this peak in roll angle response, ϕ_{peak}, can be found approximately by applying a modified final value theorem, since "a" is much smaller than ω_{nr} or ω_{np}.

First, rewriting the expression for $\phi_{(S)}$ with the denominator of the left hand side in factored form, we have:

$$\phi_{(S)} = \frac{S\beta_0\left[\left(L_r + \dfrac{K_\psi}{S}\right)(N_\beta) - L_\beta(-S + \underline{N}_r)\right]}{(S^2 + b'S + c')(S^2 + bS + c)(S + a)}$$

Applying the modified final value theorem, we have for the cruise conditions and A/P gains under consideration:

$$\phi_{peak} = \lim_{S \to u} S \phi_{(S)} = \frac{\beta_o K_\psi N_\beta}{c\ c'} \approx \frac{\beta_o K_\psi}{K_\phi}$$

where:

$$a < \mu < \omega_{nr}, \ \omega_{np}$$

From the expression we can see that for a given step wind decreasing the ratio of $\frac{K_\psi}{K_\phi}$ would decrease ϕ peak and therefore the roll remaining after switchover to the weathercocking mode.

However, this ratio also determines the first order time constant associated with the heading response, that is:

$$\tau_{HLT} = \frac{1}{a} = \frac{E}{F} = \frac{U_1}{g} \ \frac{K_\phi}{K_\psi}$$

so that a decrease ϕ_{peak} is accompanied by an increase in τ_{HLT}.

D2 Heading Loop with "Wings Leveler" Inner Loop

This configuration is shown in Figure B2.

The control equations are:

$$\delta_a = \delta_{ap}p + \delta_{ar}r + \delta_{a\psi}\frac{r}{S}$$

$$\delta_r = \delta_{rr}r$$

Combining the control equations with the vehicle equations of motion and expressing the result in matrix form, we have:

$$
\begin{bmatrix}
-S + \underline{L}_p & \underline{L}_r + \dfrac{K_\psi}{S} & L_\beta \\
0 & -S + \underline{N}_r & N_\beta \\
g/S & -U_1 & U_1(-S + Y_v)
\end{bmatrix}
\cdot
\begin{bmatrix}
p \\
r \\
\beta
\end{bmatrix}
=
\begin{bmatrix}
i(S)
\end{bmatrix}
\tag{B46}
$$

where:

$$\underline{L}_p = L_{\delta a}\,\delta_{ap} + L_p$$

$$K_\psi = L_{\delta a}\,\delta_{a\psi}$$

$$\underline{L}_r = L_{\delta a}\,\delta_{ar} + L_r$$

$$\underline{N}_r = N_{\delta r}\,\delta_{rr} + N_r$$

and

$$i(S) = \left(\frac{K_\psi \psi_{io}}{S},\ 0,\ 0\right) \quad \text{for a step in heading of } \psi_{io},\ \text{and}$$

$$i(S) = \left(0, \ 0, \ -U_1 \beta_o\right) \text{ for a step in lateral wind, } \hat{Y}_{WG_o}, \text{ where } \beta_o = \frac{-Y_{WG_o}}{U_1}$$

Response to Step Change in Heading -- With $i(S) = \left(\frac{K_\psi \psi_{io}}{S}, \ 0, \ 0\right)$, solving Equation B46, we obtain:

$$r(S) = \frac{\dfrac{K_\psi \psi_{io}}{S} \left[N_\beta \ \dfrac{g}{S}\right]}{\dfrac{-U_1}{S^2} \left[AS^5 + BS^4 + CS^3 + DS^2 + ES + F\right]}$$

where

$A = 1$

$B = -\left[\underline{N}_r + Y_v + \underline{L}_p\right]$

$C = \underline{N}_r Y_v + N_\beta + \underline{L}_p (\underline{N}_r + Y_v)$

$D = -\underline{L}_p (\underline{N}_r Y_v + N_\beta) - g\dfrac{L_\beta}{U_1}$

$E = -\dfrac{g}{U_1} \left[N_\beta L_r - L_\beta \underline{N}_r\right]$

$F = -\dfrac{g}{U_1} N_\beta K_\psi$

The steady state value of ψ can be found by applying the final value theorem to $\psi_{(S)}$, where:

$$\psi_{(S)} = \frac{1}{S} r(S)$$

Applying the Final Value Theorem:

$$\psi_{ss} = \lim_{S \to 0} S\left[\psi(S)\right] = \lim_{S \to 0} r(S) = \frac{K_\psi \, \psi_{io} \, N_\beta g}{-U_1\left[\dfrac{-g}{U_1} \, N_\beta K_\psi\right]}$$

$$= \psi_{io}$$

The transient response modes of the system can be found by approximate factoring as performed in the previous section.

The first step is to factor the fifth order polynominal into a product of first order and fourth order polynomials. As in the previous section, we have:

$$AS^5 + BS^4 + CS^3 + DS^2 + ES + F \approx$$

$$(AS^4 + BS^3 + CS^2 + DS + E)(S + a)$$

(B46a)

when:

$$a = \frac{F}{E}$$

and:

$$B >> a\,A$$
$$C >> a\,B$$
$$D >> a\,C$$
$$E >> a\,D$$

Evaluating the coefficients A through F at cruise condition and A/P gains of:

$$\delta_{ar} = 0.4; \quad \delta_{a\psi} = 0.025; \quad \delta_{rr} = 0.22; \quad \delta_{ap} = 0.$$

we have:

A = 1

B = 11.1

C = 48.5

D = 129

E = 35.4

F = 1.69

For these values we can see that the inequalities hold and therefore, the factoring is valid. Secondly, we test to see if the decoupled roll response is a factor following the procedure employed in the previous section.

The decoupled roll response can be found as before by letting $\beta = 0$ and opening up the heading loop (i.e., letting $K_\psi = 0$). Equation (B46) then reduces to:

$$\begin{bmatrix} -S + \underline{L}_p & \underline{L}_r \\[2ex] \dfrac{g}{S} & -U_1 \end{bmatrix} \cdot \begin{bmatrix} p \\[2ex] r \end{bmatrix} = \begin{bmatrix} i(S) \\[2ex] \end{bmatrix}$$

The characteristic equation of this system is:

$$S^2 - \underline{L}_p S - \underline{L}_r \frac{g}{U_1} = 0$$

Therefore we will test whether $S^2 + bS + c$ is a factor, where:

$$b = -\underline{L}_p$$

$$c = -\frac{\underline{L}_r g}{U_1}$$

However, before we proceed we note that for representative values c is much smaller for this case than for the preceding case, and the damping factor much greater. In this case the damping factor is about 3, while it was only about 0.5 in the previous case.

With such a large damping factor an additional level of factoring is possible. Thus:

$$(S^2 + bS + c) \approx (S + b) \left(S + \frac{c}{b}\right)$$

Multiplying out the right hand side, we see that the validity of the approximation requires that

$$b \gg \frac{c}{b}$$

With the values of gains and stability derivatives used in evaluating the fifth order polynomial coefficients we have:

$$b = 6.70$$
$$c = 1.422$$
$$\frac{c}{b} = 0.212$$

Therefore the inequality holds and approximation is valid.

We now return to testing whether $S^2 + bS + c$ is a factor of the fourth order polynomial of Equation (46a).

Dividing the fourth order polynomial by the quadratic, we have, as obtained previously:

$$\frac{AS^4 + BS^3 + CS^2 + DS + E}{S^2 + bS + c} = S^2 + b'S + c' + \frac{r_1 S + r_2}{S^2 + bS + c}$$

where:

$$b' = B - b$$

$$c' = C - c - bb'$$

$$r_1 = D - cb' - bc'$$

$$r_2 = E - cc'$$

Expressing the b' and c' in terms of aircraft stability derivatives and auto-pilot gains we have:

$$b' = -(\underline{N}_r + Y_v)$$

$$c' = \underline{N}_r Y_v + N_\beta + \frac{\underline{L}_r g}{U_1}$$

As was shown previously,

$$AS^4 + BS^3 + CS^2 + DS + E \approx (S^2 + bS + c)(S^2 + b'S + c')$$

if $|r_1| << D$ and $|r_2| << E$

Evaluating r_1 and r_2 for the conditions considered in this section (Page B56) we have:

$$r_1 = 4.8$$

$$r_2 = 10.4$$

Comparing to D and E respectively, we see the inequalities hold and the approximation is good.

Recapitulating, we have:

$$AS^5 + BS^4 + CS^3 + DS^2 + ES + F =$$

$$(S^2 + b'S + c')\ (S^2 + bS + c) \cdot (S + a) =$$

$$(S^2 + b'S + c')\ (S + b)\ (S + \frac{c}{b})\ (S + a)$$

where

$$b = -\underline{L}_p$$

$$c = \frac{-\underline{L}_{rg}}{U_1}$$

$$b' = -(N_r + Y_v)$$

$$c' = \underline{N}_r Y_v + N_\beta + \frac{\underline{L}_{rg}}{U_1}$$

$$a = \frac{F}{E}$$

The critical frequency of the response for yaw disturbances is:

$$\omega_{nr} = \sqrt{c'}$$

with a damping factor of:

$$\zeta_{nr} = \frac{b'}{2\sqrt{c'}}$$

For roll we have:

$$\omega_{np} = \sqrt{c}$$

$$\zeta_{np} = \frac{b}{2\sqrt{c}}$$

which can be expressed approximately as two single order terms with crossover frequencies at:

$$\omega_{p_1} = b$$

$$\omega_{p_2} = \frac{c}{b}$$

And the lowest cross-over frequency:

$$a = \frac{F}{E}$$

Evaluating these terms at the conditions given on page B56, we have:

$$\omega_{nr} = 4.2 \ \text{rad/sec}$$

$$\zeta_r = 0.53$$

$$\omega_{np} = 1.19 \ \text{rad/sec}$$

$$\zeta_p = 2.8$$

$$a = 0.048 \ \text{rad/sec}$$

$$\omega_p = 1.42 \ \text{rad/sec}$$

$$\omega_{p_2} = 0.212 \ \text{rad/sec}$$

We are now ready to find the roll response to a lateral wind step input.

Roll Response to Lateral Wind Step -- The roll response to step wind can be found by letting:

$$i(s) = [0, 0, -U_1\beta_o]$$

and solving Equation B46 for p

$$p = \frac{-U_1\beta_o [N_\beta (\underline{L}_r + \frac{K_\psi}{S}) - L_\beta(-S + \underline{N}_r)]}{\frac{-U_1}{S^2} [AS^5 + BS^4 + CS^3 + DS^2 + ES + F]}$$

Applying the final value theorem to $\phi = \frac{1}{S} p$, we find that the steady state value, ϕ_{ss} equals zero.

However as indicated previously, for dual mode application we are interested in the peak value of the initial response, ϕ_{peak}.

As in the previous heading loop investigation we will use a modified final value theorem.

First we write the expression for ϕ using the factored form for the denominator of the right hand side:

Thus:

$$\phi = \frac{1}{S} p = \frac{1}{S} \frac{\beta_o [N_\beta (\underline{L}_r + \frac{K_\psi}{S}) - L_\beta(-S + \underline{N}_r)]}{\frac{1}{S^2} \left[(S^2 + b'S + c')(S + b)(S + \frac{c}{b})(S + a)\right]}$$

We can find ϕ_{peak} by applying a modified form of the final value theorem:

$$\phi_{peak} = \lim_{S \to \mu} S\phi = \lim_{S \to \mu} \frac{\beta_o [\, N_\beta (\underline{L}_r + \frac{K_\psi}{S}) - L_\beta (-S + \underline{N}_r)]}{\frac{1}{S^2}(S^2 + b'S + c')(S + b)(S + \frac{c}{b})(S + a)}$$

where

$$b > \mu > \frac{c}{b}$$

Since

$$\frac{K_\psi}{\mu} << L_r$$

$$\underline{N}_r >> \mu$$

$$a << \mu$$

$$\mu^2 + b'\mu + c' \approx c'$$

we have

$$\phi_{peak} = \frac{+\beta_o (N_\beta \underline{L}_r - L_\beta \underline{N}_r)}{c'b} = \frac{-\beta_o (N_\beta \underline{L}_r - L_\beta \underline{N}_r)}{(\underline{N}_r Y_v + N_\beta + \frac{\underline{L}_{rg}}{U_1})(\underline{L}_p)}$$

or

$$\phi_{peak} \approx \frac{-\beta_o (N_\beta \underline{L}_r - L_\beta \underline{N}_r)}{\underline{L}_p N_\beta}$$

This shows that the magnitude of ϕ_{peak} can be reduced by increasing the size of $\underline{L}_p$.

Increasing $\underline{L}_p$, however, also increases the damping of the roll response, which has a marked effect on the settling time of the heading loop.

As in the previous case, we find that a compromise is required between limiting ϕ_{peak} and providing adequate heading loop response.

D3 Heading Loop with "Wings Leveler" Inner Loop; Heading Error Feedback to Rudder

The block diagram for this configuration is shown in Figure B3.

The control equations are:

$$\delta_a = \delta_{ap} p + \delta_{ar} r$$

$$\delta_r = \delta_{rr} r + \delta_{r\psi} \frac{r}{S}$$

Combining the control equations with the vehicle equations of motion and expressing the result in matrix form, we have:

$$
\begin{bmatrix}
-S + \underline{L}_p & \underline{L}_r & L_\beta \\
0 & -S + \underline{N}_r + \dfrac{K_\psi}{S} & N_\beta \\
\dfrac{g}{S} & -U_1 & U_1(-S+Y_v)
\end{bmatrix}
\cdot
\begin{bmatrix}
p \\
r \\
\beta
\end{bmatrix}
=
\begin{bmatrix}
i(S)
\end{bmatrix}
\qquad (B47)
$$

where

$$\underline{L}_r = L_{\delta a} \delta_{ar} + L_r$$

$$\underline{L}_p = L_{\delta a} \delta_{ap} + L_p$$

$$K_\psi = N_{\delta r} \delta_{r\psi}$$

$$\underline{N}_r = N_{\delta r} \delta_{rr} + N_r$$

and $i(S) = \left\{ 0, \dfrac{K_\psi \psi_{io}}{S}, 0 \right\}$ for a step change of ψ_{io} in heading, and:

$$i(S) = \left\{ 0, \ 0, \ -U_1\beta_o \right\} \text{ for a step change in lateral wind magnitude, } \dot{Y}_{WG_o}$$

where

$$\beta_o = - \frac{\dot{Y}_{WG_o}}{U_1}$$

Response to Step Change in Heading -- With $i(S) = \ 0, \ \dfrac{K_\psi \psi_{io}}{S}, \ 0 \quad ,$
solving Equation B47 we obtain:

$$r = \frac{\dfrac{K_\psi \psi_{io}}{S} \left[(-S+\underline{L}_p)(U_1)(-S+Y_v) - L_\beta \dfrac{g}{S} \right]}{\dfrac{-U_1}{S^2} \left[AS^5 + BS^4 + CS^3 + DS^2 + ES + F \right]}$$

where

$$A = 1$$

$$B = -\left[\underline{N}_r + Y_v + \underline{L}_p \right]$$

$$C = \underline{N}_r Y_v + \underline{L}_p (Y_v + \underline{N}_r) + N_\beta - K_\psi$$

$$D = -\left[\underline{L}_p (\underline{N}_r Y_v + N_\beta) - K_\psi(\underline{L}_p + Y_v) \right] - g\frac{L_\beta}{U_1}$$

$$E = -\frac{g}{U_1} \left[N_\beta \underline{L}_r - L_\beta \underline{N}_r \right] - L_p Y_v K_\psi$$

$$F = g\frac{L_\beta K_\psi}{U_1}$$

The steady state value of ψ can be found by applying the final value theorem to $\psi_{(S)}$ where

$$\psi_{(S)} = \frac{1}{S} r(S)$$

Thus:

$$\psi_{ss} = \lim_{S \to o} S \psi_{(S)} = \lim_{S \to o} r_{(S)} = \frac{K_\psi \psi_{io} L_\beta g}{L_\beta g K_\psi} = \psi_{io}$$

As in the preceding discussion, we may find the form of the transient response mode in terms of the aircraft stability derivatives and A/P gains.

The inequalities of the preceding section are found to hold for cruise conditions and the following A/P gains:

$$\delta_{ar} = 0.4$$

$$\delta_{ap} = 0$$

$$\delta_{r\psi} = 0.1$$

$$\delta_{rr} = 0.22$$

Therefore, by following the procedures of the preceding section, we find as the approximate factors of the fifth order polynomial:

$$\left[S^2 + b'S + c' \right] \left[S^2 + bS + c \right] \left[S + a \right]$$

or

$$\left[S^2 + b'S + c' \right] \left[S + b \right] \left[S + \frac{c}{b} \right] \left[S + a \right]$$

where

$$b = -\underline{L}_p$$

$$c = -\frac{\underline{L}_r g}{U_1}$$

$$b' = -(\underline{N}_r + Y_v)$$

$$c' = N_\beta - K_\psi + \underline{N}_r Y_v + \frac{\underline{L}_r g}{U_1}$$

$$a = \frac{F}{E}$$

The critical frequencies and damping factors for the response modes are:

$$\omega_{nr} = \sqrt{c'}$$

$$\zeta_{nr} = \frac{b'}{2\sqrt{c'}}$$

$$\omega_{np} = \sqrt{c}$$

$$\zeta_{np} = \frac{b}{2\sqrt{c}}$$

$$a = \frac{F}{E}$$

$$\omega_{p_1} = b$$

$$\omega_{p_2} = \frac{c}{b}$$

Evaluating these frequencies at the representative condition (Page B67) we have:

$$\omega_{nr} = 4.52 \text{ rad/sec}$$

$$\zeta_{nr} = 0.491$$

$$\omega_{np} = 1.2$$

$$\zeta_{np} = 2.8$$

$$\omega_{p_1} = 6.7$$

$$\omega_{p_2} = 0.21$$

$$a = 0.0966$$

For convenience in checking the numerical results of this section the values of the fifth order polynomial coefficients are given for these conditions:

$$A = 1$$

$$B = 10.6$$

$$C = 28.2$$

$$D = 134$$

$$E = 35.5$$

$$F = 3.43$$

We can now proceed to find the roll response to a lateral wind step.

Roll Response to a Lateral Wind Step -- The roll response to a lateral wind can be found by letting

$$i(S) = \left\{ 0,\ 0,\ -U_1 \beta_o \right\}$$

and solving th Equation for p

$$p = \cfrac{-U_1 \beta_o \left[\underline{L}_r N_\beta - L_\beta \left(-S + \underline{N}_r + \dfrac{K_\psi}{S} \right) \right]}{\dfrac{-U_1}{S^2} \left[AS^5 + BS^4 + CS^3 + DS^2 + ES + F \right]}$$

Applying the final value theorem to $\phi_{(S)} = \dfrac{1}{S} P_{(S)}$, we find that the steady state value, ϕ_{ss} is zero.

To find the peak value attained by the roll angle, ϕ_{peak}, during the transient, we proceed as in the previous sections, using a modified final value theorem.

First, expressing $\phi_{(S)}$, with the denominator of the right hand side of the equation in its factored form we have:

$$\phi_{(S)} = \frac{\frac{\beta_o}{S}\left[\underline{L}_r N_\beta - L_\beta\left(-S + \underline{N}_r + \frac{K_\psi}{S}\right)\right]}{\frac{1}{S^2}\left[S^2 + b'S + c'\right]\left[S + b\right]\left[S + \frac{c}{b}\right]\left[S + a\right]}$$

Applying a modified form of the final value theorem to $\phi_{(S)}$ we have:

$$\phi_{peak} = \lim_{S \to \mu} S\phi = \lim_{S \to \mu} \frac{\beta_o\left[\underline{L}_r N_\beta - L_\beta\left(-S + \underline{N}_r + \frac{K_\psi}{S}\right)\right]}{\frac{+1}{S^2}\left[S^2 + b'S + c'\right]\left[S + b\right]\left[S + \frac{c}{b}\right]\left[S + a\right]}$$

where

$$b < \mu < \frac{c}{b}$$

Since

$$\frac{K_\psi}{\mu} << \underline{N}_r$$

$$\underline{N}_r >> \mu$$

$$a << \mu$$

$$\mu^2 + b'\mu + c' \approx c'$$

we have

$$\phi_{peak} = \frac{+\beta_o\left[\underline{L}_r N_\beta - L_\beta \underline{N}_r\right]}{c'b} = \frac{+\beta_o\left[\underline{L}_r N_\beta - L_\beta \underline{N}_r\right]}{\left[\frac{L_{rg}}{U_1} + N_\beta K_\psi + \underline{N}_r Y_v \underline{L}_p\right]}$$

or

$$\phi_{peak} \approx \frac{-\beta_o \left[\underline{L}_r N_\beta - L_\beta \underline{N}_r \right]}{\underline{L}_p N_\beta}$$

This is the same result we obtained in the preceding section and as before we note that increasing $\underline{L}_p$ will decrease ϕ_{peak}.

Also, as in the preceding heading loop an increase in $\underline{L}_p$ increases the damping of the roll response, lengthening the heading loop settling time following a disturbance. Thus, as before a compromise between limitation of ϕ_{peak} and fast heading loop settling time is necessary.

E. "CONSTANT HEADING" FLIGHT PATH CONTROL

The configuration is shown in block diagram form in Figure 48.

The control equations are:

$$\delta_a = \delta_{a\phi}\frac{p}{S} + \delta_{a\beta}\beta + \delta_{ap}p$$

$$\delta_r = \delta_{rr}r + \delta_{r\psi}\frac{r}{S}$$

Combining the control equations with the vehicle equations of motion, and expressing the result in matrix form, we have for a step change in lateral wind, $\dot{Y}_{WG_o}$, where $\beta_o = -\dfrac{\dot{Y}_{WG_o}}{U_1}$, we have:

$$
\begin{bmatrix}
-S + \underline{L}_p + \dfrac{K_\phi}{S} & L_r & \underline{L}_\beta \\[3ex]
o & -S + \underline{N}_r + \dfrac{K_\psi}{S} & N_\beta \\[3ex]
\dfrac{g}{S} & -U_1 & U_1(-S + Y_v)
\end{bmatrix}
\cdot
\begin{bmatrix}
p \\[3ex] r \\[3ex] \beta
\end{bmatrix}
=
\begin{bmatrix}
o \\[3ex] o \\[3ex] -U_1\beta_o
\end{bmatrix}
\qquad \text{(B58)}
$$

where

$$K_\phi = L_{\delta a}\delta_{a\phi}$$

$$\underline{L}_p = L_{\delta a}\delta_{ap} + L_p$$

$$\underline{L}_\beta = L_{\delta a}\delta_{a\beta} + L_\beta$$

$$\underline{N}_r = N_{\delta r}\delta_{rr} + N_r$$

$$K_\psi = N_{\delta r}\delta_{r\psi}$$

$$\beta_o = \frac{-\dot{Y}_{WG_o}}{U_1}$$

To describe the performance of this flight path control concept we must obtain expressions for the steady values of yaw, ψ_{ss} and sideslip β_{ss} following a step change in the lateral winds, since:

$$\dot{Y}_{G_{ss}} = \dot{Y}_{WG_o} + U_1 \ (\beta_{ss} + \psi_{ss}) \qquad \text{See B8}$$

Therefore, for:

$$\dot{Y}_{G_{ss}} = 0$$

$$\beta_{ss} + \psi_{ss} = -\frac{\dot{Y}_{WG_o}}{U_1} = \beta_o \qquad\qquad (B59)$$

Yaw Response to Step in Lateral Winds -- Solving Equation B58 for $r_{(S)}$, we obtain:

$$r_{(S)} = \frac{+U_1 \beta_o \left[N_\beta \left(-S + \underline{L}_p + \frac{K_\phi}{S} \right) \right]}{-\dfrac{U_1}{S^2} \left[AS^5 + BS^4 + CS^3 + DS^2 + ES + F \right]}$$

where

$A \quad = \ 1$

$B \quad = \ -\left[\underline{N}_r + Y_v + \underline{L}_p \right]$

$C \quad = \ \underline{N}_r Y_v + \underline{L}_p (Y_v + \underline{N}_r) + N_\beta - K_\psi - K_\phi$

$D \quad = \ -\left[\underline{L}_p(\underline{N}_r Y_v + N_\beta) - K_\psi(\underline{L}_p + Y_v) - K_\phi(\underline{N}_r + Y_v) \right] - \dfrac{g\underline{L}_\beta}{U_1}$

$E \quad = \ -\dfrac{g}{U_1} \left[N_\beta L_r - \underline{L}_\beta \underline{N}_r \right] - K_\phi \left[\underline{N}_r Y_v + N_\beta - K_\psi \right] - \underline{L}_p Y_v K_\psi$

$F \quad = \ \dfrac{g}{U_1} \left[\underline{L}_\beta K_\psi \right] - \left[K_\phi Y_v K_\psi \right]$

To find ψ_{ss} we apply the final value theorem to $\psi_{(S)}$

where

$$\psi_{(S)} = \frac{1}{S} r_{(S)}$$

Thus:

$$\psi_{ss} = \lim_{S \to o} \frac{U_1 \beta_o \left[N_\beta \right] \left[-S + \underline{L}_p + \dfrac{K_\phi}{S} \right]}{\dfrac{-U_1}{S^2} \left[AS^5 + BS^4 + CS^3 + DS^2 + ES + F \right]}$$

We note that $\psi_{ss} = 0$, unless $F = 0$.

For $F = 0$, ψ_{ss} becomes

$$\psi_{ss} \bigg|_{F = 0} = \frac{-\beta_o N_\beta K_\phi}{E} \tag{B60}$$

Sideslip Response to Step in Lateral Wind

Solving Equation for $\beta_{(S)}$, we obtain:

$$\beta_{(S)} = \frac{-U_1 \beta_o \left(-S + \underline{L}_p + \dfrac{K_\phi}{S} \right) \left(-S + \underline{N}_r + \dfrac{K_\psi}{S} \right)}{\dfrac{-U_1}{S^2} \left[AS^5 + BS^4 + CS^3 + DS^2 + ES + F \right]}$$

To find β_{ss} we apply the final value theorem:

As for ψ_{ss} we find $\beta_{ss} = 0$, unless $F = 0$. With $F = 0$, however then by the final value theorem:

$$\beta_{ss} \bigg|_{F = 0} = \frac{\beta_o K_\phi K_\psi}{E} \tag{B61}$$

Steady State Value of the Sum of β and ψ -- It was shown at the beginning of this discussion that the relationship:

$$\beta_{ss} + \psi_{ss} = \beta_{o}$$

must be satisfied for zero error in $\dot{Y}_G$.

We have already noted that unless $F = 0$, β_{ss} and ψ_{ss} will both be zero in the steady state (for $F > 0$) or divergemt (for $F < 0$).

With $F = 0$, however, we have by combining our previous results:

$$(\beta_{ss} + \psi_{ss}) \Big|_{F=0} = \frac{-\beta_{o}\left[N_\beta K_\phi - K_\psi K_\phi\right]}{E} = \frac{-\beta_{o}K_\phi\left[N_\beta - K_\psi\right]}{E} \qquad (B62)$$

Before substituting for E, we note that E can be written as:

$$E = \frac{-g}{U_1} N_\beta L_r - K_\phi (N_\beta - K_\psi) + \left[\frac{L_\beta g}{U_1} - K_\phi Y_v\right] N_r$$

But:

$$F = K_\psi\left[\frac{L_\beta g}{U_1} - K_\phi Y_v\right]$$

Substituting in expression for E, we obtain:

$$E = \frac{-g}{U_1} N_\beta L_r - K_\phi (N_\beta - K_\psi) + F \cdot \frac{N_r}{K_\psi}$$

For $F = 0$, therefore

$$E\Big|_{F=0} = \frac{-g}{U_1} N_\beta L_r - K_\phi(N_\beta - K_\psi)$$

and:

$$(\beta_{ss} + \psi_{ss})\Big|_{F=0} = \frac{-\beta_o K_\phi (N_\beta - K_\psi)}{\frac{-g}{U_1} N_\beta L_r - K_\phi (N_\beta - K_\psi)}$$

and the error in $(\beta_{ss} + \psi_{ss})$ can be expressed as:

$$\epsilon(\beta_{ss} + \psi_{ss}) = \beta_o \frac{g}{U_1} \frac{N_\beta L_r}{K_\phi (N_\beta - K_\psi)} \tag{B63}$$

The error in $\dot{Y}_G$ is therefore:

$$\epsilon \dot{Y}_G = U_1 \epsilon(\beta_{ss} + \psi_{ss}) = \beta_o \frac{g N_\beta L_r}{K_\phi (N_\beta - K_\psi)} \tag{B64}$$

It is important to note that Equations (B63) and (B64) are valid as long as F = 0. If F ≠ 0 then Equations (B63) and (B64) are valid after the initial transient, and then β and ψ converge to zero (F positive) or diverge (F negative). The convergence or divergence is exponential, and the associated time constant can be expressed by borrowing the results of previous sections, as:

$$\tau = \frac{E}{F} = \frac{\frac{-g}{U_1}\left[N_\beta L_r - L_\beta \underline{N}_r\right] - K_\phi\left[\underline{N}_r Y_v + N_\beta - K_\psi\right] - \underline{L}_p Y_v K_\psi}{\frac{+g}{U_1}\left[L_\beta K_\psi\right] - \left[K_\phi Y_v K_\psi\right]} \tag{B65}$$

A Physical Interpretation of F = 0

The condition that F = 0 for a stable non-zero steady state is equivalent to the requirement that the conditions for static stability with a non-zero side-slip be satisfied.

For static stability the summation of roll moment and side forces must equal zero. The conditions which must exist to achieve this state with $\beta \neq 0$ can be found from Equation (B58).

From Side Force Equation:

$$g\phi + U_1 Y_v \beta = 0$$

or

$$\frac{\phi}{\beta} = -\frac{U_1 Y_v}{g} \qquad (B66)$$

From roll moment equation

$$K_\phi \phi = -\underline{L}_\beta \beta$$

or

$$\frac{\phi}{\beta} = -\frac{\underline{L}_\beta}{K_\phi} \qquad (B67)$$

In order to satisfy both Equation (B66) and (B67) simultaneously, we must have

$$-\frac{\underline{L}_\beta}{K_\phi} = \frac{-U_1 Y_v}{g}$$

or

$$g\frac{\underline{L}_\beta}{U_1} - K_\phi Y_v = 0$$

which we can see is equivalent to having F = 0.

$\underline{L}_\beta$ can be chosen to make F= 0 by the appropriate amount of β feedback to aileron.

Roll Response to a Wind Step

In a manner similar to that used to find $\psi_{ss}\big|_{F=0}$ and $\beta_{ss}\big|_{F=0}$ it can be shown that:

$$\phi_{ss}\bigg|_{F=0} = \frac{-\beta_o \underline{L}_\beta K_\psi}{E} \tag{B68}$$

APPENDIX C
ANALOG COMPUTER DIAGRAMS AND POTENTIOMETER SETTINGS

COMPUTER DIAGRAMS

The linearized equations of motion were used for the simulation of the Cessna 310. These equations are listed for the pitch axis in this appendix and in Appendix B for the lateral axis. They have also been noted on the analog diagrams (Figures C1 and C2) for ease in comparing the equations to the simulation.

The aerodynamic data has been estimated for the Cessna 310 and is typical of twin-engine light aircraft. The flight conditions have been selected for the cruise, approach and climb phase.

Not all of the concepts are shown on the computer diagrams. Typical feedbacks are shown on the diagrams so that a correlation can be made with the block diagrams in the text. The block diagrams list the over-all gain for each feedback for ease in duplicating the simulation in the future.

The pitch and lateral potentiometer settings are listed and correspond to the computer diagrams.
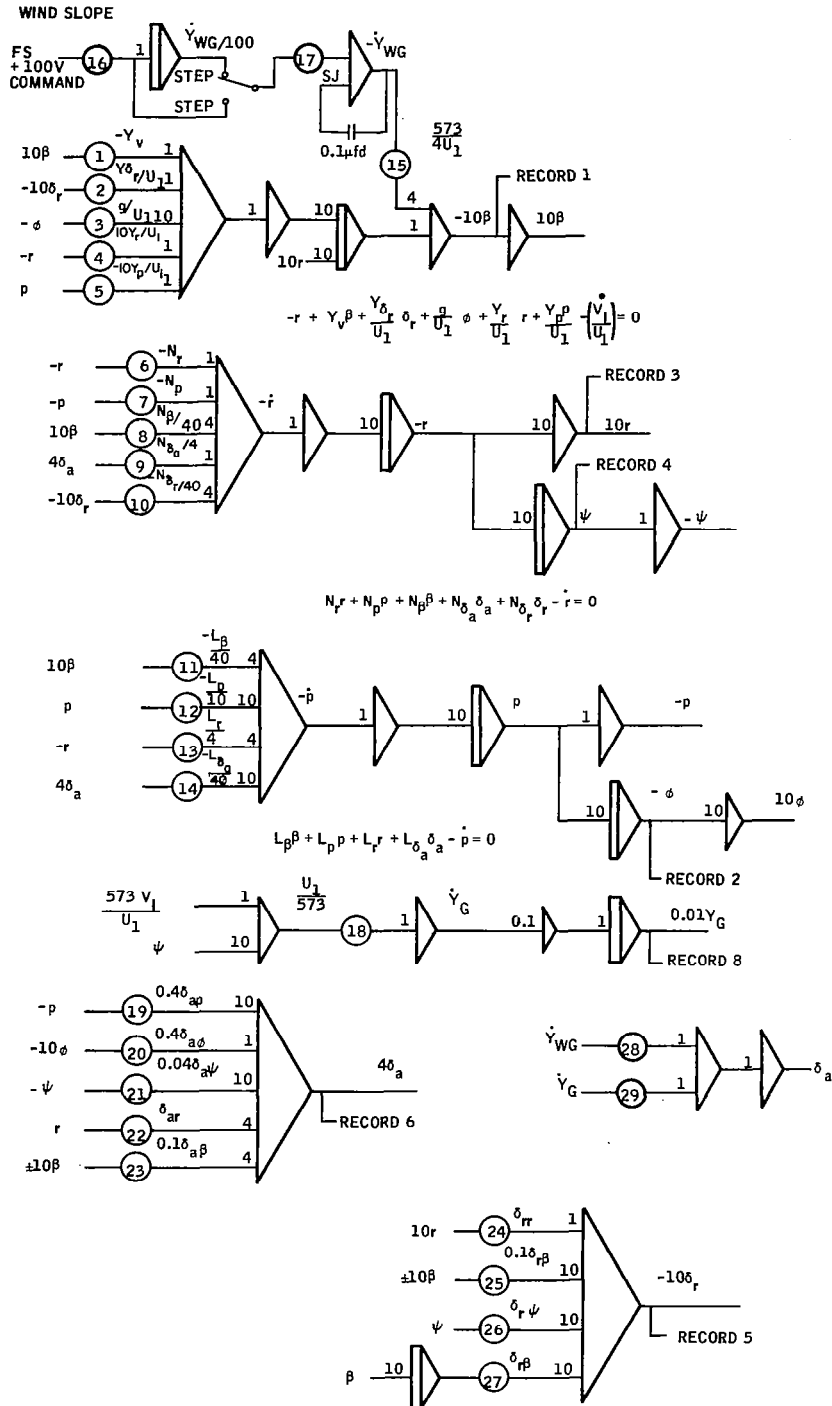
Figure C1.   Lateral Axis Computer Diagram
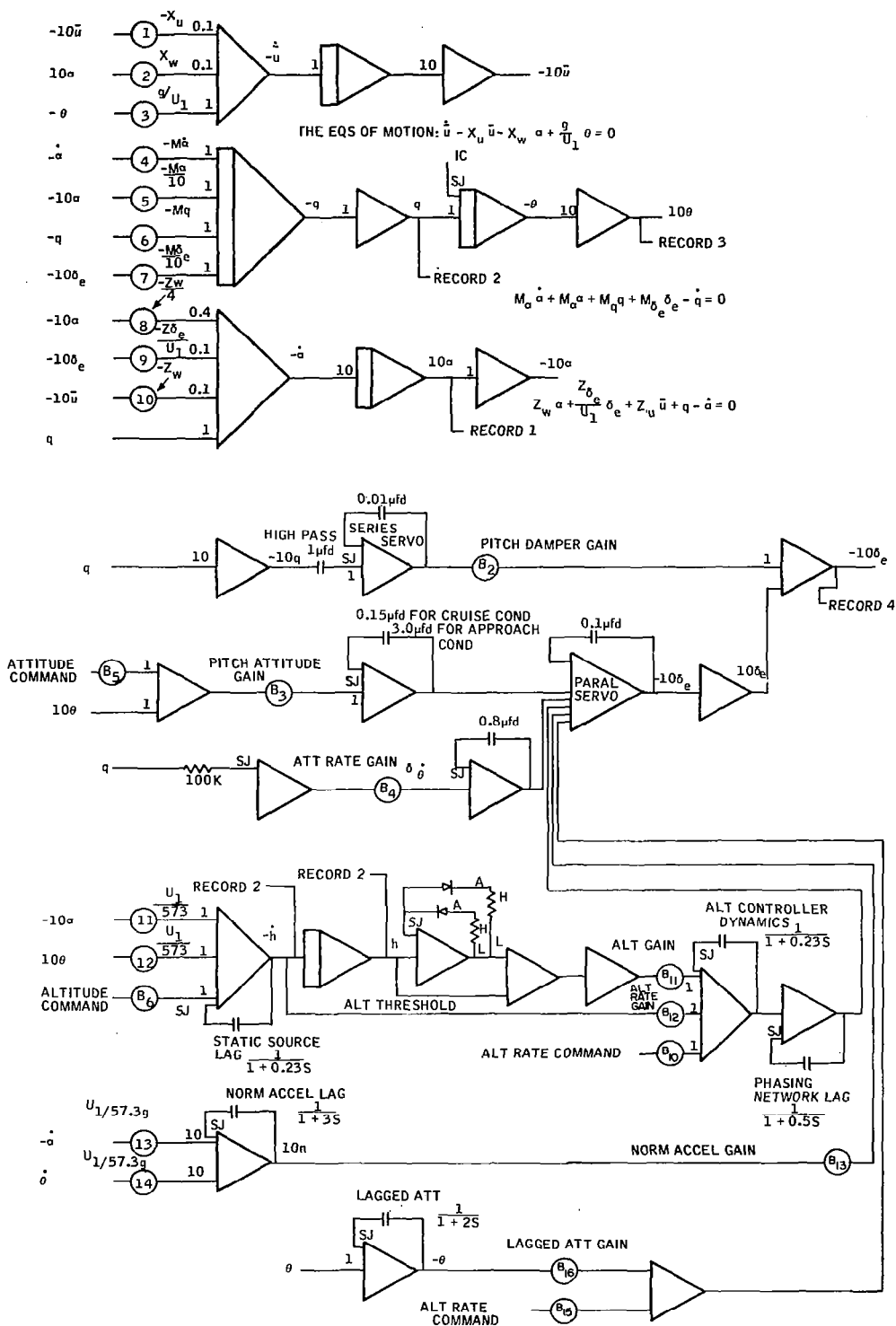
Figure C2.   Pitch Axis Computer Diagram

POTENTIOMETER SETTINGS

Lateral

Pot	Quantity	Cruise	Climb	Approach
A1	Y_v	-0.240	-0.159	-0.114
A2	$Y_{\delta r}/U_1$	+0.083	+0.063	+0.049
A3	g/U_1	+0.103	+0.179	+0.233
A4	$10\,Y_r/U_1$	+0.072	+0.093	+0.092
A5	$10\,Y_p/U_1$	-0.0277	-0.054	-0.075
A6	N_r	-1.06	-0.841	-0.809
A7	N_p	-0.184	-0.335	-0.424
A8	$N_\beta/40$	+0.446	+0.210	0.134
A9	$N_{\delta a}/4$	+0.539	+0.545	0.543
A10	$N_{\delta r}/40$	-0.356	-0.157	-0.092
A11	$L_\beta/40$	-0.585	-0.215	-0.132
A12	$L_p/10$	-0.672	-0.512	-0.409
A13	$L_r/4$	0.223	0.403	0.431
A14	$L_{\delta a}/40$	-0.920	-0.400	-0.235
A15	$573/4U_1$	+0.458	+0.796	+1.038
A16	Wind Slope			
A17	$Y_{WG}/100$	Varies with input		
A18	$U_1/573$	0.5463	0.3141	0.2409

Pitch Axis Settings - Cessna 310

Pot	Quantity	Cruise 8000 ft 313 ft/sec	Climb S.L. 180 ft/sec	Approach S.L. 138 ft/sec
A1	X_u	-0.021	-0.028	-0.069
A2	X_w	+0.044	+0.086	+0.103
A3	g/U_1	+0.103	+0.179	+0.233
A4	$M_{\dot{\alpha}}$	-0.036	-0.053	-0.041
A5	$M_{\alpha}/10$	-0.600	-0.640	-0.695
A6	M_q	-0.072	-0.105	-0.090
A7	$M_{\delta e}/10$	-0.990	-0.477	-0.242
A8	$Z_w/4$	-0.395	-0.303	-0.230
A9	$Z_{\delta e}/U_1$	-0.263	-0.226	-0.148
A10	Z_u	-0.206	-0.362	-0.466
A11	$U_1/573$	+0.546	+0.314	-0.241
A12	$U_1/573$	+0.546	+0.314	+0.241
A13	$U_1/573$	+0.170		-0.075
A14	$U_1/57.3g$	+0.170	+0.0975	+0.075

NOTE: The value given for $C_{m\delta e}$ in the Cessna aerodynamic data looks like it is off by a factor of 10 in comparison to other aircraft. Accordingly, it was reduced for these studies.

EQUATIONS OF MOTION

For pitch and lateral axis stability the following simplified equations of motion have been used:

1. $\dot{\bar{u}} - X_u \bar{u} - X_w \alpha + \dfrac{g}{U_1} \theta = 0$

2. $M_{\dot{\alpha}} \dot{\alpha} + M_\alpha \alpha + M_q q + M_{\delta e} \delta_e = 0$

3. $Z_w \alpha + \dfrac{Z_{\delta e}}{U_1} \delta_e + Z_u \bar{u} + q - \dot{\alpha} = 0$

4. $Y_v \beta + \dfrac{Y_{\delta r}}{U_1} \delta_r + \dfrac{g}{U_1} \phi + \dfrac{Y_r\, r}{U_1} + \dfrac{Y_p\, p}{U_1} - \left(\dfrac{\dot{V}_a}{U_1}\right) = 0$

5. $N_r r + N_p p + N_\beta \beta + N_{\delta a} \delta_a + N_{\delta r} \delta_r - \dot{r} = 0$

6. $L_\beta \beta + L_p p + L_r r + L_{\delta a} \delta_a - \dot{p} = 0$

APPENDIX D

CESSNA 310 AERODYNAMIC DATA

Condition	Altitude (ft)	Density (slug/ft^3)	Velocity U_1 (ft/sec)	Weight (lbs)	Dynamic Pressure (lbs/ft^2)
Cruise	8,000	0.0018	313	4,600	91.6
Climb	0	0.00238	180	4,600	38.6
Approach	0	0.00238	138	4,600	22.6

Wing area (S)	175 ft^2
Mean aero. chord (C)	5.08 ft
Span	35.8 ft
Aspect ratio	7.3
Tail length	15 ft (estimated)
Aileron area (one)	6.38 ft^2
Aileron chord	1.13 ft
Elevator area	21.7 ft^2
Elevator chord	1.29 ft
Rudder area	11 ft^2
Rudder chord	1.75 ft
I_x	2585 slug ft^2
I_z	4446 slug ft^2
I_y	1789 slug ft^2

Center of gravity at 33 percent MAC

APPENDIX E
DEFINITION OF SYMBOLS

A, B, C, D, E, F polynominal coefficient

$a = \dfrac{F}{E}$

a_{ij} direction cosine matrix

b used as the coefficient of the S term in certain forms of the characteristic equations

b wing span, ft

b' coefficient of S term in certain forms of characteristic equations

C_D drag coefficient

$C_{D\alpha} = \dfrac{\partial C_D}{\partial \alpha}$

C_L lift coefficient

$C_{L\alpha} = \dfrac{\partial C_L}{\partial \alpha}$

$C_{L\delta e} = \dfrac{\partial C_L}{\partial \delta_e}$

C_l rolling moment coefficient

$C_{lp} = \dfrac{\partial C_l}{\partial \left(\dfrac{pb}{2U}\right)}$

$C_{lr} = \dfrac{\partial C_l}{\partial \left(\dfrac{rb}{2U}\right)}$

$C_{l\beta} = \dfrac{\partial C_l}{\partial \beta}$

$C_{l\delta a} = \dfrac{\partial C_l}{\partial \delta_a}$

C_m pitching moment coefficient

$$C_{mq} = \frac{\partial C_m}{\partial\left(\frac{qc}{2U}\right)}$$

$$C_{m\alpha} = \frac{\partial C_m}{\partial\alpha}$$

$$C_{m\dot{\alpha}} = \frac{\partial C_m}{\partial\left(\frac{\dot{\alpha}c}{2U}\right)}$$

$$C_{m\delta e} = \frac{\partial C_m}{\partial\delta_e}$$

C_n yawing moment coefficient

$$C_{np} = \frac{\partial C_n}{\partial\left(\frac{pb}{2U}\right)}$$

$$C_{nr} = \frac{\partial C_n}{\partial\left(\frac{rb}{2U}\right)}$$

$$C_{n\beta} = \frac{\partial C_n}{\partial\beta}$$

$$C_{n\delta a} = \frac{\partial C_n}{\partial\delta_a}$$

$$C_{n\delta r} = \frac{\partial C_n}{\partial\delta_r}$$

C_Y side-force coefficient

$$C_{Yp} = \frac{\partial C_Y}{\partial\left(\frac{pb}{2U}\right)}$$

$$C_{Yr} = \frac{\partial C_Y}{\partial\left(\frac{rb}{2U}\right)}$$

$$C_{Y\beta} = \frac{\partial C_Y}{\partial\beta}$$

$$C_{Y_{\delta r}} = \frac{\partial C_Y}{\partial \delta_r}$$

C_Z sought wind velocity

C_1 known wind velocity

c   mean aerodynamic chord

c   used as a constant term in certain forms of the characteristic equations

c'   constant term in certain forms of characteristic equations

$c\theta$ cosine θ

$c\phi$ cosine ϕ

$c\psi$ cosine ψ

D   drag, lb

F_x forces acting on vehicle in X direction, lb

F_y forces acting on vehicle in Y direction, lb

F_z forces acting on vehicle in Z direction, lb

f_z coefficients

f_1 coefficients

g   acceleration due to gravity, ft/sec^2

I_x moment of inertia in roll, slug/ft^2

I_y moment of inertia in pitch, slug/ft^2

I_z moment of inertia in yaw, slug/ft^2

i(s)   forcing function

K_β effective increment in the stability derivative due to sideslip feedback

K_ϕ effective increment in the stability derivative due to bank angle feedback

K_ψ effective increment in the stability derivative due to heading feedback

$$L_p = \frac{\bar{q}Sb}{I_x} \left(\frac{b}{2U}\right) C_{lp}$$

$$L_r = \frac{\bar{q}Sb}{I_x} \left(\frac{b}{2U}\right) C_{lr}$$

$$L_\beta = \frac{\bar{q}Sb}{I_x} C_{l\beta}$$

$$L_{\delta a} = \frac{\bar{q}Sb}{I_x} C_{l\delta a}$$

$$M_q = \frac{\bar{q}Sc}{I_y} \left(\frac{c}{2U}\right) C_{Mq}$$

$$M_\alpha = \frac{\bar{q}Sc}{I_y} C_{M\alpha}$$

$$M_{\dot{\alpha}} = \frac{\bar{q}Sc}{I_y} \left(\frac{c}{2U}\right) C_{M\dot{\alpha}}$$

$$M_{\delta e} = \frac{\bar{q}Sc}{I_y} C_{M\delta e}$$

m   vehicle mass, slugs

$$N_p = \frac{\bar{q}Sb}{I_z} \left(\frac{b}{2U}\right) C_{np}$$

$$N_r = \frac{\bar{q}Sb}{I_z} \left(\frac{b}{2U}\right) C_{nr}$$

$$N_\beta = \frac{\bar{q}Sb}{I_z} C_{n\beta}$$

$$N_{\delta a} = \frac{\bar{q}Sb}{I_z} C_{n\delta a}$$

$$N_{\delta r} = \frac{\bar{q}Sb}{I_z} C_{n\delta r}$$

P   a constant for a particular location

p   aircraft roll rate, deg/sec

p(s)   transfer function for roll rate

q	aircraft pitch rate, deg/sec
$\bar{q}$	dynamic pressure, lb/ft^2
r	aircraft yaw rate, deg/sec
r(s)	transfer function for yaw rate
r_1	remainder of S coefficient
r_2	remainder of constant
S	Laplace operator; also wing area, ft^2
$s\theta$	sine θ
$s\phi$	sine ϕ
$s\psi$	sine ψ
T	reset time, sec
T_a	airplane time constant, sec
T_D	time lost in detecting onset of the lateral wind change in effecting the switchover, sec
t	time, sec
t_o^+	time immediately after gust is applied, sec
t_o^-	time before gust is applied, sec
U	body velocity with respect to an inertial space, forward, ft/sec
U_a	body velocity with respect to the surrounding air mass, forward-aft, ft/sec
U_1	aircraft longitudinal velocity, ft/sec
$\bar{u}$	dimensionless change in perturbation velocity
V	wind speed
V	body velocity with respect to an inertial space, lateral, ft/sec
V_a	body velocity with respect to the surrounding air mass, lateral, ft/sec
V_z	vertical wind speed at altitude

V_0 vertical wind speed at reference level

W   aircraft weight, lb

W   body velocity with respect to an inertial space, vertical, ft/sec

W_a body velocity with respect to the surrounding air mass, vertical, ft/sec

$$X_u = -\frac{\bar{q}S}{mU}\left(2C_D\right)$$

$$X_W = \frac{\bar{q}S}{mU}\left(C_L - C_D\alpha\right)$$

$\dot{X}_{WG}$ inertially-fixed winds along flight path, ft/sec

x   distance from aircraft x-axis to engine thrust line, ft

Y_G lateral displacement from flight path, ft

$\dot{Y}_G$ lateral velocity, ft/sec

$$Y_p = \frac{\bar{q}Sb}{m2U}\,C_{yp}$$

$$Y_r = \frac{\bar{q}Sb}{m2U}\,C_{yr}$$

$$Y_v = \frac{\bar{q}S}{mU}\,C_{y\beta}$$

$$Y_{\delta r} = \frac{\bar{q}S}{m}\,C_{y\delta r}$$

$\dot{Y}_{WG}$ inertially fixed winds, lateral to flight path, ft/sec

$\dot{Y}_{WG_o}$ lateral wind, ft/sec

Z   altitude, ft

$$Z_u = -\frac{\bar{q}S}{mU}\left(2C_L\right)$$

$$Z_w = -\frac{\bar{q}S}{mU}\left(C_{L\alpha} + C_D\right)$$

$\dot{Z}_{WG}$ inertially fixed winds, normal to ground, ft/sec

$$Z_{\delta e} = -\frac{\bar{q}S}{m}\,C_{L\delta e}$$

Z_0 altitude at reference level

α	angle of attack, deg
β	sideslip angle, deg
β	sought angle or deviation of the wind direction at level Z from the given wind direction
γ	flight path angle, deg
Δ	denominator of the airframe transfer function
δ_a	aileron deflection, deg
δ_{ap}	autopilot gain, deg aileron/deg/sec roll rate
δ_{ar}	autopilot gain, deg aileron/deg/sec yaw rate
δ_{ar_w}	autopilot gain, deg aileron/deg/sec yaw rate weathercock mode
$\delta_{a\beta}$	autopilot gain, deg aileron/deg sideslip
$\delta_{a\beta_s}$	autopilot gain, deg aileron/deg servoed sideslip
$\delta_{a\phi}$	autopilot gain, deg aileron/deg roll angle
$\delta_{a\psi}$	autopilot gain, deg aileron/deg heading
$\delta_{a\psi_s}$	autopilot gain, deg aileron/deg heading sensor
δ_e	elevator deflection, deg
δ_r	rudder deflection, deg
δ_{rr}	autopilot gain, deg rudder/deg/sec yaw rate
δ_{rv}	autopilot gain, deg rudder/side velocity
$\delta_{r\beta}$	autopilot gain, deg rudder/deg sideslip
$\delta_{r\beta_{int}}$	autopilot gain, deg rudder/integral of sideslip
$\delta_{r\psi}$	autopilot gain, deg rudder/deg heading
δ_z	coefficient
δ_1	coefficient

ϵ_{Y_G}	lateral flight path error, ft
$\epsilon_{\dot{Y}_G}$	lateral velocity error, ft/sec
$\epsilon_{\psi_{ss}}$	error in steady state yaw angle, deg
$\epsilon_{\psi^*_{(t)}}$	error in heading after the initial transient, deg
ζ	damping of the short transient response in heading
ζ_{np}	damping of the roll response
ζ_{nr}	damping of the yaw response
θ	pitch attitude, deg
ρ	air density, slugs/ft^3
τ	time constant, sec
τ_{HLT}	long term response in heading, sec
ϕ	roll angle, deg
ϕ_{peak}	value of the roll angle at the end of the short term heading transient, deg
$\phi(s)$	transfer function for the roll angle
$\phi^*(t)$	roll angle at the end of the initial transient, deg
ψ	yaw angle, deg
ψ_d	heading drift angle, deg
ψ_{FP}	flight path bearing, deg
ψ_H	aircraft heading, deg
ψ_{io}	input step in heading
$\psi(s)$	transfer function for heading
$\psi^*(t)$	heading at the end of the initial transient, deg
ω_n	natural frequency of the short term transient response in heading

ω_{np} natural frequency of roll response

ω_{nr} natural frequency of yaw response

Subscripts:

o   initial value

ss   steady state or final value

ss(des)   steady state value desired

(t)   function of time

      A bar under the stability derivative signifies that this is the effective value modified by a feedback quantity.

      A dot over a quantity indicates the differentiation with respect to time

APPENDIX F
ENGINE THRUST DIFFERENTIAL

The magnitude of twin engine thrust mismatch was estimated, in order to evaluate its effect on flight path control accuracy. For the Cessna 310 at cruise (213 mph, 8 K feet):

$$C_{D_{cruise}} = 0.031$$

x = 6.12 feet (distance from aircraft x axis to engine thrust line)

α = 2.5 degrees

ρ = 1.87×10^{-3} (air density)

S = 175 ft^2 (wing area)
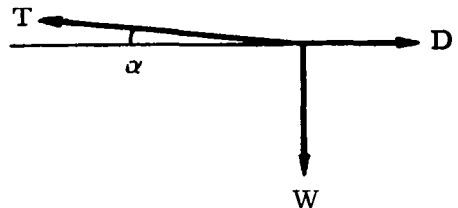
U_1 = 313 ft/sec

W = 4600 lbs

$$D = \text{Drag} = 1/2 \, C_D \, \rho \, S \, V^2$$
$$= 1/2 \, (0.031) \, (1.87 \times 10^{-3}) \, (175) \, (313)^2$$
$$= 498 \text{ lbs}$$

Engine Thrust = $D \cos \alpha + mg \sin \alpha$

$$= 498 + 4600 \times 2.5/57.3$$

$$= 498 + 201$$

$$= 699 \text{ lbs}$$

$$= 350 \text{ lbs/engine}$$

Assuming engines are matched to 3 percent thrust

Differential thrust = 0.03 (350) = 10.50 lbs

Moment = 10.50 (6.12) = 64.3 ft-lbs

At cruise

$N_{\delta r}$ = 14.24

I_Z = 4446

Rudder moment = $\dfrac{14.24\ (4446)}{57.3}$ = $1100\ \dfrac{\text{ft-lbs}}{\text{deg}\ \delta_r}$

Required rudder to trim engine mismatch = $\dfrac{64.3}{1100}$ = 0.058 degree

A similar procedure was used to estimate effect of engine mismatch at climb and approach conditions. Following is a summary of the results:

Flight Condition	Moment Due to Engine Mismatch (ft-lbs)	Required Rudder to Trim (deg)
Cruise	64.1	0.058
Climb	129	0.26
Approach	89	0.31

APPENDIX G
VERTICAL AND LATERAL WIND PROFILES

VERTICAL WIND PROFILES

A literature search was made to obtain vertical wind profile data for low altitudes (to 10K feet).

One study (Ref. 1) provides data for determining the vertical wind gradient under conditions of high winds (>26 mph), where thorough mixing reduces thermal stability effects. It is concluded that the vertical wind gradient may be approximated by the exponential law $\frac{V_Z}{V_0} = \left(\frac{Z}{Z_0}\right)^P$, where V = wind speed, Z = altitude, P = a constant for a particular location, and subscript 0 is a reference level. P was found to vary from approximately 0.1 to 0.3, depending primarily on the terrain at a given location. For fairly flat terrain the value is 0.1 to 0.15.

A second study (Ref. 2) provides data which permits calculation of the wind velocity profile - when data on the wind at any given level is known.

The following formula is used to calculate the velocity and direction of the wind at any height:

$$C_z = C_1 \frac{f_z}{f_1} \text{ and } \beta = \delta_z - \delta_1$$

where C_z is the sought wind velocity, C_1 is the known wind velocity at any fixed level z_1, β is the sought angle of deviation of the wind direction at level z from the given wind direction at level z_1 (positive, if $z > z_1$, i.e., the wind at level z deviates to the right of the wind at level z_1).

The values f_z, f_1, δ_z, and δ_1 are determined from Table G1.

Table G1. Coefficients f and δ for Unstable, Equilibrium and Stable Conditions

Height (meters)	Unstable Condition		Equilibrium		Stable Condition	
	f	δ	f	δ	f	δ
1	0.46	0	0.39	0	0.36	0
3	0.57	0	0.50	0	0.47	0
5	0.61	0	0.54	0	0.53	1°
10	0.66	0	0.60	0	0.61	1°
15	0.68	0	0.63	0	0.66	2°
20	0.70	0	0.66	1°	0.69	2°
30	0.73	0	0.69	1°	0.74	2°
50	0.75	0	0.73	1°	0.80	3°
80	0.77	0	0.76	1°	0.88	5°
100	0.78	0	0.78	2°	0.91	6°
150	0.80	1°	0.82	2°	0.98	10°
200	0.81	1°	0.85	3°	1.0	13°
300	0.84	1°	0.91	5°	1.0	17°
400	0.86	1°	0.96	7°	1.0	19°
500	0.88	2°	0.99	9°	1.0	20°
600	0.90	2°	0.99	10°		
800	0.94	3°	1.0	13°		
1000	0.97	5°	1.0	15°		
1200	0.98	6°	1.0	17°		
1500	1.0	7°				
2000	1.0	9°				
2500	1.0	11°				
3000	1.0	13°				

Example: The wind velocity at z = 10m is equal to 5m/sec. The condition of the atmosphere is unstable. Find the velocity and direction of the wind at z = 500m.

From the table we find the values of the coefficients f_{10} and δ_{10} in the "unstable condition" for 10m, and f_{500} and δ_{500} for 500m.

In the given example f_{10} = 0.66, δ_{10} = 0, f_{500} = 0.88, δ_{500} = 2°. Then C_{500} = 6.7m/sec., i.e., the velocity at z = 500m is equal to 6.7m/sec., and the direction is 2 degrees to the right of the surface wind.

The two methods check reasonably well, depending on the value of P chosen for the equation of Ref. 1.

It is expected that the wind profile data will be helpful in approximating wind variations during changing-altitude flight conditions (approach, climbout, letdown). Additional studies will be made of wind gradients at constant altitude to realistically simulate wind variations for the cruise condition.

LATERAL WIND PROFILES

A literature search failed to disclose relevant information on horizontal wind profiles. As a result, the following wind profiles were arbitrarily selected for evaluating the cruise mode:

    Step Crosswind Changes   10, 20, 40 fps

    Ramp Crosswind Changes   0.66, 1.33, 2.66 fps/min

Selection of the minimum ramp wind change is probably the most critical consideration, since this establishes sensor threshold requirements for

several concepts. The minimum ramp of 0.66 fps/min was chosen because it represents a wind change which, undetected, produces a cross-course deviation within the accuracy tolerances previously set up (assuming that approximately half the total tolerance can be assigned to this source).